Harbor Branch Oceanographic Institution
5600 North U.S. Highway 1
Fort Pierce, Florida 34946

# Final Report

## Hawk Channel Transport Study: Pathways and Processes

January 1, 1996 - December 31, 1997

Submitted December 1, 1998 by:
Ned P. Smith, Principal Investigator
Patrick A. Pitts, Research Specialist

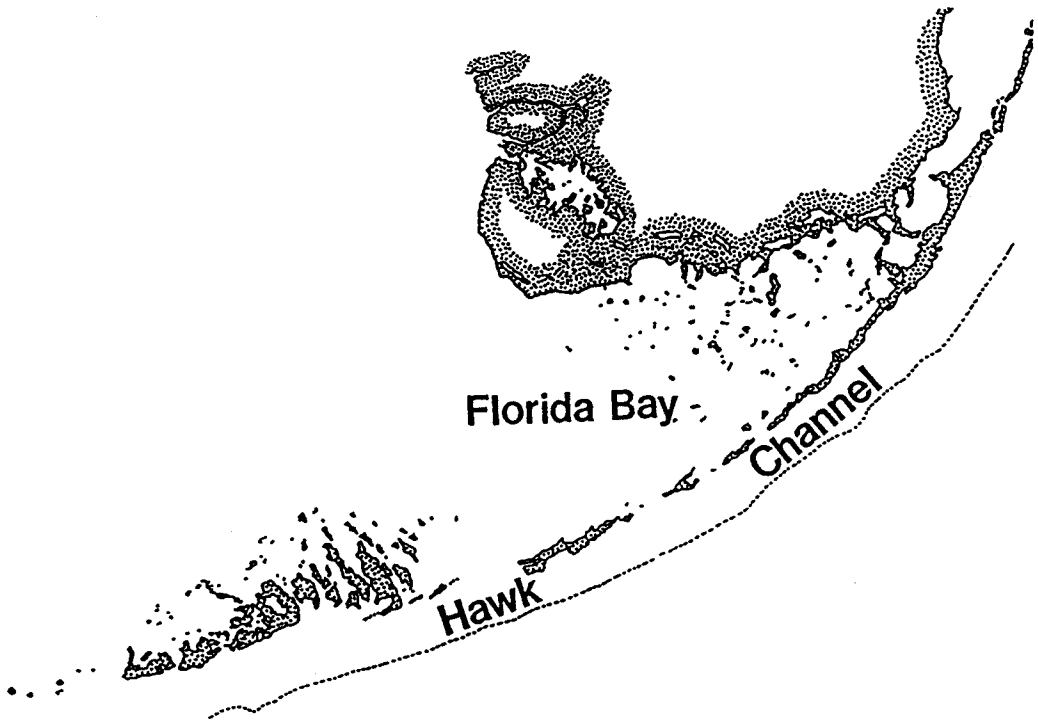


**Figure 1.** Map of the Florida Keys showing the location of Florida Bay and the Florida reef tract (hatched line). Hawk Channel lies between and parallels the reef tract and Florida Keys.

CONTENTS



## SUMMARY


Historical data from the previous ten years are combined with new data collected during 1996 and 1997 to describe several aspects of the transport of water across Florida Bay, through tidal channels that connect the Gulf and Atlantic sides of the Florida Keys, across Hawk Channel and into the Straits of Florida at the reef tract.

A tidal pumping mechanism is identified as the primary mechanism for the west-to-east net flow of water across Florida Bay. The long-term net Gulf-to-Atlantic transport is the principal exchange mechanism for carrying salt, heat and mass through tidal channels. Tidal exchanges, along with mixing on each half tidal cycle, also produce an exchange of Florida Bay water and Hawk Channel water. Hydrographic data, intended to track plumes of high-salinity Florida Bay water across Hawk Channel, identifies Florida Bay water only to the middle of Hawk Channel. Data from the reef tract do not indicate the presence of Florida Bay water, but hydrographic data are limited and the transect may not have stayed within the ebb tide plume. A comparison of transport processes that can move Florida Bay water seaward across Hawk Channel indicates that a seaward deflection of the near-bottom current is more effective than turbulent mixing. Local and temporary exceptions can occur where the deflection of the current is minimal, or where across-channel concentration gradients are large. Winter and summer studies of near-surface and near-bottom flow patterns at study sites off the Middle and Upper Keys suggest that wind forcing is the primary mechanism for exchanging water between Hawk Channel and the Straits of Florida. Results indicate that this flushing mechanism at the open boundary varies both seasonally and with location along the reef tract. Tidal exchanges are small, and the loss of Hawk Channel water through near-bottom density currents is also of secondary importance. Major wind events such as hurricanes produce a distinct mark on current meter time series, but effects are transient. Data from tidal channels suggest that the net effect can be quite small, and that the perturbation itself is often of the same order of magnitude as that produced by winter cold fronts. Data from the reef tract indicate a relatively subtle response to storms included in this study.

## INTRODUCTION

This Final Report describes work done by Harbor Branch scientists during a two-year study (January 1996 - December 1997) designed to describe the transport of Florida Bay water into, across and out of Hawk Channel. Hawk Channel is an elongated, shallow basin that serves as the continental shelf on the Atlantic Ocean side of the Florida Keys (**Figure 1**). It is approximately 10 km wide, and extends 230 km from Fowey Rocks, off Key Biscayne, to Sand Key, off Key West. Water depths along the center of the channel are 7-8 m off the Upper Keys, and generally between 12-15 m off the Middle and Lower Keys.

Many of the environmental issues involving the Florida reef tract, including nutrient and larval transport, require an understanding of transport processes and the pathways taken by dissolved and suspended material moving between Florida Bay and the reef tract. Hawk Channel provides the connecting link between these two regions, and an understanding of transport processes that move water along and especially across Hawk Channel is fundamental to understanding exchanges between Florida Bay and the reef tract.

The overall **goal** of this project was to identify the mechanisms and pathways by which dissolved and suspended materials are transported through major tidal channels, across Hawk Channel and into the Florida Straits at the reef tract. **Specific objectives** included: (a) quantifying the cumulative volume transport over seasonal and annual time scales through selected tidal channels connecting Florida Bay with Hawk Channel, and documenting the perturbing effect of intense but short-lived episodic forcing; (b) determining the relative importance of the steady and time-varying components of heat, salt and mass transport through selected tidal channels; (c) identifying mechanisms that exchange water between Hawk Channel and the Florida Straits, and determining if they vary in magnitude and relative importance over the course of a year; and (d) determining if, in a given season, wind-driven exchanges between Hawk Channel and the Florida Straits vary along the reef tract as a function of wind direction relative to the local orientation of the reef tract. The **justification** for the project stems from concerns that Florida Bay water may have a negative impact on water quality in the Florida Keys National Marine Sanctuary, especially the reef tract, and thus a negative influence on resources in the Sanctuary.

In a geographic sense, the transport study has three **components**: (1) a tidal channel component, to quantify long-term and episodic transport between Florida Bay and Hawk Channel; (2) a Hawk Channel component, to quantify advective and diffusive transport rates, and (3) a reef tract component, designed to determine how actively and by what mechanisms water in Hawk Channel is exchanged with Florida Straits water at the reef tract. The **approach** was to supplement historical data with new data to obtain an integrated picture of the transport of Florida Bay water across Hawk Channel. Field studies were designed to fill gaps in the historical data base.

To provide a focus for the individual components of our study, six **hypotheses** were formulated and then tested with both new and historical data:

**(1)** We hypothesized that transport from Florida Bay to Hawk Channel exhibits a distinctly fortnightly transition as tidal waves entering western Florida Bay alternate from spring to neap conditions, or from tropic to equatorial conditions. Results from this part of the study quantified the magnitude of the transport mechanism described by Wang et al. (1994).

**(2)** We hypothesized that tidal pumping is the principal transport mechanism through tidal channels of the Upper Keys, while a nontidal, quasi-steady outflow is the principal transport mechanism in the Middle and Lower Keys. Results quantified the relative importance of time-varying and steady transport in the tidal channels selected for this study.

(3) We hypothesized that Florida Bay water retains its hydrographic characteristics in near-bottom layers as it is transported across Hawk Channel, and that it can be detected through its hydrographic properties at the reef tract. Results showed the extent to which Florida Bay water is diluted by mixing as it moves from the tidal channels to the reef tract.

(4) We hypothesized that advection is more important than diffusion for transporting Florida Bay water across Hawk Channel. Results showed the relative importance of these two processes in carrying water of low quality to the reef tract.

(5) We hypothesized that seasonally shifting winds alternately increase and decrease the near-bottom export of Florida Bay water from Hawk Channel to the Florida Straits. Results of our seasonal field studies at the reef tract showed whether the loss of Hawk Channel water to the Florida Straits is a function of season and/or location.

(6) Finally, we hypothesized that episodic wind events have major perturbing effects on Keys circulation patterns, transporting in a few days volumes of water that are commonly transported in several weeks. Results put in perspective the importance of short-lived transport events that import Florida Bay water into Hawk Channel, advect it across Hawk Channel, and export it to the Florida Straits.

We have divided this final report into six sections, each addressing one of the above hypotheses. Each section has its own introduction, data, methods, results and discussion sub-sections specific for the given hypotheses. Structuring the report in this way should provide optimal clarity and readability.

## HYPOTHESIS #1: Transport from Florida Bay to Hawk Channel exhibits a distinct fortnightly transition.

### Introduction

Primary attention in this first section is given to the transport through tidal channels that connect the Gulf and Atlantic sides of the Florida Keys. Smith (1994) showed that the long-term net volume transport through the major tidal channels of the Lower and Middle Keys is upwind, indicating that wind forcing plays a secondary role at most in the export of Florida Bay water into Hawk Channel. Wang et al. (1994) have postulated that frictionally damped tidal waves entering Florida Bay from the Gulf of Mexico set up water levels on the western side of the bay and force an outflow through the tidal channels on the southeast side of the bay. This would produce a fortnightly fluctuation in outflow. In this section we describe the relationship between flow through Bahia Honda and Long Key Channels and tidal conditions in western Florida Bay. Specifically, we test the hypothesis that flow from Florida Bay exhibits a distinct fortnightly transition as tides in western Florida Bay alternate from spring to neap conditions, or from tropic to equatorial conditions. Results are directly related to the transport mechanism described by Wang et al. (1994).

### Data Base

To investigate the importance of tidal forcing in driving water across Florida Bay and through the tidal channels, current meter data were analyzed in conjunction with bottom pressure measurements. Two study periods were singled out from historical data. The first was a 120-day time period from October 24, 1987 to February 21, 1988. The second was a 76-day period from January 18 to April 4, 1995. In the first study, current meter data from Bahia Honda Channel (24°39.15'N, 81°17.30'W) were combined with bottom pressure data from the Gulf side of the

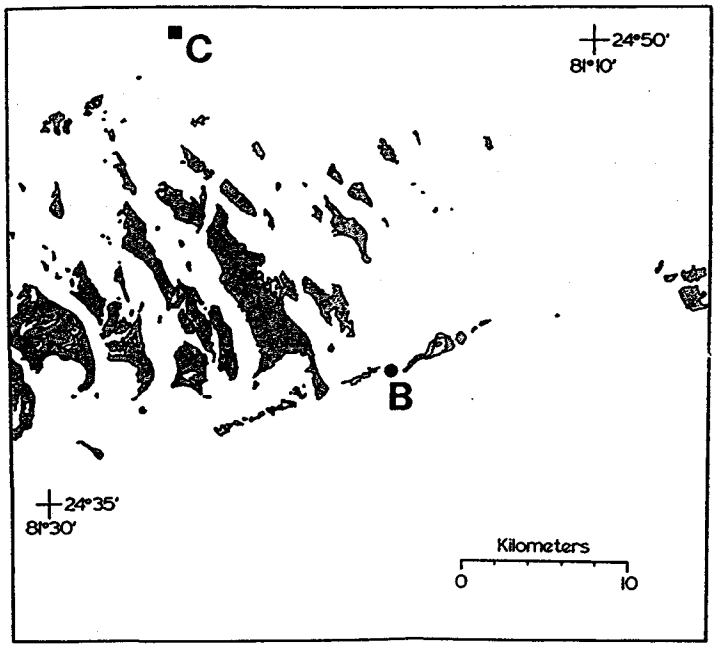


**Figure 2.** Map of the study sites used in the investigation of tidal pumping through Bahia Honda Channel. The solid square labeled "C" at the top of the figure indicates the location of the pressure recorder near the Content Keys. The solid circle labeled "B" shows the location of the current meter in Bahia Honda Channel.

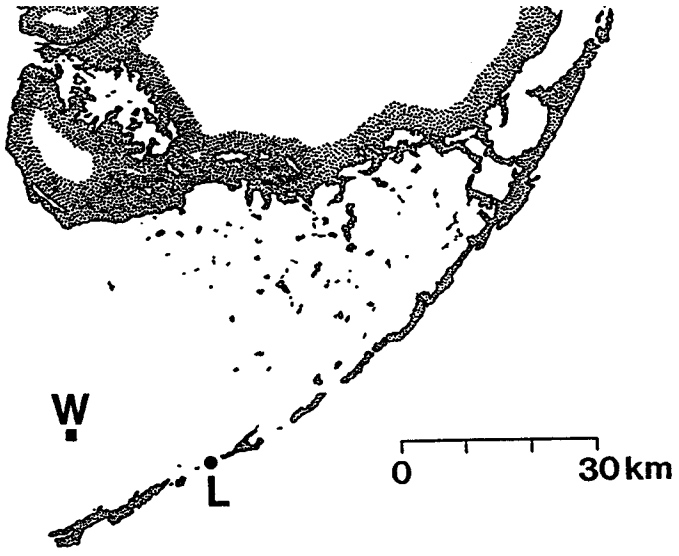


**Figure 3.** Map of the study sites used in the investigation of tidal pumping through Long Key Channel. The solid square labeled "W" indicates the location of the pressure recorder in southern Florida Bay, north of Marathon. The solid circle labeled "L" shows the location of the current meter in Long Key Channel.

Keys (24°50.3"N, 81°25.6'W, see **Figure 2**). In the second study, current meter data from Long Key Channel (24°47.867'N, 80°52.269'W) were combined with bottom pressure data from southern Florida Bay (24°50.005'N, 80°05.016'W, see **Figure 3**). From the data bases for these two time periods, flow through tidal channels was quantified as a response to tidal pumping on the Gulf side of the Keys.

General Oceanics currents meters were used to measure current speeds and directions with accuracies of ±1 cm $s^{-1}$ and ±2°, respectively. Current meters were suspended 2 m above the bottom in 8 m of water in Bahia Honda Channel and 1 m above the bottom in 3.5 m of water in Long Key Channel on "gallows" type moorings. Each hour, the current meters took burst samples of eight readings to filter out the effects of wave oscillations. Averages were stored in the current meter on either a cartridge or a cassette tape depending on the instrument model. Brancker and General Oceanics pressure recorders were used to record water level changes. Recorders were housed in bottom-mounted PVC tubes which were vented to expose the sensors to both temperature and pressure changes. Both recorders resolve pressure changes of ±0.004 db, which is equivalent to approximately ±0.5 cm in depth.

### Methods

Only along-channel components of the current vectors were retained for analysis. Along-channel currents were plotted as cumulative net displacement diagrams (Scientific Programming Enterprises, 1985). Displacement is defined to be the product of the current speed and the (one-hour) time interval it represents. By our convention, negative displacement represents flow into Hawk Channel.

Harmonic constants of the principal tidal constituents for along-channel currents and water pressures were quantified using a 29-day harmonic analysis program (Dennis and Long, 1971). Because the time series were substantially longer than 29 days, multiple harmonic analyses were conducted with 29-day offsets. Amplitude and phase angle pairs were then vector averaged for each constituent. Tidal constituents of particular interest included $M_2$, $S_2$, $N_2$, $K_1$, $O_1$ and $P_1$.

To investigate tidal pumping as a mechanism for forcing water through Florida Bay, time series of bottom pressures from the study site in southern Florida Bay and the time series of current speed from Long Key Channel were broken into 25-hour blocks, starting every 24th hour (one-hour overlap). This approximately one-day time period includes one diurnal tidal cycle and two semidiurnal tidal cycles, and thereby incorporates the effect of diurnal inequalities. For each block of data, the standard deviation of the bottom pressure is taken to represent the magnitude of tidal pumping, and the mean along-channel current speed is calculated to represent the response. Linear regression of current speed against standard deviation quantifies two aspects of the flow through Long Key Channel that are of particular interest. The square of the correlation coefficient indicates how much of the variance in the mean current speeds could be explained by fluctuations in tidal pumping; the y-intercept provides an indication of the along-channel flow that occurs in the absence of tidal pumping. An identical procedure quantifies tidal pumping through Bahia Honda Channel, using pressure data from the Content Keys study site.

### Results and Discussion

Results begin with a plot of the cumulative net displacement of the along-channel current components in Bahia Honda Channel from October 24, 1987 to February 21, 1988 (**Figure 4**). Negative displacements indicate a flow of water from the Gulf of Mexico into Hawk Channel. The pattern shows a remarkably steady, long-term outflow from the Gulf of Mexico. Linear

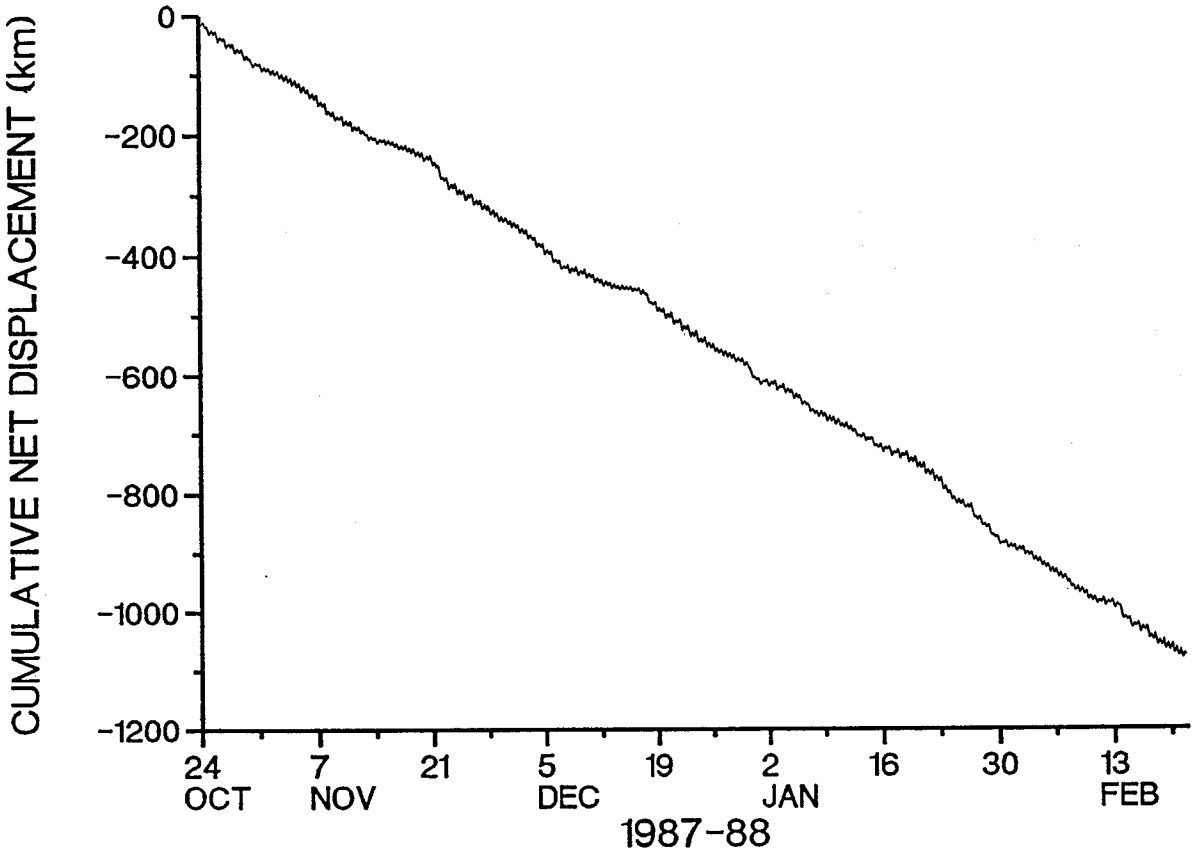


**Figure 4.** Cumulative net displacement of the along-channel current components in Bahia Honda Channel October 24, 1987 to February 21, 1988. Negative displacements indicate flow from the Gulf to the Atlantic side of the Keys.

regression of displacement against time indicates that the outflow averages 10.0 cm $s^{-1}$. Low-frequency variability appears as subtle fluctuations in the outflow rate. There is some indication of a low-frequency signal in the curve as outflow slows perceptibly for about a week then speeds up again about once a month. Superimposed onto the long-term outflow and low-frequency fluctuations are the ebb and flood of the tide. The amplitude of the principal tidal constituent for this region, $M_2$, was determined by harmonic analysis to be 63.4 cm $s^{-1}$. See **Table 1** for amplitudes and phase angles of the other principal diurnal and semidiurnal tidal constituents.

Standard deviations of 25-hour blocks of bottom pressure from the Content Keys station (top) and 25-hour averages of along-channel current speed from Station "B" in Bahia Honda Channel (bottom), October 24, 1987, to February 15, 1988 are shown in **Figure 5**. The mean of the standard deviations is approximately 0.437 db, indicating a characteristic water level fluctuation of about ±44 cm in the vicinity of the Content Keys. The scatter about the mean, quantified by the standard deviation of the 115 standard deviation values, is 0.09 db. The quasi-periodic rise and fall of the 115 standard deviation values is due in large part to the interaction of semidiurnal tidal constituents to produce the spring-neap tide sequence, or the interaction of the diurnal tidal constituents to produce the tropic-equatorial tide sequence. The 25-hour mean current speeds indicate an average outflow of 10.1 cm $s^{-1}$, and the standard deviation of the 25-hour means is 5.1 cm $s^{-1}$. Inspection of the two plots indicates an inverse relationship between tidal pumping and current speed. When tidal pumping is greatest, outflow is strongest.

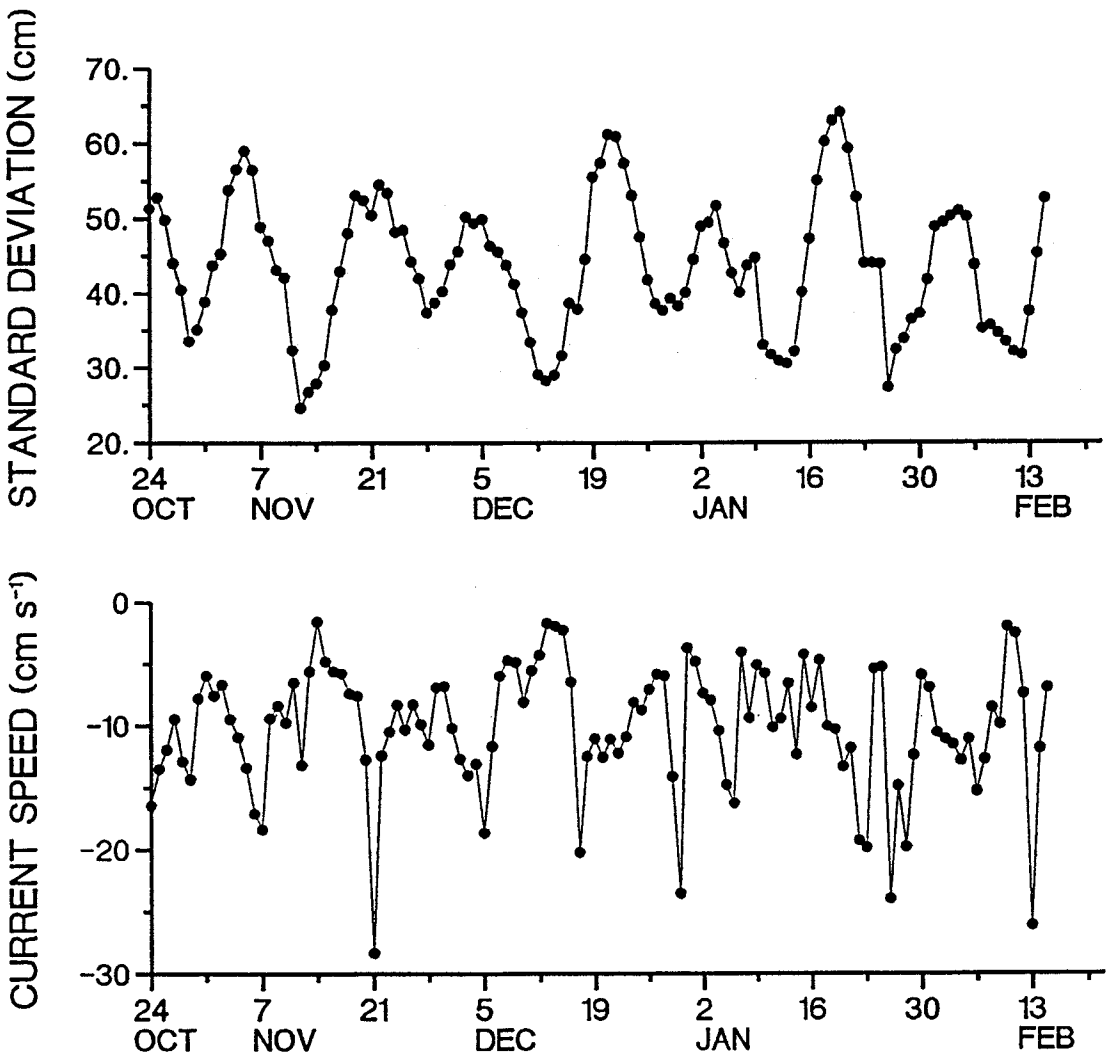


**Figure 5.** Standard deviations of 25-hour blocks of bottom pressure from the Content Keys station (top) and 25-hour averages of along-channel current speed from Station "B" in Bahia Honda Channel (bottom), October 24, 1987, to February 15, 1988.

**Figure 6** shows the mean current speed (25-hour blocks) through Bahia Honda Channel plotted as a function of the standard deviation (25-hour blocks) of hourly bottom pressures recorded at the Content Keys study site. Comparison of standard deviations with along-channel current speeds indicates that correlation is highest when blocks of currents are lagged 15 hours relative to the starting times of the blocks of bottom pressures. The linear correlation coefficient is -0.25, but this is statistically significant at the 99.9% confidence level. The slope of the regression line is -13.9 cm $s^{-1}$ per db, indicating that a 1 db increase in the standard deviation of bottom pressure will increase the outflow by approximately 14 cm $s^{-1}$. Using the slope with the mean of the standard deviations and the y-intercept, results suggest that tidal pumping explains approximately 6 cm $s^{-1}$ of the mean flow, or about 60% of the total. Given the 0.09 db standard deviation of the 25-hour average pressures, it follows that tidal pumping explains variations in the flow through Bahia Honda Channel on the order of ±1-2 cm $s^{-1}$. The standard deviation of the 25-hour average currents is 5.1 cm $s^{-1}$. Thus, tidal pumping explains on the order of 25% of the variation about the mean outflow.

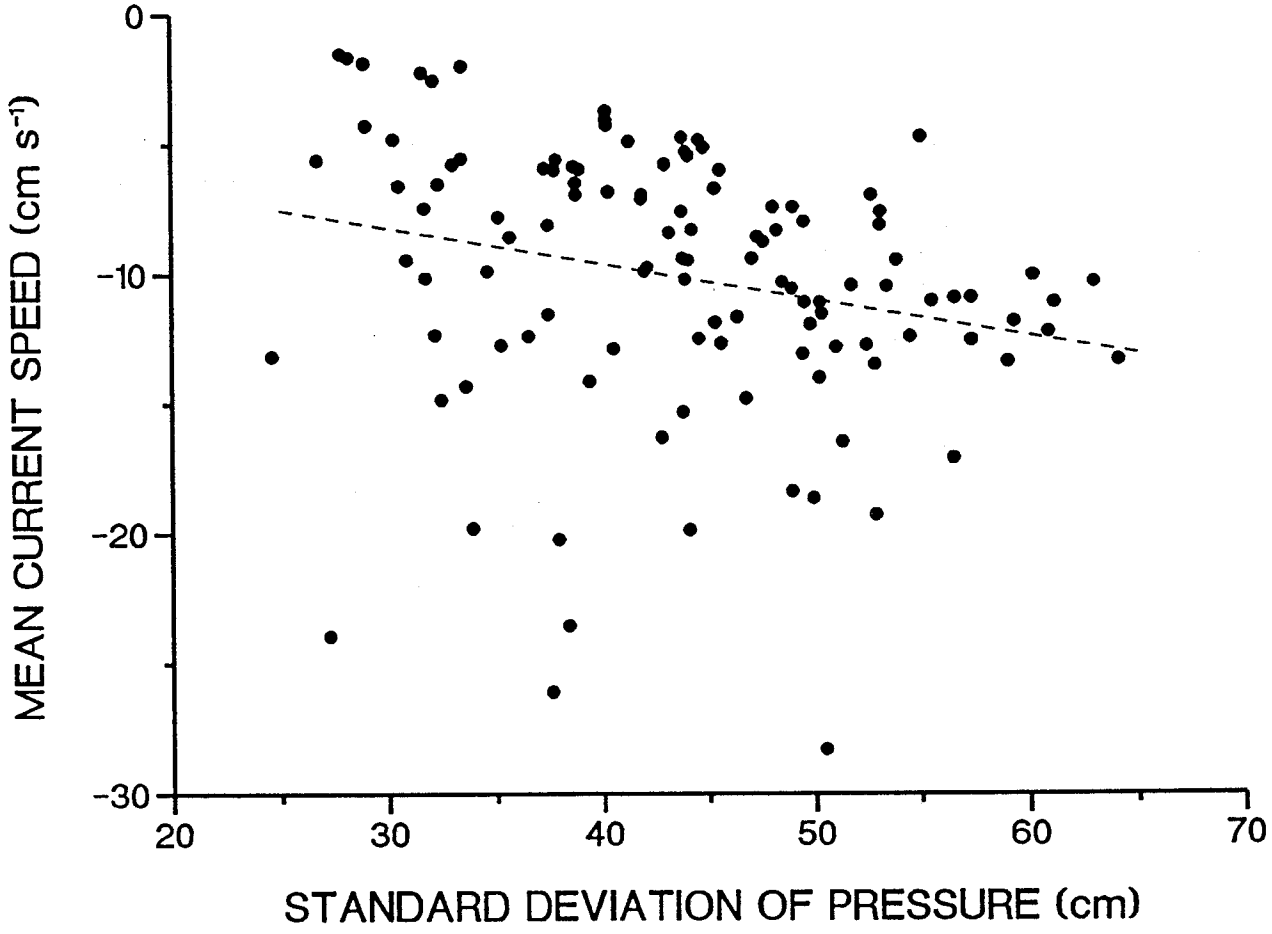


**Figure 6.** Mean current speed (25-hour blocks) through Bahia Honda Channel plotted as a function of the standard deviation (25-hour blocks) of hourly bottom pressures recorded at the Content Keys study site.

Results of the second part of the tidal pumping study begin with a plot of the cumulative net displacement of the along-channel current components in Long Key Channel (**Figure 7**). Data were recorded from January 18 to April 4, 1995. Negative displacements indicate water flowing out of Florida Bay. The pattern shows a long-term outflow from Florida Bay into Hawk Channel which linear regression indicates averages 6.7 cm $s^{-1}$. A significant reversal of the outflow occurs during the second week in March and lasts for about 5 days. Other temporary reversals occur during the month of March and last on the order of 1-3 days. Superimposed onto the long-term outflow and low-frequency fluctuations are the ebb and flood of the tide. The amplitude of the $M_2$ tidal constituent was determined by harmonic analysis to be 46.9 cm $s^{-1}$. See **Table 1** for amplitudes and phase angles of the other principal diurnal and semidiurnal tidal constituents.

Standard deviations of 25-hour blocks of bottom pressure from Station "W" in southern Florida Bay (top) and 25-hour averages of along-channel current speed at Station "L" in Long Key Channel (bottom), January 18 to April 4, 1995, are shown in **Figure 8.** The mean of the standard deviations is approximately 0.21 db, indicating a characteristic water level fluctuation

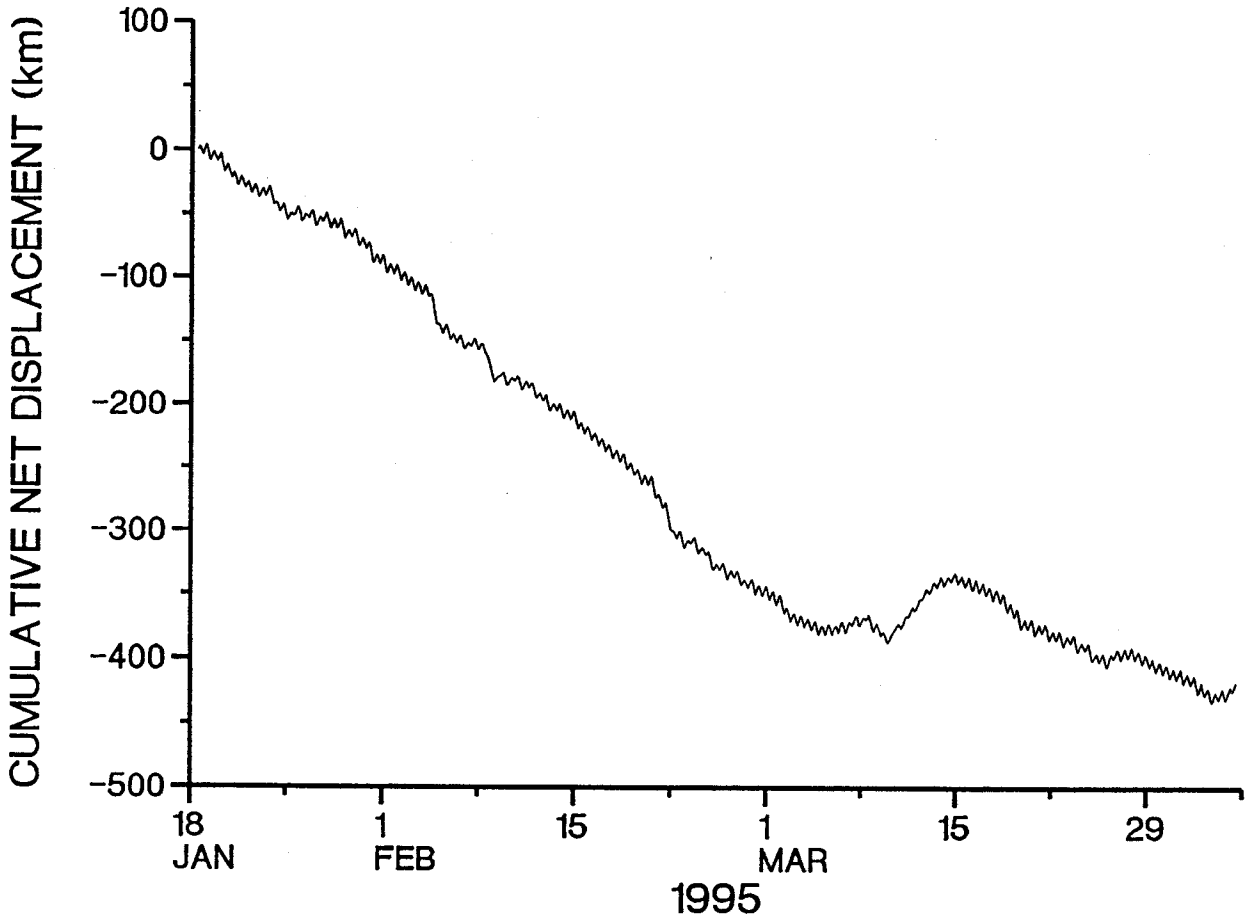


**Figure 7.** Cumulative net displacement of the along-channel current components in Long Key Channel, January 18 to April 4, 1995. Negative displacements indicate a flow of water out of Florida Bay.

of about ±21 cm at the study site in southern Florida Bay. The scatter of the mean, quantified by the standard deviation of the 76 standard deviation values, is 0.0225 db. The irregular rise and fall represents the interaction of the spring-neap tide progression of the semidiurnal constituents with the tropic-equatorial tide progression of the diurnal constituents. The 25-hour mean flow values indicate an average outflow of -7.1 cm $s^{-1}$, and the standard deviation of the 25-hour means is 7.2 cm $s^{-1}$. The 25-hour means indicate an inflow for a 5-day period in mid March, corresponding to the minimum in the standard deviations.

The mean current speed (25-hour blocks) through Long Key Channel as a function of the standard deviation (25-hour blocks) of hourly bottom pressures recorded at Station "W" in southwestern Florida Bay is shown in **Figure 9**. Correlation is highest when blocks of current speed are lagged six hours relative to the starting times of the 25-hour blocks of bottom pressures. The linear correlation coefficient of -0.52 is statistically significant at the 99.9% confidence level. The slope of the linear regression line is -167 cm $s^{-1}$ per db. Combining the slope with the 0.21 db mean value of the standard deviations, results suggest that tidal pumping drives a mean outflow of 35 cm $s^{-1}$. This is substantially larger than the 7 cm $s^{-1}$ that is observed. The difference may be related to other processes forcing water out of Florida Bay, or

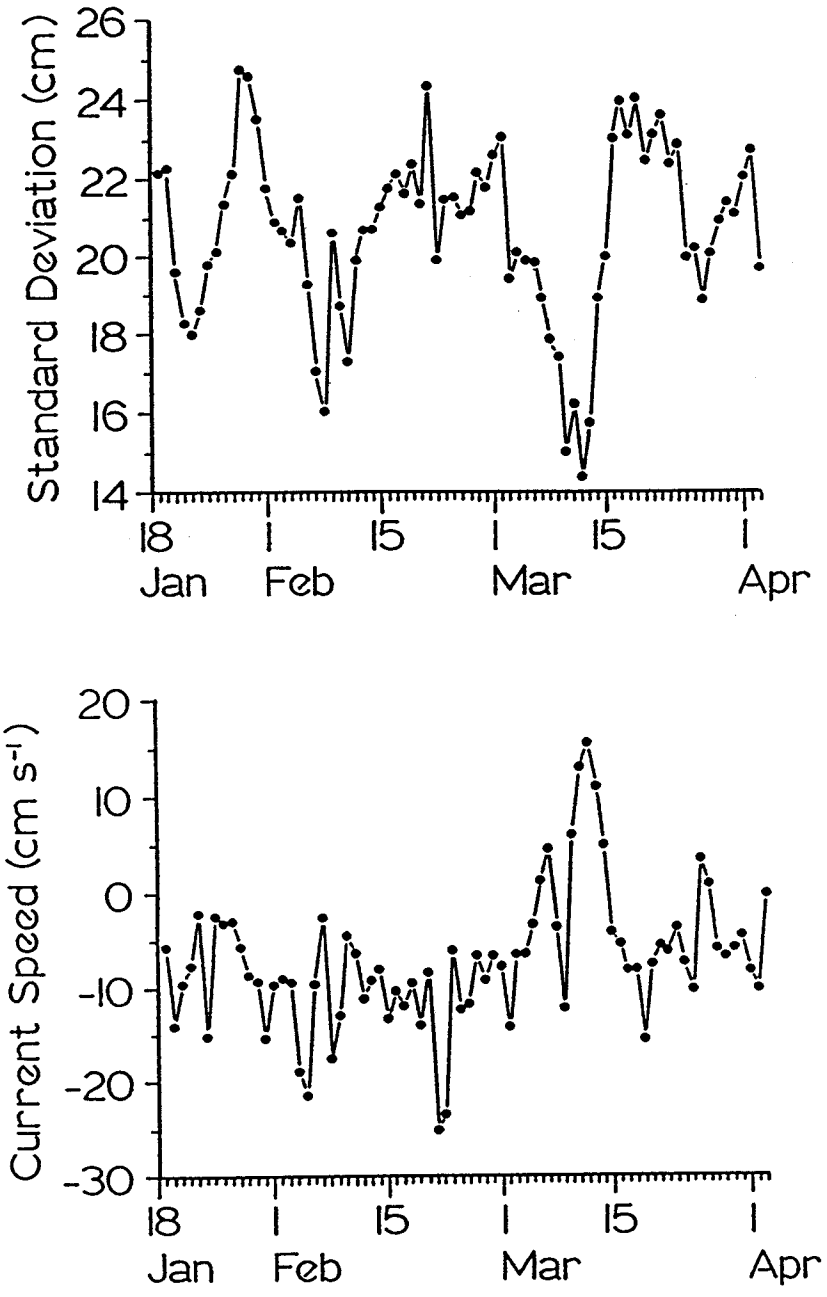


**Figure 8.** Standard deviations of 25-hour blocks of bottom pressure from Station "W" (top) and 25-hour averages of along-channel current speed at Station "L" in Long Key Channel (bottom), January 18 to April 4, 1995

it may indicate that scatter in the data has influenced the estimate of the slope. Using the 0.0225 db standard deviation of the 76 standard deviations of bottom pressure, it follows that tidal pumping explains variations on the order of ±3-4 cm $s^{-1}$ in the flow through Long Key Channel. From the scatter in the plot of 25-hour mean current speeds, and from the square of the correlation coefficient, it appears that variations in tidal pumping explain 25-30% of the variability in the averages computed from the current meter data.

**Figure 9.** Mean current speed (25-hour blocks) through Long Key Channel as a function of the standard deviation (25-hour blocks) of hourly bottom pressures recorded at Station "W" in southwestern Florida Bay.

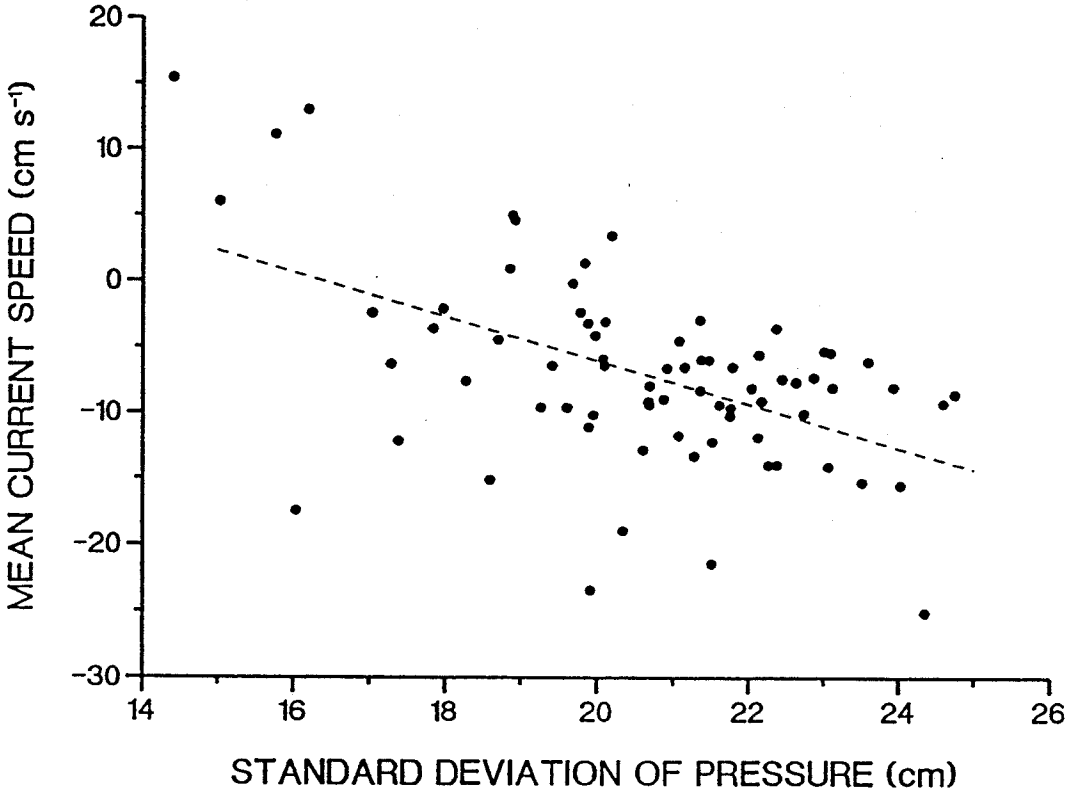


**Table 1.** Harmonic constants (amplitudes, η, in cm $s^{-1}$ for currents and in db for pressures; local phase angles, κ, in degrees) of the principal tidal constituents for the along-channel current components in Bahia Honda Channel and Long Key Channel and pressure data from study sites in the Content Keys and southwest Florida Bay.

| | | Tidal Constituent | | | | | |
|---|---|---|---|---|---|---|---|
| | | $M_2$ | $S_2$ | $N_2$ | $K_1$ | $O_1$ | $P_1$ |
| Bahia Honda Channel | η | 63.6 | 14.9 | 10.7 | 11.0 | 10.0 | 3.7 |
| | κ | 235.9 | 288.6 | 209.2 | 203.3 | 187.7 | 203.3 |
| Long Key Channel | η | 46.9 | 10.2 | 8.2 | 10.0 | 10.1 | 3.3 |
| | κ | 246.4 | 273.7 | 227.9 | 203.1 | 202.8 | 203.1 |
| Content Keys | η | 0.538 | 0.167 | 0.093 | 0.171 | 0.160 | 0.054 |
| | κ | 353.6 | 100.0 | 339.4 | 284.2 | 285.0 | 293.2 |
| Southern Florida Bay | η | 0.234 | 0.681 | 0.391 | 0.120 | 0.102 | 0.397 |
| | κ | 050.4 | 076.6 | 033.1 | 331.9 | 325.8 | 331.9 |

Results in this section investigated the west-to-east tide-induced transport of water across Florida Bay. We tested, and we conclude by accepting the hypothesis that outflow through the tidal channels exhibits a distinct fortnightly transition as tides alternate from spring to neap, or from tropic to equatorial conditions. Results from Bahia Honda Channel and from Long Key Channel support the idea that fluctuations in outflow are significantly related to tidal fluctuations in water level along the western side of the bay. Results suggest further that tidal pumping is the primary cause of the long-term net outflow through these channels. Significant scatter in the plots, however, indicate that undefined nontidal forcing also plays an important role in the Gulf-to-Atlantic transport of water through tidal channels.

**HYPOTHESIS #2: Tidal pumping is the principal transport mechanism in tidal channels of the Upper Keys, while a nontidal, quasi-steady outflow is the principal transport mechanism in the Middle and Lower Keys.**

**Introduction**

In this section we compare the relative importance of steady and time-varying salt, heat and mass transport through two tidal channels in the Middle and Lower Keys using historical data, and one tidal channel in the Upper Keys using new data. We test the hypothesis that tidal pumping is the principal transport mechanism in Tavernier Creek (Upper Keys), while a nontidal, quasi-steady outflow is the principal transport mechanism in Long Key Channel and Indian Key Channel (Middle Keys). We use salinity as a natural tracer, taking advantage of salinity differences between Hawk Channel and Florida Bay that should exist under both wet and dry season conditions.

**Data Base**

The data used for the analysis draws partially from historical data collected in 1992 and 1995-96 and includes data collected for a project funded by Everglades National Park. Specifically, we use time series of conductivity, temperature, current and pressure data recorded from study sites in three tidal channels in the middle and upper Florida Keys. Historical data include time series recorded in Long Key Channel (24° 47.867'N, 80°52.269'W) from October 12 to November 20, 1992 and Indian Key Channel (24°53.10'N, 80°40.60'W) from May 1 to July 24, 1995. Data from Tavernier Creek (25°00.32'N, 80°31.57'W) were recorded from December 7, 1995 to June 19, 1996 (see **Figure 10**).

Current speed and direction, temperature and conductivity were recorded hourly in Long Key Channel using an ENDECO Type 174SSM. Accuracies are ±2.6 cm $s^{-1}$, ±5° magnetic, ±0.2°C and ±0.55 mS $cm^{-1}$, respectively. The ENDECO senses current speed, direction, water temperature and conductivity every second. At the end of the one-hour sampling period, readings are averaged (currents are vector-averaged) and stored internally. The same four variables were recorded in Indian Key Channel and Tavernier Creek using General Oceanics Model 6011 Mark II current meters at accuracies of ±1.0 cm $s^{-1}$, ±2° magnetic, ±0.25°C and ±2.5 mS $cm^{-1}$, respectively. The current meters were suspended 1 to 2 m above the bottom on "gallows" type moorings. Total water depths at the sites were 3.5 m in Long Key Channel, 5 m in Indian Key Channel and 3 m in Tavernier Creek.

Pressure data were recorded in Tavernier Creek using a Brancker Model TG-205. Pressures were recorded in Long Key Channel and Indian Key Channel using a Sea Data TDR-3

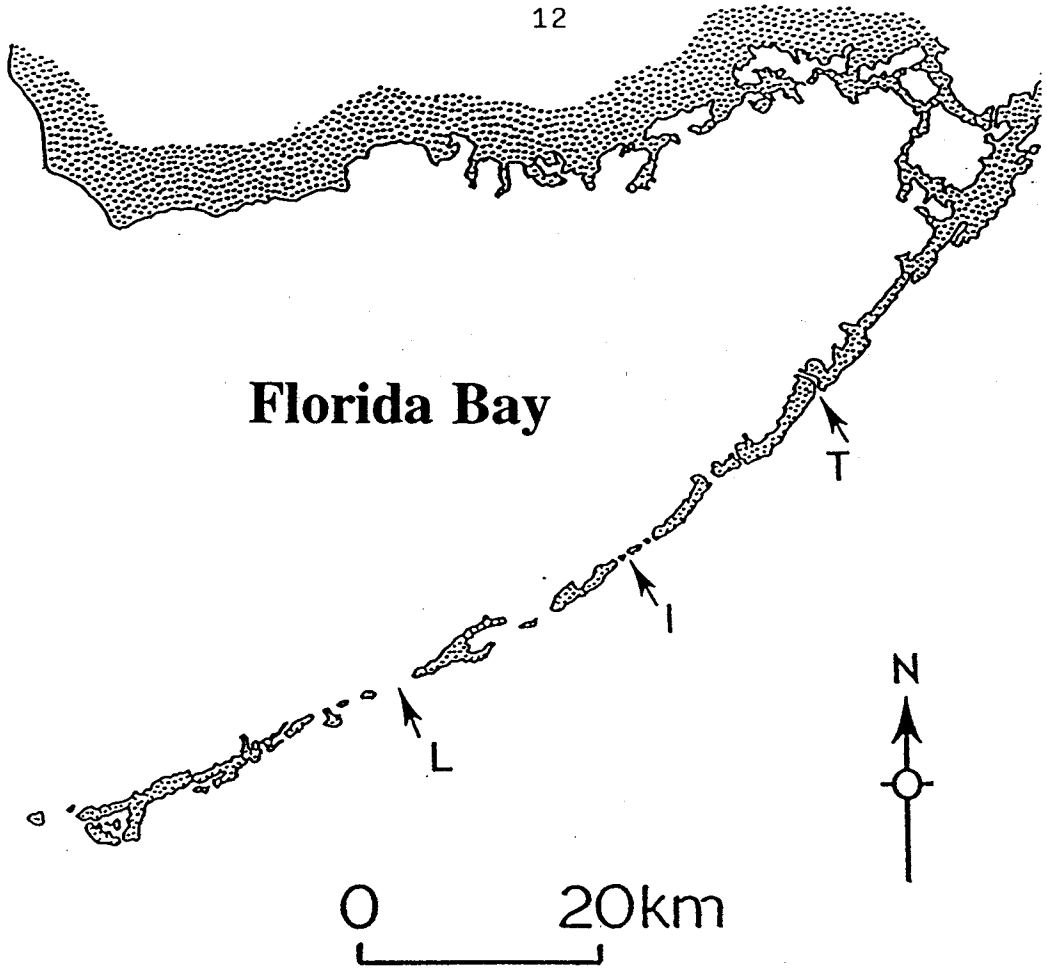


**Figure 10.** Map showing study sites in Long Key Channel ("L"), Indian Key Channel ("I") and Tavernier Creek ("T") where data were collected to investigate the relative importance of steady and time-varying transport through tidal channels.

recorder which has an accuracy similar to the Brancker recorder (see **Data** in the previous section). Both pressure recorders were moored on the bottom in a protective PVC housing.

**Methodology**

The steady and time-varying salt and heat transport in tidal channels are quantified using perturbation analysis, which decomposes salt content, heat content and volume transport into their mean and time-varying components.

Volume transport was calculated by assuming that the current profile is logarithmic, and that the measured current speed represents a one-meter width of the tidal channel. When a channel has been calibrated with anchor stations on either side of a reference station, lateral extrapolations provide additional information on the total volume transport. But without similar calibration data for water temperature and salinity, lateral extrapolation adds nothing to an investigation of salt and heat transport. The vertically averaged current speed, U, at the study site is given by

$$U = \frac{u_*}{k(Z-z_o)} \left[ Z \ln\left(\frac{Z}{z_o}\right) - (Z-z_o) \right],$$

where Z is the total water depth, k is the Kármán constant and $z_o$ is the roughness length. The friction velocity, $u_*$, is obtained by rearranging

$$u_{ref} = \frac{u_*}{k} \ln\left(\frac{z_{ref}}{z_o}\right),$$

where $u_{ref}$ is the current speed measured at the study site at a height $z_{ref}$ above the bottom. A roughness length of 0.5 cm was used in the calculations (Heathershaw and Langhorne 1988). Water depth is estimated from bottom pressure measurements using

$$Z = \frac{p}{\rho g},$$

where p is the bottom pressure, ρ is water density (assumed constant through the water column) and g is gravity. In practice, with gravity 9.79 m $s^{-2}$ and density approximately 1025 kg $m^{-3}$, the water depth in meters is approximately 0.98 times the pressure in decibars.

Time series of water temperature and conductivity are used to calculate water density (Millero and Poisson 1981) and salinity in practical salinity units (psu) (Perkin and Lewis 1980). We convert salinity, in kg of salt per kg of water, to salt content, in kg $m^{-3}$, by multiplying by water density, in kg $m^{-3}$. Then the product of the salt content and the volume transport for the channel, in $m^3$ $s^{-1}$, gives the local salt transport, in kg $s^{-1}$. Beginning with heat content, in Kcal $m^{-3}$, and density, in kg $m^{-3}$, we calculate heat and mass transport in a similar way.

Given time series of 2-dimensional (surface-to-bottom in the along-channel direction) volume transport, heat and salt content, we use perturbation analysis to quantify the quasi-steady and time varying transport of salt, heat and mass through selected tidal channels. In perturbation analysis, hourly observations of current speed (flood currents defined positive), heat and salt content and density are decomposed into the study mean, the low-frequency deviation about the mean and the high-frequency (tide-dominated) deviation about the low-frequency variation. This approach follows the suggestion of Pond and Pickard (1983), and it provides an important distinction between tidal and nontidal time-varying processes. The instantaneous heat transport and salt transport, calculated from observations made for the $i^{th}$ hour of the study ($v_ih_i$, $v_im_i$ and $v_is_i$, respectively) are then expanded to nine perturbation products, three of which have physical significance. For example, for the instantaneous salt transport:

$$t_{s,i} = \langle s\rangle\langle t\rangle + s_i'v_i' + s_i''v_i'',$$

where <s> and <v> are the study mean salt content and volume transport, s' and v' are the low-frequency fluctuations of salt content and volume transport, and s" and v" are the high-frequency fluctuations of salt content and volume transport. In most perturbation analyses, the $s_i'v_i'$ and $s_i''v_i''$ perturbation products are averaged to make them comparable to the <s><v> term. The averaging process can obscure considerable variability over tidal and low-frequency time scales, however, and useful information may be lost. In this report, we present not only the study mean values, but also plots that show the cumulative net salt, heat and mass transport. By accumulating transport values, subtle but persistent differences between flood and ebb contributions stand out clearly. For salinity, the cumulative net transport through the $k^{th}$ hour of the study is given by

$$T_{s,k} = \sum_{i=1}^{k} t_{s,i}.$$

**Results**

Results of the perturbation analyses appear in two forms. **Table 2** summarizes the mean salt, heat and mass transport values for each of the three channels under investigation. Salt and mass transport are given in kg $s^{-1}$, and heat transport is given in Kcal $s^{-1}$. Positive values represent transport into Florida Bay, and negative values indicate an export to Hawk Channel. **Figures 11-13** include plots of the cumulative volume transport, followed by plots of cumulative salt, heat and mass transport. The cumulative volume transport plots are similar in shape to the plots of cumulative total salt, heat and mass transport. Curve (a) represents transport by high-frequency (tide-dominated) exchanges, and curve (b) represents transport by low-frequency exchanges.

**Table 2** calls attention to three features of steady and time-varying salt transport through the three tidal channels we investigated. First, steady transport dominates time-varying transport in all cases. Second, there is no consistent relationship between the direction of the two time-varying terms. Finally, there is no consistent relationship regarding the relative importance of the two time-varying terms.

In each of the tidal channels studied, and for each of the three variables we could quantify using current and hydrographic data, transport by the mean flow is consistently larger--as much as four orders of magnitude larger--than transport by either low-frequency or tidal exchanges. Thus, we can immediately reject our hypothesis that tidal pumping is the most important transport mechanism in Tavernier Creek, but we must accept the same hypothesis for Long Key and Indian Key Channels. For example, salt transport through Long Key Channel calculated from the mean volume transport past the current meter (+0.048 $m^3$ $s^{-1}$) and the mean salt content (36.28 kg $s^{-1}$) is 1.746 kg $s^{-1}$. This is over two orders of magnitude larger than the -0.010 kg $s^{-1}$ transport associated with low-frequency variations in current and salinity, and the -0.005 kg $s^{-1}$ transport associated with tidal exchanges. Because of the relative importance of the mean flow, the net salt transport is into Florida Bay, even though both of the time-varying terms are exporting salt to Hawk Channel.

**Table 2** does show, however, that time-varying transport becomes more important in Tavernier Creek--at least for salt transport. Study-mean salt transport is less than an order of magnitude larger than either time-varying term. Heat transport by the mean outflow is nearly two orders of magnitude larger than heat transport by the time-varying terms, and study-mean mass transport is well over two orders of magnitude larger than the time-varying terms.

The direction of time-varying transport shows no consistent relationship from one channel to the next, nor from one variable to the next. Analysis of Tavernier Creek data shows that both low-frequency and high-frequency exchanges imported salt, heat and mass to Florida Bay. Similarly, salt transport by the time-varying processes were in the same direction in all three tidal channels. Comparison with results from the other two tidal channels, however, suggests that these patterns may have been fortuitous.

Inspection of the relative magnitudes of low-frequency and high-frequency transport reveals few consistencies. Only in Indian Key Channel are salt, heat and mass transport by low-frequency exchanges consistently smaller than transport by tidal exchanges. Because the direction of the net transport is inconsistent, it is difficult to assign any significance to the magnitude. In general, because the magnitude of the time-varying terms is so small, the steady

**Table 2.** Perturbation products of mean and time-varying salt, heat and mass transport. Sections A, B and C summarize calculations made for Long Key Channel (October 12 to November 20, 1992), Indian Key Channel (May 1 to July 24, 1995) and Tavernier Creek (December 7, 1995 to June 19, 1996). Salt and mass transport values are in kg $s^{-1}$; heat transport is in kcal $s^{-1}$. The symbols M, m' and m" represent the study-mean density (in kg $m^{-3}$), the low-frequency deviation of density about the mean, and the high-frequency (tide-dominated) deviation of density relative to the low-frequency variation. The symbols S, s' and s" are defined similarly for salt content (in kg $m^{-3}$); and the symbols H, h' and h" are defined similarly for heat content (in kcal $m^{-3}$).

| | S | s' | s" | H | h' | h" | M | m' | m" |
|---|---|---|---|---|---|---|---|---|---|
| Long Key Channel | | | | | | | | | |
| T | +1.746 | | | +14.719 | | | +49.250 | | |
| t' | | -0.010 | | | -0.039 | | | +0.006 | |
| t" | | | -0.005 | | | +0.005 | | | -0.006 |
| Indian Key Channel | | | | | | | | | |
| T | -13.436 | | | -113.855 | | | -356.459 | | |
| t' | | +0.089 | | | +0.049 | | | +0.053 | |
| t" | | | +0.240 | | | -0.110 | | | +0.231 |
| Tavernier Creek | | | | | | | | | |
| T | -3.048 | | | -29.626 | | | -100.071 | | |
| t' | | +0.641 | | | +0.466 | | | +0.369 | |
| t" | | | +0.949 | | | +0.236 | | | +0.683 |

transport is dominant regardless of how the time-varying transport terms interact.

The study-mean values listed in **Table 2** tell only part of the transport story, however, because time-varying transport can change significantly over the course of the study. Over selected shorter time periods, transport by tidal or low-frequency exchanges can become temporarily dominant. To investigate time-varying transport over time periods of days to weeks, we present plots of cumulative salt, heat and mass transport. These plots are directly related to the values listed in **Table 2.** Slopes of the cumulative transport curves are virtually identical to the mean values summarized in the table. If the import or export of salt, heat and mass were steady in time, then plots of cumulative transport would be straight lines. It is apparent, however, that during any given study the accumulation curve can deviate significantly from the slope. This shows graphically that transport by tidal exchanges, for example, can vary significantly with time as a result of changes in regional hydrography or differing tidal conditions.

a. Long Key Channel

**Figure 11** shows the cumulative volume transport, followed by the cumulative tidal

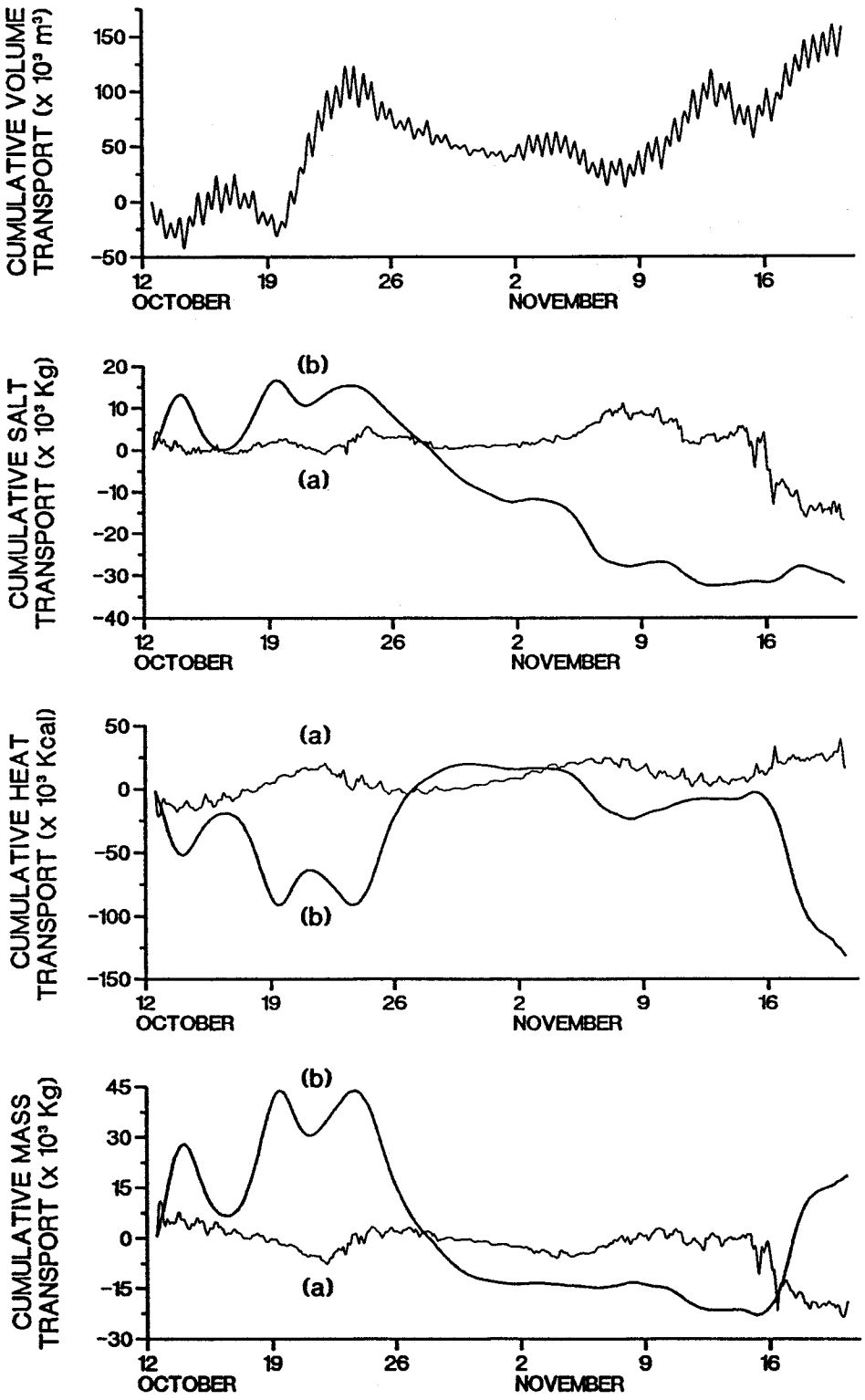


**Figure 11.** Cumulative net transport of volume (top plot), salt (second from top), heat (third from top) and mass (bottom) through a 1-meter-wide water column in the middle of Long Key Channel, October 12 to November 20, 1992. Curves (a) and (b) show transport by tidal and low-frequency exchanges, respectively. Ascending curves indicate transport into Florida Bay.

(curve a) and low-frequency (curve b) transport of salt, heat and mass through a 1-m-wide water column at the study site in Long Key Channel from October 12 to November 20, 1992. Ascending curves indicate a transport into Florida Bay from Hawk Channel. During this study period, the net volume transport was into Florida Bay. It follows that the total salt, heat and mass transport was into the bay, regardless of temporal variations in salt content, heat content and density. Curve (a) in the second plot shows that during the first four weeks of the study salt transport by tidal processes was minimal. This suggests weak salinity gradients between Florida Bay and Hawk Channel, because the ebb and flood of the tide were strong during this time. After a minor net import of salt to Florida Bay during the first week of November, tidal transport was out of the bay for the last two weeks of the study. By the end of the nearly seven week study, the cumulative net transport of salt by tidal exchanges was $-16 \times 10^3$ kg. The low-frequency salt transport shows reversals occurring over time scales of a few days for approximately the first 2 weeks of the study, resulting in a transport of about $+15 \times 10^3$ kg of salt. During the next three and a half weeks of the record, a quasi-steady transport of salt out of Florida Bay averages approximately -0.02 kg $s^{-1}$. Salt transport was minimal during the final 10 days, and by the end of the study, the cumulative net transport of salt by low-frequency exchanges was $-32 \times 10^3$ kg, about double the export by the ebb and flood of the tide.

The third plot in **Figure 11** shows that heat transport due to tidal exchanges is relatively inactive compared to transport by low-frequency processes. There are indications of diurnal and semidiurnal variations in the tidal transport curve. Curve (a) also varies over longer time periods, as Florida Bay warms and cools more rapidly than Hawk Channel in response to changes in weather conditions. Tidal fluctuations are generally around $\pm 10 \times 10^3$ Kcal while low-frequency fluctuations range between $\pm 30\text{-}40 \times 10^3$ Kcal. Curve (b) shows large fluctuations occurring over time scales of 2-7 days, with heat transport over any 2-3-day time period ranging between $\pm 30\text{-}100 \times 10^3$ Kcal. Little net heat transport is indicated by the end of the fifth week. During the last five days of the record, a relatively rapid heat export averages 0.3 Kcal $s^{-1}$.

Tide-induced mass transport (bottom plot, curve (a)) is largely a mirror image of the tidal transport of heat through most of the record, indicating that water temperature controls density changes during this time period. Tidal fluctuations are on the order of $\pm 3\text{-}5 \times 10^3$ kg while low-frequency, weather-related variations are generally $\pm 8\text{-}12 \times 10^3$ kg. The cumulative net mass transport by tidal exchanges was $-18 \times 10^3$ kg over the 39-day study. Large fluctuations in the low-frequency mass transport occur over time scales of 2-3 days during the first 2 weeks of the study and result in a net import to Florida Bay of $+44 \times 10^3$ kg. During the third week, low-frequency mass transport was out of the bay, averaging -0.098 kg $hr^{-1}$. While this relatively rapid mass transport is an order of magnitude greater than the average low-frequency mass transport it is still three orders of magnitude less than the steady mass transport. Little mass transport occurred due to low-frequency processes over the next three weeks, but was followed by a rapid import of $+42 \times 10^3$ kg over the final 5 days of the study. The cumulative net mass transport by low-frequency exchanges over the study period was nearly $+20 \times 10^3$ kg.

b. Indian Key Channel

**Figure 12** contains the cumulative transport curves for Indian Key Channel from May 1 to July 24, 1995. Note that the y-axis transport scales are 1-2 orders of magnitude greater than those used for plotting transport through Long Key Channel. This is partly because of the longer study period for Indian Key Channel, but also because of the greater salt, heat and mass transport rates through this channel. The cumulative volume transport shown in the top plot indicates a relatively steady nontidal outflow. This is consistent with **Table 2**, which shows an export of

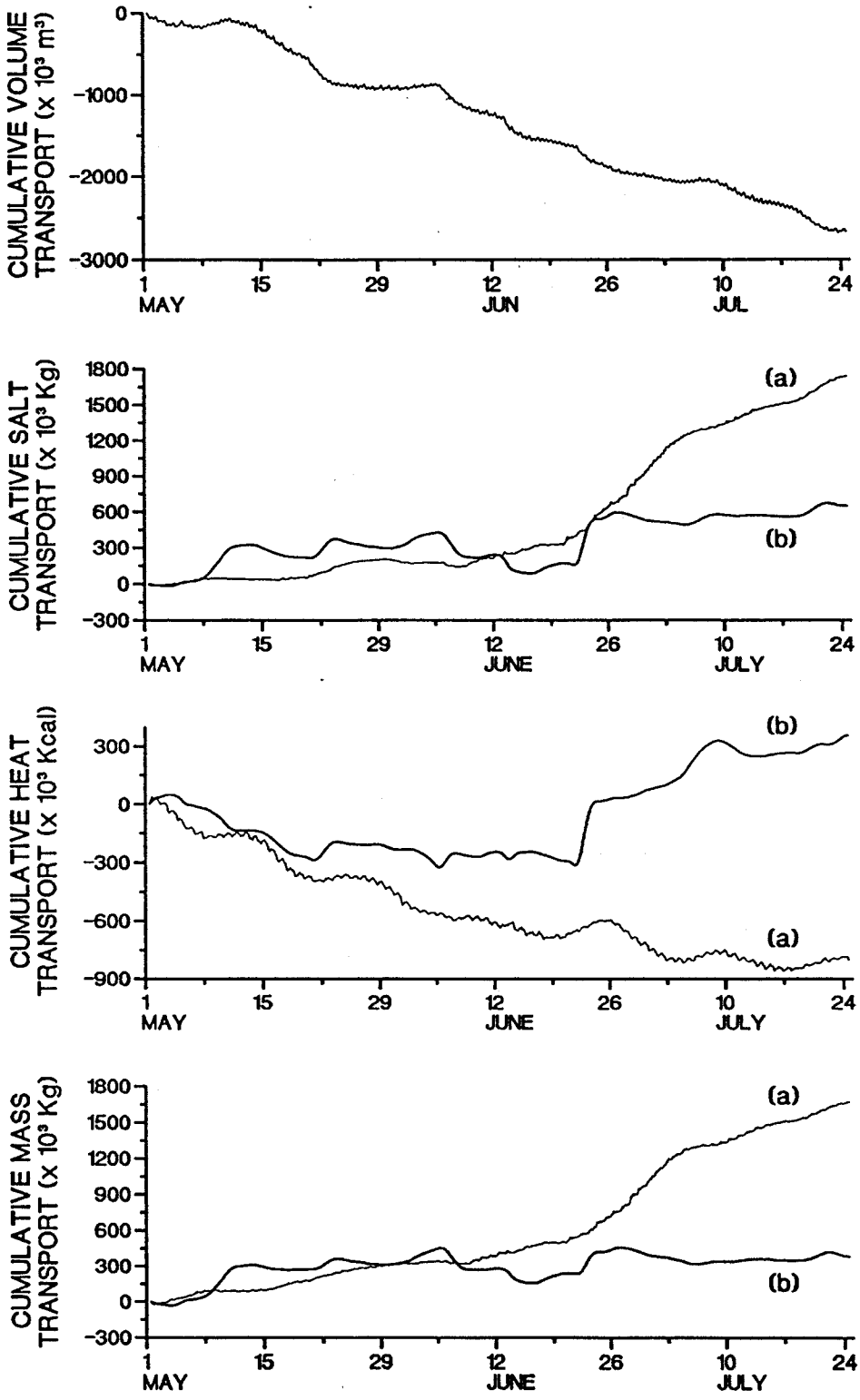


**Figure 12.** Cumulative net transport of volume (top plot), salt (second from top), heat (third from top) and mass (bottom) through a 1-meter-wide water column in the middle of Indian Key Channel, May 1 to July 24, 1995. Curves (a) and (b) show transport by tidal and low-frequency exchanges, respectively. Ascending curves indicate transport into Florida Bay.

salt, heat and mass to Hawk Channel by the mean flow. Curve (a) in the second plot shows that salt transport by tidal exchanges is relatively small during the first half of the study. Over the last 5 weeks the rate of salt transport into the bay increases steadily. By the end of the 12-week study the import of salt to Florida Bay by tidal processes is +1800 x $10^3$ kg. The low-frequency transport of salt is irregular and relatively small throughout study. The net gain of salt by Florida Bay due to low-frequency exchanges is +800 x $10^3$ kg, or roughly a third of that transported into the bay by tides. The strong tidal transport of salt into the bay during the final four weeks of the study coincides with negligible low-frequency transport. This indicates that significant salinity gradients existed between Florida Bay and Hawk Channel at a time when nontidal currents were minimal.

The third plot in **Figure 12** shows an irregular heat loss from Florida Bay by tidal exchanges at a time when low-frequency transport processes were importing heat to the bay. Again, heat loss by high-frequency exchanges occurs over both tidal and low-frequency time scales. The cumulative net heat loss from Florida Bay by tidal exchanges was approximately 800 x $10^3$ Kcal. The low-frequency heat transport curve shows a gradual heat loss from the bay for the first 8 weeks, followed by a net transport of heat into the bay. The total heat gain to Florida Bay was about 400 x $10^3$ Kcal. This is about half the heat lost due to tidal exchanges.

The curves for cumulative tidal and low-frequency mass transport through Indian Key Channel show a slow transport into Florida Bay for the first five weeks of the study period. During the sixth week, the curves diverge as tidal mass transport increases sharply, while low-frequency transport is minimal. By the end of the study, mass transport by tidal exchanges is about +1700 x $10^3$ kg, which is four times that imported by low-frequency exchanges.

c. Tavernier Creek

**Figure 13** shows the transport of volume, salt, heat and mass through Tavernier Creek from December 7, 1995 to June 19, 1996. Cumulative volume transport indicates a net outflow, although the direction changed for a five-week period from mid April through late May. Both tidal and low-frequency transport of salt are into Florida Bay through most of this six and a half month study period. The rate of salt imported to the bay by tidal processes decreases from +4.9 x $10^3$ kg during the first eleven weeks of the study to +0.7 x $10^3$ kg over the last four weeks. By the end of the the study, over 1600 x $10^3$ kg of salt have been transported into Florida Bay. The low-frequency transport curve indicates that the import of salt into the bay occurs relatively steadily, except for the rapid increase during the last week in April and first 3 weeks in May. Over the last month of the study period salt transport by low-frequency processes is minimal. The cumulative net transport of salt into Florida Bay by low-frequency processes was about 11 x $10^6$ kg, or about 70% that imported by tidal exchanges.

Curves for cumulative tidal and low-frequency heat transport through Tavernier Creek show a nearly equal transport into Florida Bay through the first 20 weeks of the study (third plot from top). After that time tidal transport is minimal. Meanwhile, low-frequency transport into the bay increases dramatically for four weeks during May. During the final month of the study, low-frequency transport is negligible.

The bottom plot of **Figure 13** shows tidal and low-frequency mass transport into Florida Bay through most of the study period. The rate of tidal transport into the bay decreases gradually from 0.9 kg $s^{-1}$ during the first 10 weeks to 0.2 kg $s^{-1}$ over the last month of the study. Low-frequency mass transport into the bay occurs in relatively short bursts, with most of the transport occurring during four periods in mid December, early January, late February and early May.

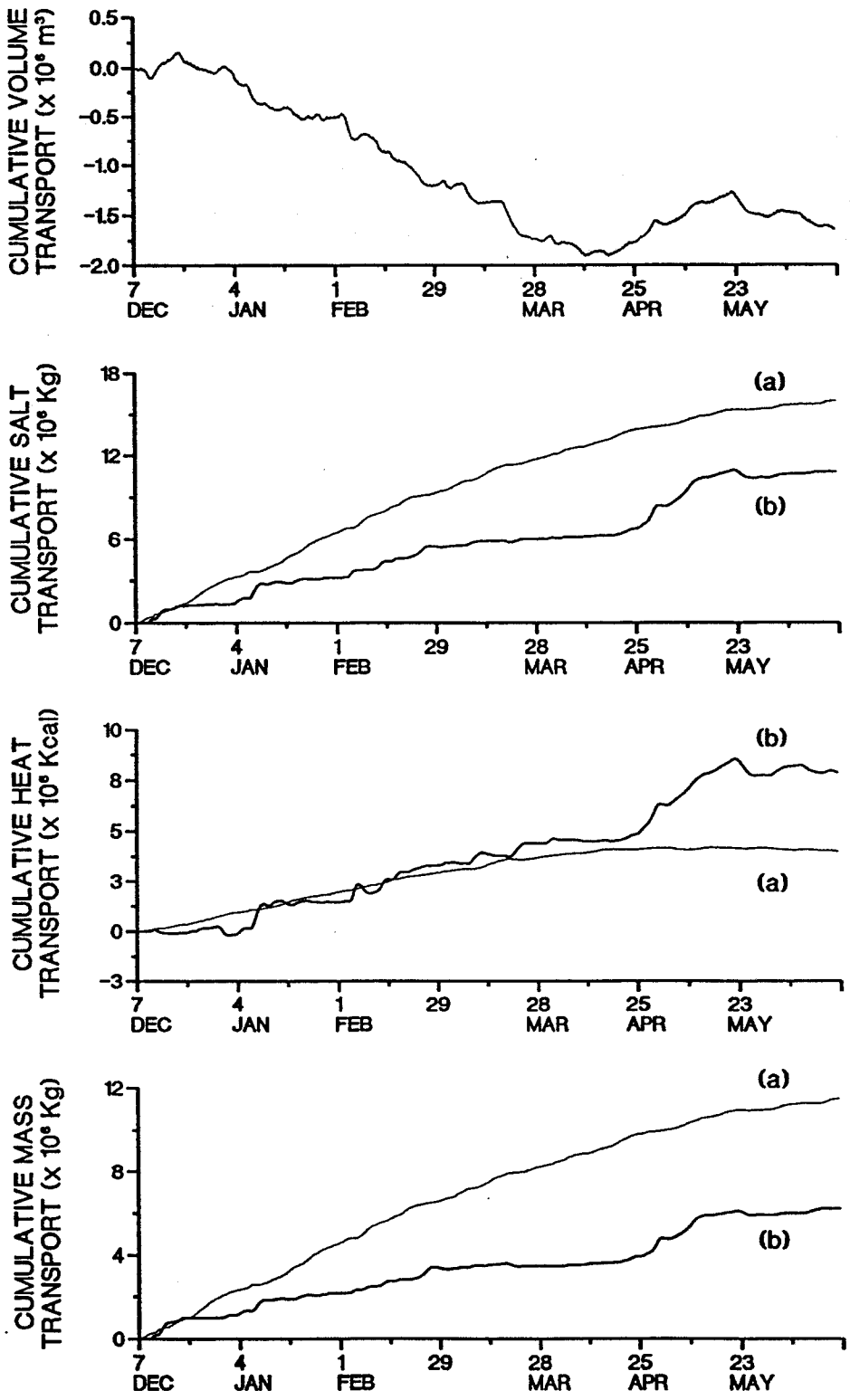


**Figure 13.** Cumulative net transport of volume (top plot), salt (second from top), heat (third from top) and mass (bottom) through a 1-meter-wide water column in the middle of Tavernier Creek, December 7, 1995 to June 19, 1996. Curves (a) and (b) show transport by tidal and low-frequency exchanges, respectively. Ascending curves indicate transport into Florida Bay.

**Discussion**

It is important to distinguish clearly between what perturbation analysis can and cannot reveal about transport through the tidal channels separating the Florida Keys. The steady transport terms, ST for salt transport for example, are straightforward. During the time of each study, this is the average salt content carried by the average volume transport. The time-varying terms can be more confusing, because there are three prerequisites. All must be met, but they can vary significantly in terms of their relative importance. The first is that there must be a time-varying current. In our analysis, we distinguish only between the tidal current and the low-frequency, nontidal current. The second prerequisite is that there must be hydrographic differences in the water on either side of the tidal channel. For example, because the water in Florida Bay is shallower than the water in Hawk Channel, we might expect that Florida Bay water would warm and cool more quickly, or that it would be somewhat less saline during the wet season. Third and finally, mixing must occur on either or both halves of the tidal or low-frequency exchanges to ensure that the water moving through the tidal channel on any half cycle does not simply turn around and come back on the following half cycle. If all three conditions are met, then perturbation analysis will quantify the time-varying transport, and results can be compared in magnitude and direction with the steady transport.

Confusion may arise once time-varying transport has been quantified, because variations in transport cannot be traced back, individually and unambiguously, to variations in volume transport, mixing or hydrographic gradients. Perturbation analysis is useful for characterizing effects, but it is of limited usefulness for understanding causes. For example, **Figure 13** shows little cumulative salt transport by tidal exchanges during the first half of the study. Presumably, there were strong tidal currents during this time period. Also, although tidal mixing may fluctuate between spring tide and neap tide conditions, it is unlikely that mixing remains low for extended periods of time. Thus, it is likely that hydrographic gradients were minimal from mid October to early November, but the available data do not confirm this. It is noteworthy that during this same time low-frequency transport was relatively active. This is probably a direct effect of low-frequency variations in volume transport, which are independent of both hydrographic gradients and mixing on opposite sides of the channel.

Using the same line of reasoning, the minimal low-frequency transport noted from early November through the end of the study is probably a result of minimal low-frequency volume transport through the channel, although the mixing associated with low-frequency exchanges may have been slight as well. Salinity differences on either side of the channel were probably significant, because tidal transport during this same time period indicates a significant export of salt to Hawk Channel.

It is clear that tidal transport of salt, for example, says nothing about the tidal transport of heat. The relationship of either salt transport or heat transport to mass transport is significant, however, because density is a function of both salinity and temperature. Again, using the Long Key Channel data as an example (**Figure 13**), we note that during late October low-frequency exchanges through the channel were exporting salt, but they were importing heat. At the very end of the study, salt transport by low-frequency exchanges were minimal, while heat was being exported to Hawk Channel rapidly. The important point here is that results of a perturbation analysis of one variable may have no relationship to results stemming from measurements of another variable.

An alternate way to express the means of the time-varying transport terms (**Table 2**) involves calculating the slope of the least-squares linear regression line. It is clear from **Figures**

**11-13** that the best-fit line through the cumulative transport curves may differ from the lines that connect the end points of the curves (equivalent to the arithmetic average). For example, the mean of the low-frequency mass transport values calculated from the Long Key Channel data (**Figure 11**, bottom) is +0.006 (see **Table 2**). The least squares regression line, on the other hand, suggests that a better value for the low-frequency mass transport would be -0.138 kg $s^{-1}$. In general, the differences between the arithmetic means of the hourly values and the slopes of the least-squares regression lines calculated from the cumulative transport values are subtle. In some cases, however, the magnitude can change by a significant percent. This example shows that the algebraic sign can also change.

**HYPOTHESIS #3: Florida Bay water retains its hydrographic characteristics in near-bottom layers as it is transported across Hawk Channel, and it can be detected through its hydrographic properties at the reef tract.**

### Introduction

In this section we combine new and historical hydrographic data to describe salinity gradients across Hawk Channel from Long Key Viaduct to the reef tract. We use salinity as a natural tracer on consecutive half tidal cycles to determine how far into Hawk Channel Florida Bay water penetrates on the ebb tide. We examine salinity cross-sections to determine if Florida Bay water can be detected at the reef tract. The analysis is based on historical data collected in 1991-92 and new data collected in March 1997.

### Data Base

The data base used for our analysis of Hawk Channel shelf hydrography consists of Sea-Bird SeaCat SBE-19 CTD profiles. Historical data were provided by the SEAKEYS SeaCat (Keys Marine Laboratory on Long Key); new data were provided by the Harbor Branch SeaCat. The two instruments are virtually identical, although the SEAKEYS instrument contains sensors that were not used in our hydrographic study. Calibration data are generally not taken with SeaCat casts, because the conductivity sensor has such slow and slight drift. This was confirmed by factory recalibration work done on both the SEAKEYS and the Harbor Branch instruments.

The resolution of the temperature sensor is 0.001°, and the resolution of the conductivity sensor is 0.0001 Siemens/meter (S $m^{-1}$). This permits the SeaCat profiler to record salinity to the nearest 0.0001‰. It is noteworthy that the coefficients appearing in the 1978 practical salinity scale (Perkin and Lewis, 1980; Lewis, 1980) have only three significant figures, thus permitting salinity calculations to the nearest 0.001‰. Whether we let the SeaCat profiler make the salinity calculations, or whether we use the SeaCat temperature and conductivity to make our own salinty calculations, the resulting values are more than accurate enough for characterizing Hawk Channel salinity, where across-channel differences may be several parts per thousand. Note that for purposes of this report the terms "practical salinity units" and "parts per thousand (‰)" are used interchangeably.

Surface-to-bottom SeaCat profiles were taken from Long Key Channel to the reef tract, west-southwest of Tennessee Reef (**Figure 14**). Usually, 11 profiles were taken on each transect (one per 0.5 nautical mile). In some cases rough seas prohibited occupying one or more of the stations at the seaward end of the transect, and as few as eight stations were obtained on one occasion.

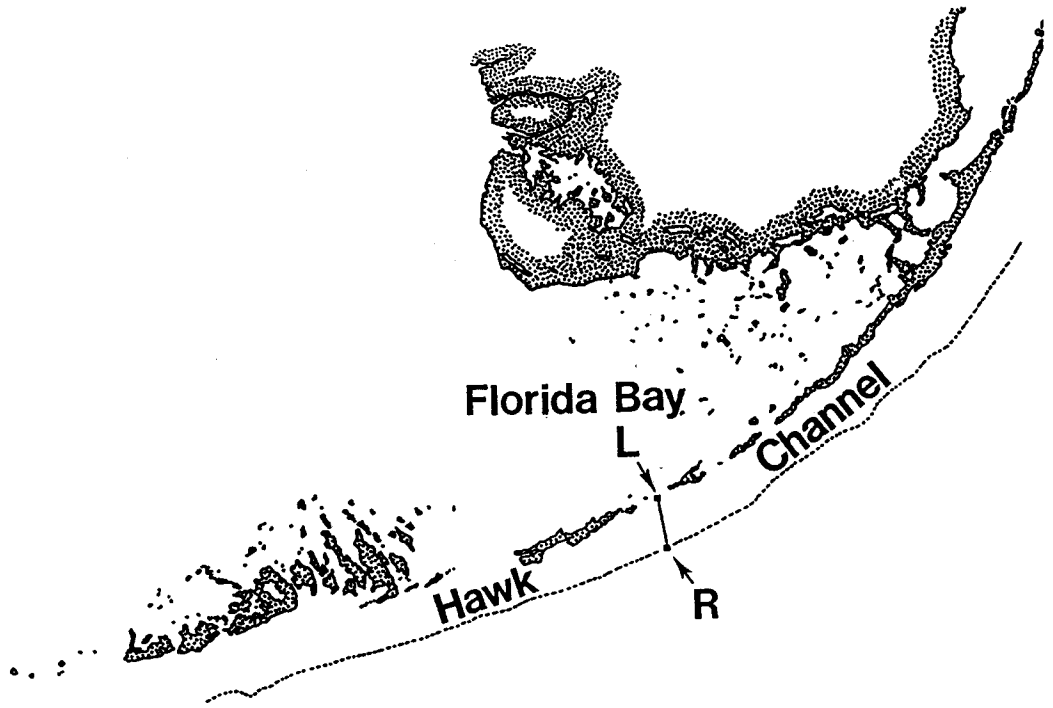


**Figure 14.** Map showing the location of the hydrographic transect across Hawk Channel from Long Key Viaduct (marked "L") to the reef tract southwest of Tennessee Reef ("R").

Across-shelf hydrographic transects are available from 8 time periods. Data were collected during adjacent half tidal cycles on February 7, 1991; May 2, 1991; May 23, 1991; June 14, 1991; August 20, 1991; November 1, 1991; January 9, 1992; and March 19, 1997. Spacing the transects throughout the year provided information that reflected a variety of wind and rainfall conditions.

**Methodology**

Hawk Channel cross-sections of salinity were constructed by plotting surface-to-bottom salinity profiles to the nearest 0.5 or 1.0‰, then contouring the isohalines. Salinity cross-sections were constructed with data taken at times of predicted slack water (Schureman, 1958) for Long Key Channel. The cross-section at slack water following the ebb will show how far into Hawk Channel Florida Bay water penetrated. The cross-section at slack water following the flood will show the extent to which Florida Bay water retreated into Florida Bay through Long Key Channel. A third cross-section was constructed from salinity differences throughout the cross-section. The difference cross-section shows which parts of Hawk Channel alternately have, then do not have Florida Bay water over tidal time scales.

Using salinity as a natural tracer in this way raises three issues. We note them here in passing, then return to them in the discussion section. First, this approach assumes that the hydrographic transect remains within the plume of Florida Bay water. In reality, however, we cannot be sure that in some cases the plume was swept off to the east or west by the current in Hawk Channel. Second, the approach depends upon a measurable salinity difference between Hawk Channel water and Florida Bay water. In fact, some of our transects suggest that no salinity differences existed, making salinity useless as a natural tracer. Third, this technique can

be influenced greatly by effects of diurnal inequalities in the flood and ebb currents. Studies of tidal currents in Long Key Channel have shown that diurnal inequalities can be significant. In this case, however, a careful interpretation of the data can take this into account.

The strength of the technique lies in the ease with which data can be obtained and interpreted. With appropriately qualified interpretation, this approach provides useful information regarding how far into Hawk Channel Florida Bay water can penetrate on any single ebb half of the tidal cycle.

**Results**

To put results in perspective, we begin with a time series of salinity recorded in Long Key Channel during an approximately 11-month time period from late August 1994 to late July 1995 (**Figure 15**). Salinity was calculated from hourly observations of conductivity and temperature made at about mid depth and near the mid point of the channel (the square marked "L" in **Figure 14**). The study site is well positioned to document salinity differences between Florida Bay (recorded during the latter part of the ebb half of the tidal cycle) and Hawk Channel (recorded during the latter part of the flood). The presence or absence of salinity differences such as these are directly related to the value of salinity as a natural tracer for tide-induced exchanges.

The plot shows time periods with large fluctuations in salinity, as well as time periods with small and even negligible variations in salinity. Largest salinity fluctuations occur in

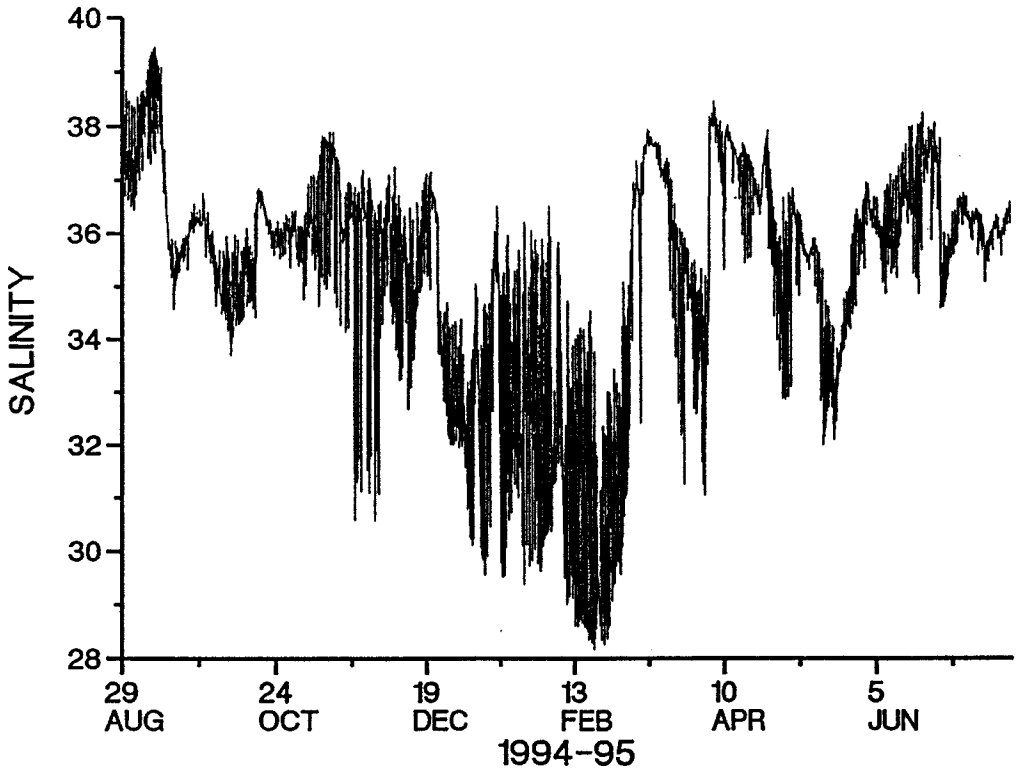


**Figure 15.** Salinity recorded in Long Key Channel August 29, 1994 to July 24, 1995.

midwinter months. This is normally the dry season, but current meter data recorded at the study site during this time indicate that low salinity water from Florida Bay was moving through Long Key Channel during the ebb. For relatively short time periods throughout the study (e.g., early March and at the very end of the record), either very weak tidal exchanges or very small salinity differences result in negliglble fluctuations at the study site in Long Key Channel.

February 7, 1991

**Figure 16** shows salinity cross-sections obtained at slack water after the ebb ("SAE," top), from 1115-1220 EST, and at slack water after the flood ("SAF," middle), from 1550-1735 EST on February 7, 1991. For this pair of transects, the diurnal inequality did not seem to be a factor: The exhaling of Florida Bay water on the ebb was approximately equal and opposite to the inhaling of water from Hawk Channel on the following flood. Strongest ebb currents preceding SAE were -20 cm $s^{-1}$ (according to tidal predictions), and strongest flood currents preceding SAF

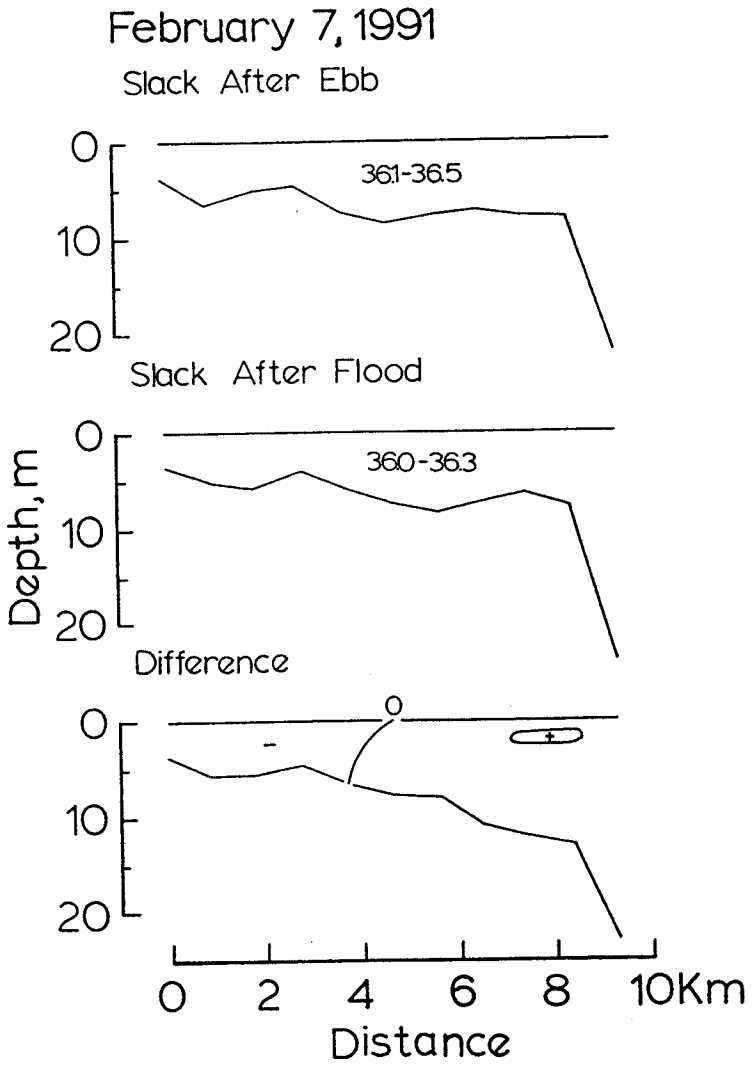


**Figure 16.** Salinity cross-sections from data collected February 7, 1991.

were +21 cm $s^{-1}$. The figure is useful for introducing the methodology, but it does not provide an example of how salinity can be used as a natural tracer to track the seaward movement of water toward the reef tract. Either because freshwater gains by rainfall were similar to freshwater losses due to evaporation, or because strong onshore winds were temporarily reversing the nontidal outflow through Long Key Channel, salinity gradients were minimal. All salinity readings on the SAE were within the range of 36.1 to 36.5‰, and all salinity readings on the SAF were within the range of 36.0 to 36.3‰. Thus, the salinity differences (bottom) are minimal and do not provide useful information relating to the movement of Florida Bay water.

May 2, 1991

**Figure 17**, however, taken from data obtained in early May at the end of the dry season, is a good example of how salinity can be used as a natural tracer. The salinity cross-section obtained during the SAE shows a plume of high salinity water extending seaward from Long Key Viaduct approximately half way across Hawk Channel. At the landward side of the cross-section,

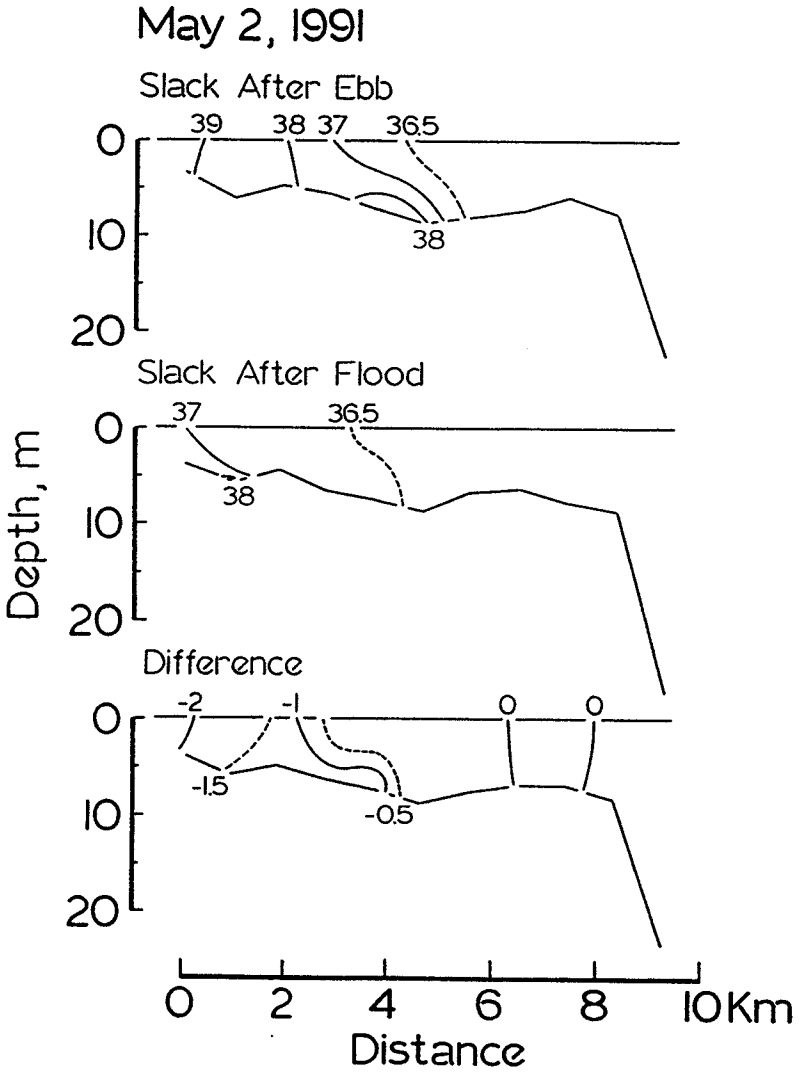


**Figure 17.** Salinity cross-sections from data collected May 2, 1991.

the water column is relatively well mixed, and isohalines are nearly vertical. Across the middle of Hawk Channel, however, there is indication of vertical stratification as high-salinity water continues seaward in the lower half of the water column. Salinity data collected during the SAF show that the high salinity water has either been forced back into Long Key Channel, or it has moved laterally--snipped off by the along-channel current in Hawk Channel. Current meter data from Hawk Channel are not available to explore this in detail, but as noted above this is a possibility in all of our pairs of salinity cross-sections. Whatever the underlying causes, the salinity difference cross-section shows that in surface layers the innermost 2 km of Hawk Channel is alternately influenced by Florida Bay water and then Hawk Channel water. In near-bottom layers, the impacted part of Hawk Channel extends about 5 km from Long Key Viaduct. Again, unequal maximum ebb and flood current speeds do not seem to be a factor. Strongest ebb speeds preceding the slack at about 0800 EST were -34 cm $s^{-1}$, while strongest flood speeds preceding the slack at about 1315 EST were +32 cm $s^{-1}$.

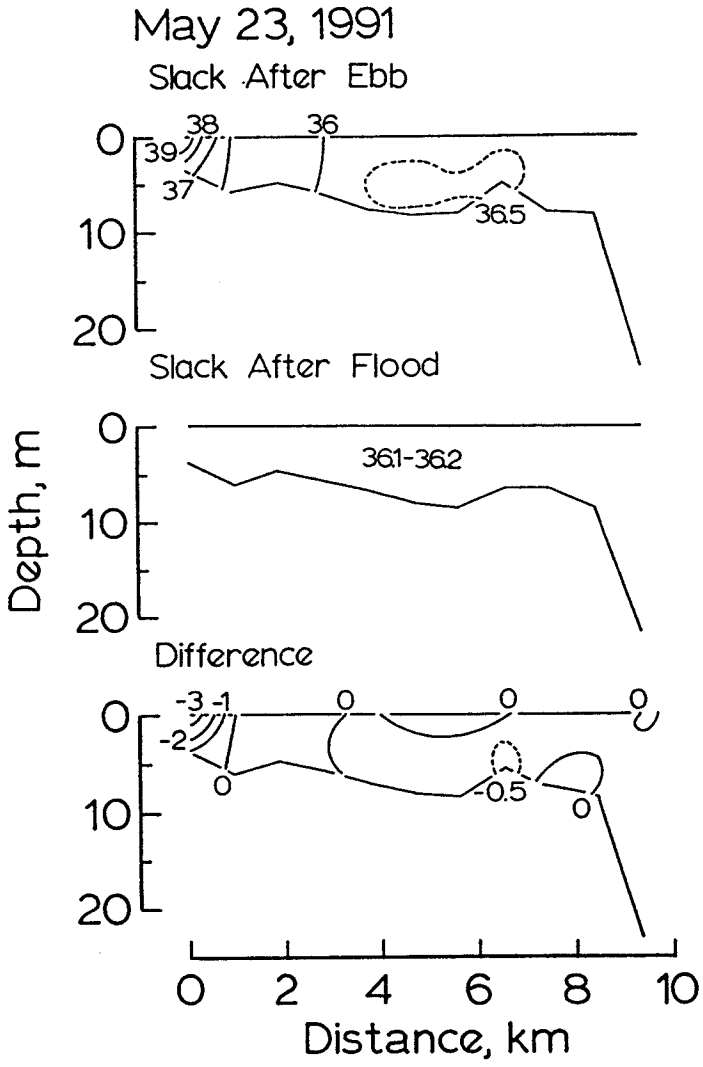


**Figure 18.** Salinity cross-sections from data collected May 23, 1991.

May 23, 1991

Hydrographic data from May 23, 1991 (**Figure 18**) provide an example of Florida Bay water penetrating a short distance into Hawk Channel on the ebb, then disappearing completely from the transect on the following ebb. Ironically, this occurred for a tidal cycle that included a relatively strong ebb (-57 cm $s^{-1}$) and a relatively weak flood (+32 cm $s^{-1}$). Again, however, it is not clear whether hypersaline Florida Bay water was drawn back into Florida Bay, or whether the plume was transported perpendicular to the transect by the nontidal along-channel flow in Hawk Channel. Taking the 36‰ isohaline as the boundary separating Florida Bay water and Hawk Channel water, the SAE plot at the top of the figure suggests that Florida Bay water penetrated little more than 1 km into Hawk Channel. For the purpose of tracking Florida Bay water, the 0 and 0.5‰ isohalines on the difference plot have little relevance.

June 14, 1991

Intense solar heating at the time of the summer solstice confines a shallow lens of slightly

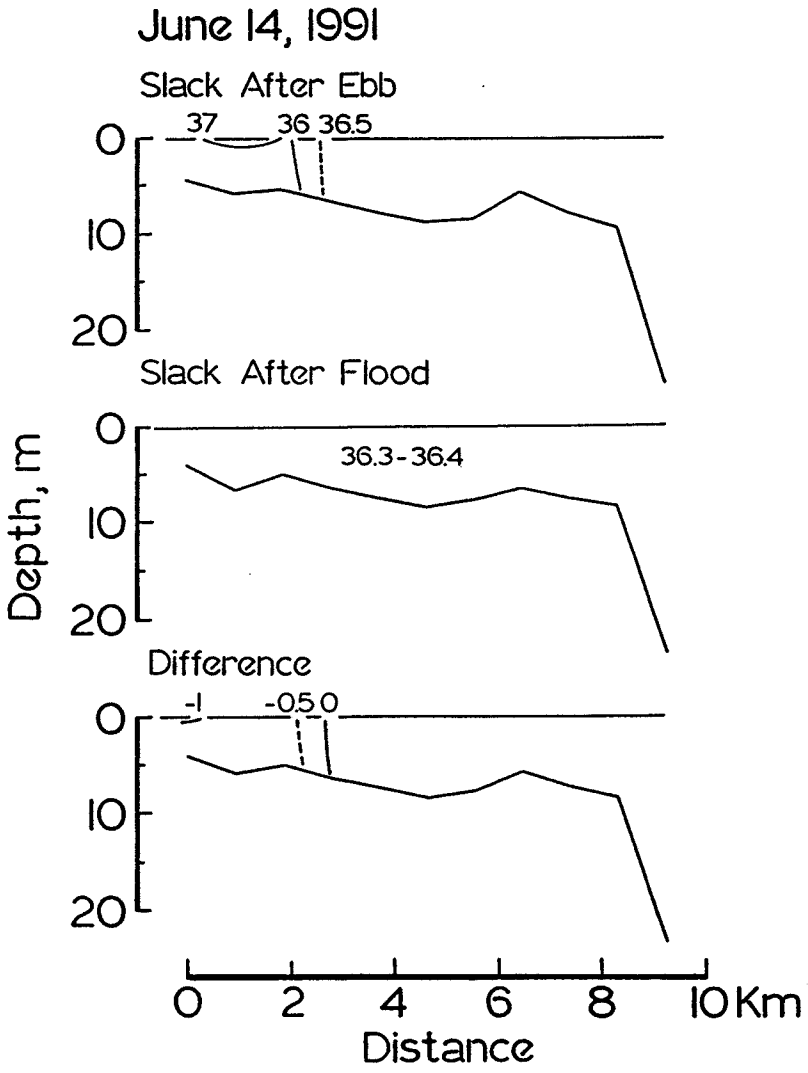


**Figure 19.** Salinity cross-sections from data collected June 14, 1991.

higher salinity Florida Bay water to the top few meters of the water column following the ebb half of the tidal cycle (**Figure 19**). This water has moved approximately 2 km seaward from Long Key Viaduct. Again, Hawk Channel water has very nearly constant salinity across its entire width following the flood, and seaward of a point about 2 km following the ebb. In this example, direct effects of Florida Bay are restricted to the inner shelf. The minor SAE-to-SAF differences are surprising, in view of the fact that maximum ebb and maximum flood currents were very strong during this tidal cycle, and there was a significant diurnal inequality. Maximum mid-morning flood current speeds were +64 cm $s^{-1}$, while strongest late-afternoon ebb current speeds were -81 cm $s^{-1}$. In view of the magnitude of the transport mechanism carrying Florida Bay water back and forth through Long Key Channel, the small differences must be a result of correspondingly small hydrographic gradients.

August 20, 1991

Data from August 20, 1991, present a relatively complex pattern, with both vertical and horizontal gradients found throughout the transect (**Figure 20**). The SAF cross-section indicates

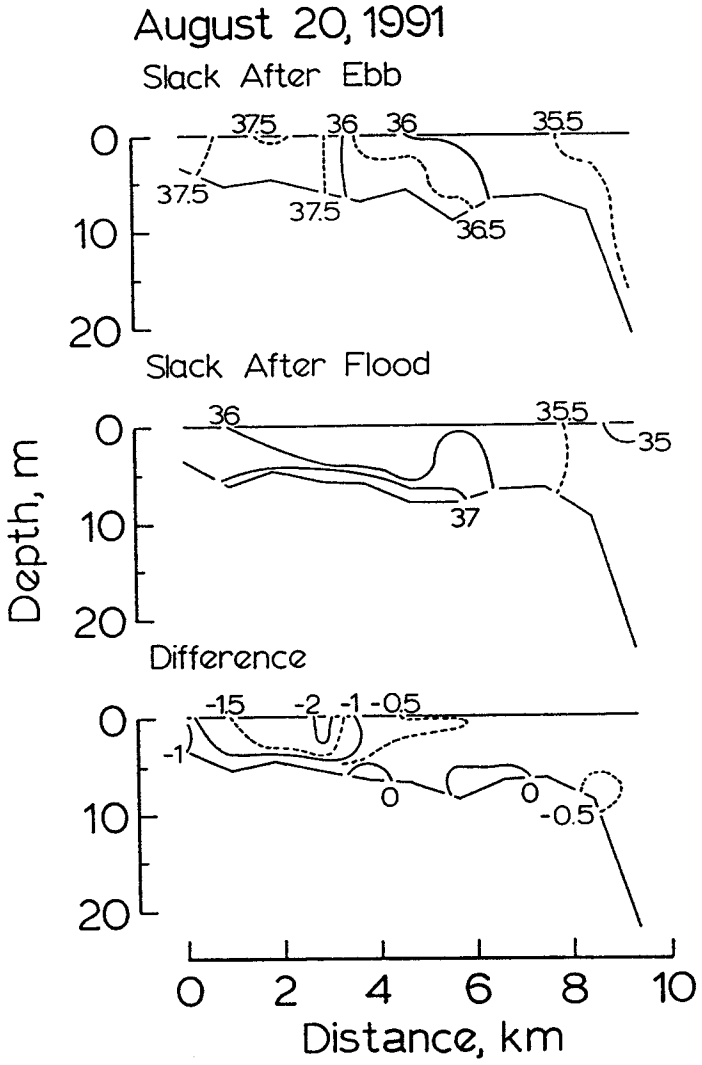


**Figure 20.** Salinity cross-sections from data collected August 20, 1991.

that the 37‰ water that left Florida Bay on the ebb tide remained in Hawk Channel as a near-bottom layer during the following flood half of the tidal cycle. The plot of salinity difference over the full tidal cycle indicates that approximately half of Hawk Channel felt the direct effects of Florida Bay water, although in this instance the largest salinity differences occurred in the upper part of the water column. The diurnal inequality during this tidal cycle is consistent with the high salinity water layer that extended well into Hawk Channel. Strongest ebb current speeds preceding the 1540 EST SAE were -64 cm $s^{-1}$, while strongest flood current speeds preceding the 0700 EST slack were only 21 cm $s^{-1}$.

November 1, 1991

Both the SAE and SAF cross-sections suggest that the water column was well mixed (**Figure 21**), perhaps a result of stronger winds in fall months. Across-shelf salinity gradients are weak as well, and data from these two transects do not provide much information regarding how much of Hawk Channel is impacted directly by tidal exchanges. Based upon the salinity

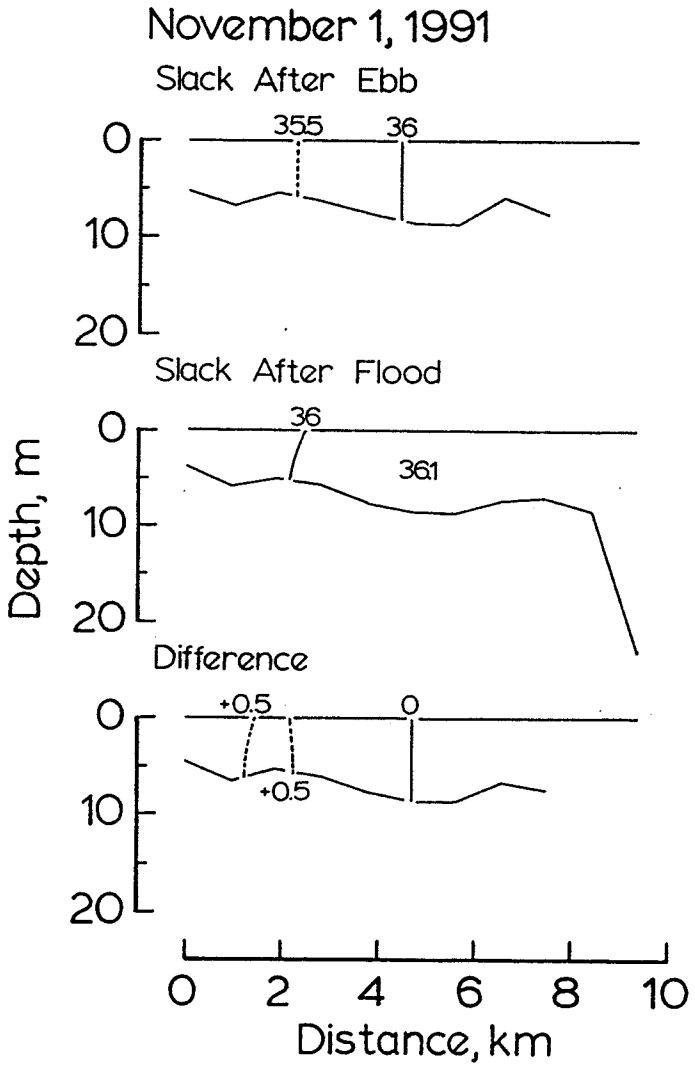


**Figure 21.** Salinity cross-sections from data collected November 1, 1991.

difference map, however, the data suggest that Florida Bay water moved approximately 2 km out of Long Key Viaduct. This tidal cycle included a relatively large diurnal inequality, with flood current speeds reaching 35 cm $s^{-1}$ prior to the 0650 EST SAF, and ebb current speeds just over -55 cm $s^{-1}$ preceding the 1405 EST SAE. It is likely that large salinity differences between Hawk Channel and Florida Bay did not exist at this time.

January 9, 1992

The final pair of transects from the 1991-92 historical data base provide another example of how salinity can be used as a natural tracer if conditions are right (**Figure 22**). Tidal current predictions for Long Key Channel indicate a modest diurnal inequality, with strongest ebb currents of -53 cm $s^{-1}$ before the SAE at about 0850 EST, and strongest flood currents of +46 cm $s^{-1}$ preceding the SAF at about 1500 EST. The SAE transect cross-section shows a relatively low-salinity plume leaving Florida Bay and extending about 5 km into Hawk Channel. The SAF

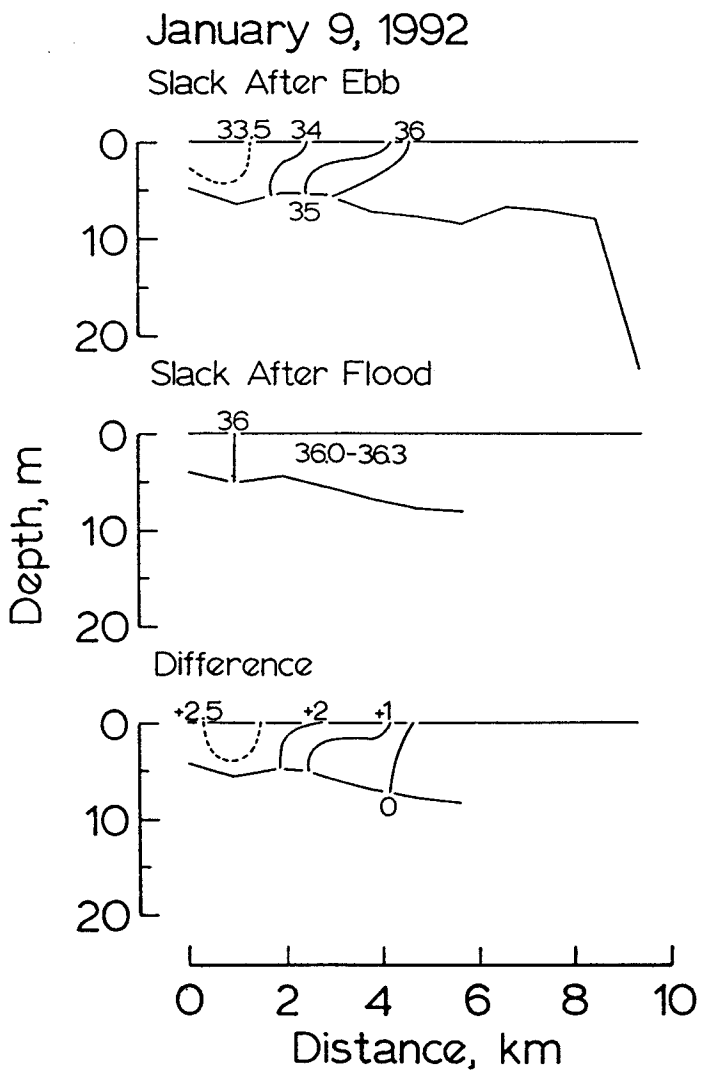


**Figure 22.** Salinity cross-sections from data collected January 9, 1992.

transect shows that the low-salinity plume is missing from the transect, with most of Hawk Channel containing relatively constant salinity water just above 36‰. Florida Bay water penetrated approximately 4 km into Hawk Channel on this tidal cycle. Perhaps more importantly, this pair of hydrographic transects shows that low-salinity water leaving Florida Bay in the surface layer is as suitable for tracking purposes as is high-salinity water in near-bottom layers.

March 18, 1997

A pair of hydrographic transects used to infer the movement of Florida Bay water across Hawk Channel were constructed from new data obtained at the end of the fifth quarter (**Figure 23**). The diurnal inequality of the flood and ebb currents was minimal, with maximum flood speeds of +30 cm $s^{-1}$ prior to the SAF at 0805 EST and strongest ebb current speeds of -32 cm $s^{-1}$ preceding the SAE at 1415 EST. Shelf waters were nearly homogeneous in terms of salinity, and there is virtually no indication of any Florida Bay water plume in the SAE transect. The minimal vertical stratification, and perhaps to some extent the lack of across-shelf gradients, can

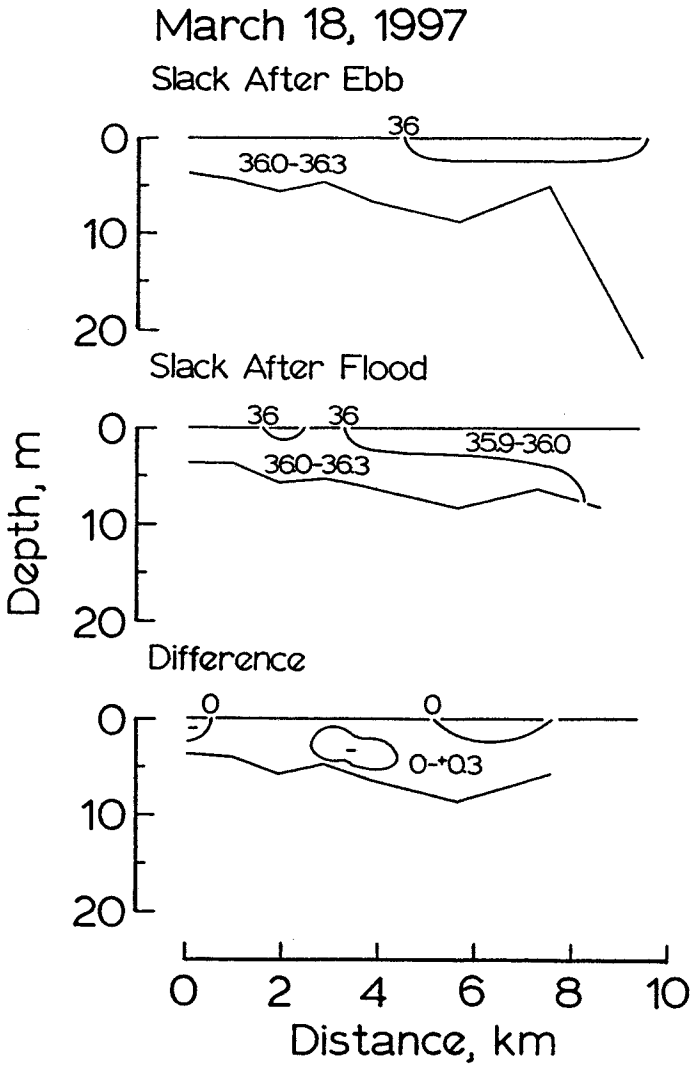


**Figure 23.** Salinity cross-sections from data collected March 18, 1997.

be attributed to strong winds that occurred the day before and the day that the hydrographic data were collected. This was not the best way to wrap up the sampling program, but it serves to reinforce the point that the methodology will work only under favorable conditions. All the data contribute to a better understanding of shelf hydrography, but not all the data will contribute as well to a better understanding of transport processes.

**Discussion**

While salinity has limitations as a natural tracer, data presented here indicate that under the right conditions it can be a convenient and low-cost approach to tracking Florida Bay water as it enters Hawk Channel. In our data base, we find evidence that Florida Bay water often penetrates 2-4 km into Hawk Channel whether the plume favors near-surface or near-bottom layers by virtue of its density. Details of the movement of the plume cannot be explored here, if only because we can never be certain whether the transect remained in the plume or left it at some point. But as a first look at this phenomenon, the approach taken here has served a useful purpose.

An important component of the data base is the tidal prediction needed to describe the flood and ebb tide conditions that preceded each hydrographic transect. The limited number of cross-sections we present does not permit any generalizations regarding how the strength of the tide affects the salinity distribution, but it is clear that the distribution of isohalines across the transect is related to the strength of the tide as much as it is related to salinity differences between Hawk Channel and Florida Bay, or the lateral movement of the plume once it enters Hawk Channnel.

This study was designed to test the hypothesis that Florida Bay water retains its hydrographic properties in near-bottom layers as it moves across Hawk Channel, and that it can be detected through its hydrographic properties at the reef tract. The hypothesis can be accepted in part, but it must also be rejected in part. The salinity cross-sections show that Florida Bay water retains its hydrographic properties as it emerges from Long Key Channel. But unless the salinity of Florida Bay water differs appreciably from that of Hawk Channel, the seaward movement of Florida Bay water, even at the mouth of Long Key Channel, cannot be tracked with salinity cross-sections.

Results suggest that there was no need to place the focus on the movement of Florida Bay water in near-bottom layers. Under high rainfall conditions, a near-surface plume of Florida Bay water can be tracked as easily as a near-bottom plume obtained during the dry season. The last part of our hypothesis must be rejected, at least temporarily. Using salinity as a natural tracer, we found no evidence of Florida Bay water at the reef tract. This is not to suggest that Florida Bay water is not reaching the shelf break, however. It almost certainly arrives at the seaward side of Hawk Channel in a diluted state, but unless we are able to track the plume as it moves across Hawk Channel, it will not be possible to determine at what rate and to what degree dilution occurs.

## HYPOTHESIS #4: Advection is more important than diffusion for transporting Florida Bay water across Hawk Channel.

**Introduction**

The two mechanisms which transport dissolved and suspended material across Hawk

Channel are investigated in this section. We test the hypothesis that advection is more important than diffusion for transporting Florida Bay water across Hawk Channel. For this component of the project we will use historical data both to characterize the across-channel deflection of the mean flow (Pitts 1994), and to quantify transport by turbulent diffusion.

**Data Base**

The data used to test this hypothesis were assembled entirely from archived data that were collected between 1991 and 1994. We include nine time series of current meter data from four study sites in Hawk Channel between Key Largo and Key West (**Figure 24**) as follows:

Key Largo Site (25°05.22' N, 80°20.58' W)

1. August 2, 1991 to December 6, 1991
2. December 18, 1991 to February 10, 1992

Long Key Site (24°47.12' N, 80°46.21' W)

3. August 9, 1990 to February 6, 1991
4. November 20, 1992 to February 18, 1993
5. July 22, 1993 to February 18, 1994

Bahia Honda Site (24°36.40' N, 81° 16.7' W)

6. August 1, 1991 to December 5, 1991
7. July 2, 1992 to July 22, 1993

Key West Site (24°30.22' N, 81°50.44' W)

8. July 1, 1992 to August 27, 1992
9. October 12, 1993 to January 27, 1994

General Oceanics currents meters were used to measure current speeds and directions. The current meters were suspended 2 or 4 m above the bottom on "gallows" type moorings. Total water depths at the sites ranged from 7-14 m but most were in depths of 7-8 m.

To quantify both advective and diffusive transport, we need values for nutrient concentrations: Local concentrations are needed for advective transport, and concentration gradients are needed for transport by turbulent diffusion. We have obtained values from the literature (Szmant and Forrester 1996) which include both gradients across Hawk Channel and point values representative of near-bottom layers in the middle of Hawk Channel.

**METHODOLOGY**

We use progressive vector diagrams (PVDs) to characterize flow patterns at each of our study sites. PVDs are constructed by plotting hourly current vectors (representing both speed and direction) head-to-tail (Scientific Programming Enterprises, 1985) to show how water moved past the study site. This is especially well suited for depicting flow patterns over time scales in excess of a few days. In some cases, our current meter records are on the order of one year in length. Results show only how water moved past the current meter. A PVD cannot be used to infer where a water parcel moved after it left the study site; nor can be used to suggest where a water parcel came from.

Advective transport is given by the product of the across-shelf volume transport and the

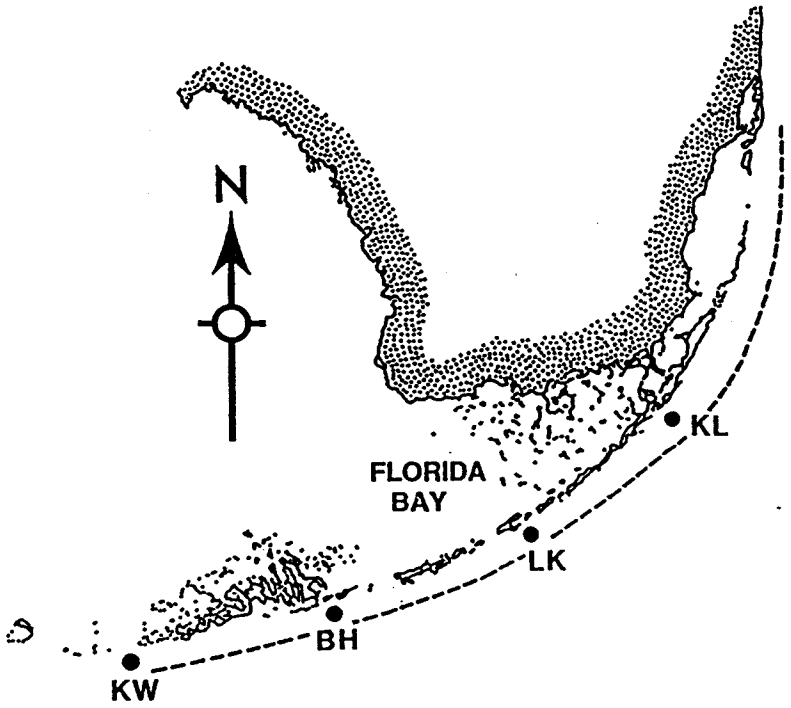


**Figure 24.** Map of the Florida Keys showing the location of study sites in Hawk Channel off Key Largo ("KL"), Long Key ("LK"), Bahia Honda Key ("BH") and Key West ("KW"). The hatched line represents the Florida reef tract.

nutrient concentration:

$$T_a = T_v C_n \ ,$$

where $T_v$ is the across-shelf component of the volume transport, in $m^3\ s^{-1}$, and $C_n$ is the nutrient concentration. Both terms can vary significantly in magnitude.

Diffusive transport is given by the product of the effective diffusion coefficient, $K_e$, and the concentration gradient, $\Delta C_n/\Delta y$,

$$T_d = \frac{\Delta C_n}{\Delta y} K_e \ ,$$

where $C_n$ is the concentration of the nutrient in μmoles $liter^{-1}$. The effective diffusion coefficient is given by the product of the diffusion time, $t_L$, and the mean square velocity of the current speed at the study site:

$$K_e = \langle v^2 \rangle \ t_L \ .$$

Bowden (1983) notes that the diffusion time can be interpreted as a "persistence time" for the turbulent speed of the dissolved or suspended material. Also, the product of the diffusion time

and the square root of the mean square velocity can be thought of as the average distance traveled during that time. Because we are concerned with turbulent transport across Hawk Channel toward the reef tract, calculations involve the across-shelf component of the current vector. The diffusion time is given by the integral of the autocorrelation function (Bowden 1983), which is obtained by summing the products of the autocorrelation functions and the one-hour lag increments:

$$t_L = \sum_{L=0}^{30} a_L \, \Delta\tau,$$

where $\Delta\tau$ is the one-hour interval separating autocorrelation calculations. The autocorrelation coefficient for time lag L is defined by

$$a_L = \frac{\frac{1}{N-L}\sum_{i=1}^{N-L} [\,(v_i - V)\,(v_{i+L} - V)\,]}{\frac{1}{N}\sum_{i=1}^{N} v_i^2},$$

where V is the mean across-isobath current speed, $v_i$ are the hourly observations of the unlagged and lagged time series, N is the number of observations used in the calculations, and L is the number of time lags. Bowden (1983) defines autocorrelation in terms of the velocity of dissolved or suspended material at successive time steps--a Lagrangian approach. To utilize historical current meter data, we take an Eulerian approach by calculating the autocorrelation from currents measured at a fixed location--the speed at which dissolved and suspended material passes the study site. Currents were decomposed into along- and across-isobath components--u and v, respectively--and we worked with only the v-component currents to quantify transport across Hawk Channel. The autocorrelation function was calculated for time lags of 1 to 30 hours. This includes the periodicities of semidiurnal and diurnal tides, as well as inertial periods at latitudes of 24-25°.

Harmonic constants of the principal tidal constituents for across-shelf currents were quantified using the 29-day harmonic analysis program as described above (Dennis and Long, 1971). Results are shown in **Table 4**, which includes both the amplitude of the across-shelf current component and the across-shelf tidal excursion. The across-shelf tidal excursion (TE) is obtained by multiplying the $M_2$ tidal constituent amplitude of the across-shelf current component by the period of that constituent (12.4206 hrs.) and dividing by $\pi$.

**Results**

**Figure 25** shows the progressive vector diagram constructed from currents recorded off Key Largo from August 2 to December 6, 1991. For the first seven weeks of the study, the net flow past the current meter was in an approximately along-shelf direction toward the northeast. The resultant speed was 0.4 cm $s^{-1}$. The flow reversed in direction in mid September, and the net flow was southwestward through the end of the record. The resultant speed of the southwestward current was approximately 1.0 cm $s^{-1}$. During August, September and in late November there were occasional periods of highly irregular flow. Across-shelf transport is relatively slight at this location, coming during short periods when along-shelf current speeds weaken.

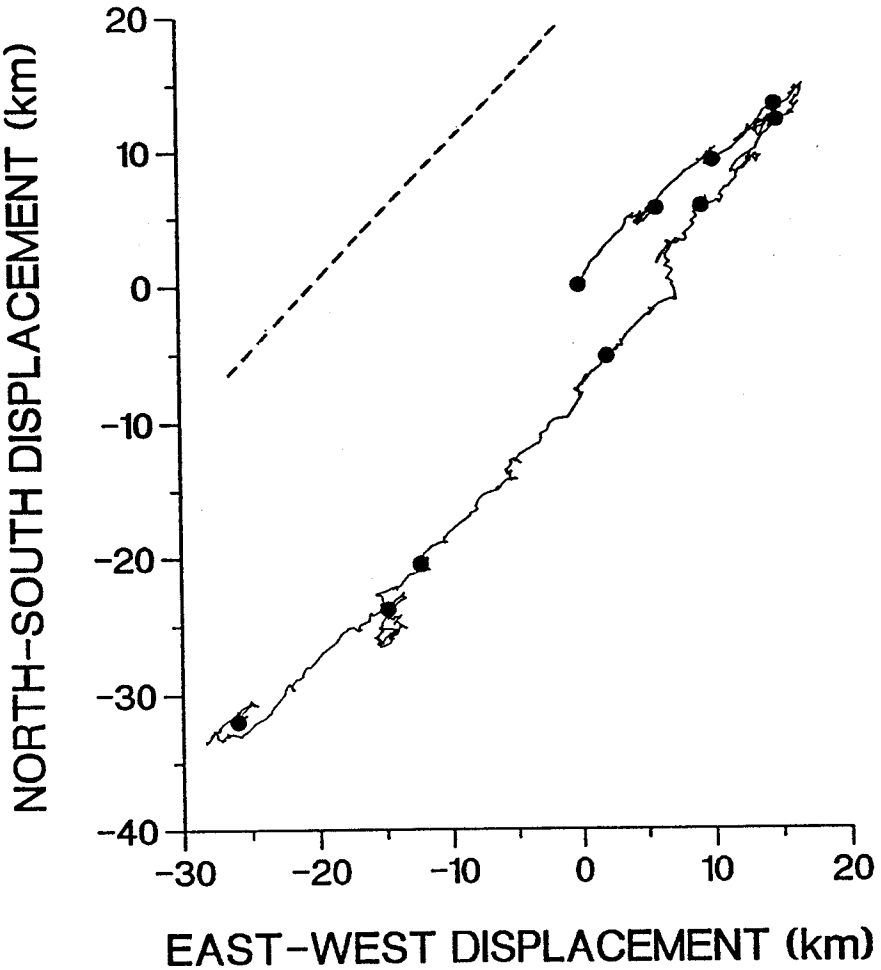


**Figure 25.** Progressive vector diagram of currents recorded 2 m above the bottom in 7 m of water in Hawk Channel off Key Largo from August 2 to December 6, 1991 (see **Figure 24** for station location). Dots have been entered at 14-day intervals. The hatched line represents the orientation of isobaths at the study site (approximately 044-224°).

Tidal currents at the study site have small amplitudes, and rotary tidal ellipses are not apparent in the progressive vector diagram (see **Table 3**). The amplitudes of the along-shelf and across-shelf components of the $M_2$ tidal constituent are 1.5 and 0.3 cm $s^{-1}$, respectively. The amplitude of the across-shelf component is within the accuracy of the current meter used to make the measurements.

The effective diffusion coefficient calculated from the across-shelf current components was 1.2 $m^2$ $s^{-1}$ (**Table 4**), which is consistent with the small amplitude of the $M_2$ tidal constituent. Combining the effective diffusion coefficient with a nitrogen concentration difference of 8 µmoles $liter^{-1}$ across the 10 km width of Hawk Channel (0.8 µmole $m^{-3}$ per meter), one obtains a diffusive transport rate of 1 µmole $m^{-2}$ $s^{-1}$. The mean across-shelf current component during this 126-day time period was a seaward flow of 0.03 cm $s^{-1}$ (also within the accuracy of the current meter). Applying this to a cross-sectional area of 1 $m^2$ and combining the volume transport rate of 3 x $10^{-4}$ $m^3$ $s^{-1}$ with a local nitrogen concentration of 12 µmoles $liter^{-1}$ (equal to 12,000 µmoles $m^{-3}$), representing mid Hawk Channel, one obtains an advective transport rate of 3.6 µmole $m^{-2}$ $s^{-1}$. Taken at face value, advective transport appears to be about four times the value of diffusive transport. However, because the mean across-shelf transport is within the accuracy of the current meter, we cannot quantify advective transport with confidence. For the time and place at which

historical current meter data are available, both advective and diffusive transport are small, and their relative roles cannot be established.

**Figure 26** shows the progressive vector diagram constructed from a second current meter time series recorded off Key Largo, starting approximately two weeks after the end of the previous record. The study period is December 18, 1991 to February 10, 1992. The pattern is basically similar to the previous record, with flow confined mainly to the local along-isobath direction, and a net flow toward the southeast. Again, across-shelf flow is minimal, and rotary tidal ellipses are not apparent in the record.

The effective diffusion coefficient for this time series was determined to be 1.62 $m^2 s^{-1}$. Combining this with the 0.8 µmole $m^{-3}$ per meter total nitrogen concentration gradient yields a diffusive transport rate of 1.3 µmole $m^{-2} s^{-1}$ for the near-bottom layer in the middle of Hawk Channel. The mean across-shelf current component during this mid-winter study period was -0.15 cm $s^{-1}$, a landward flow which is equivalent to $-0.15 \times 10^{-2}$ $m^3 s^{-1}$ through a cross-sectional area of 1 $m^2$. Combining this volume transport rate with a total nitrogen concentration gradient

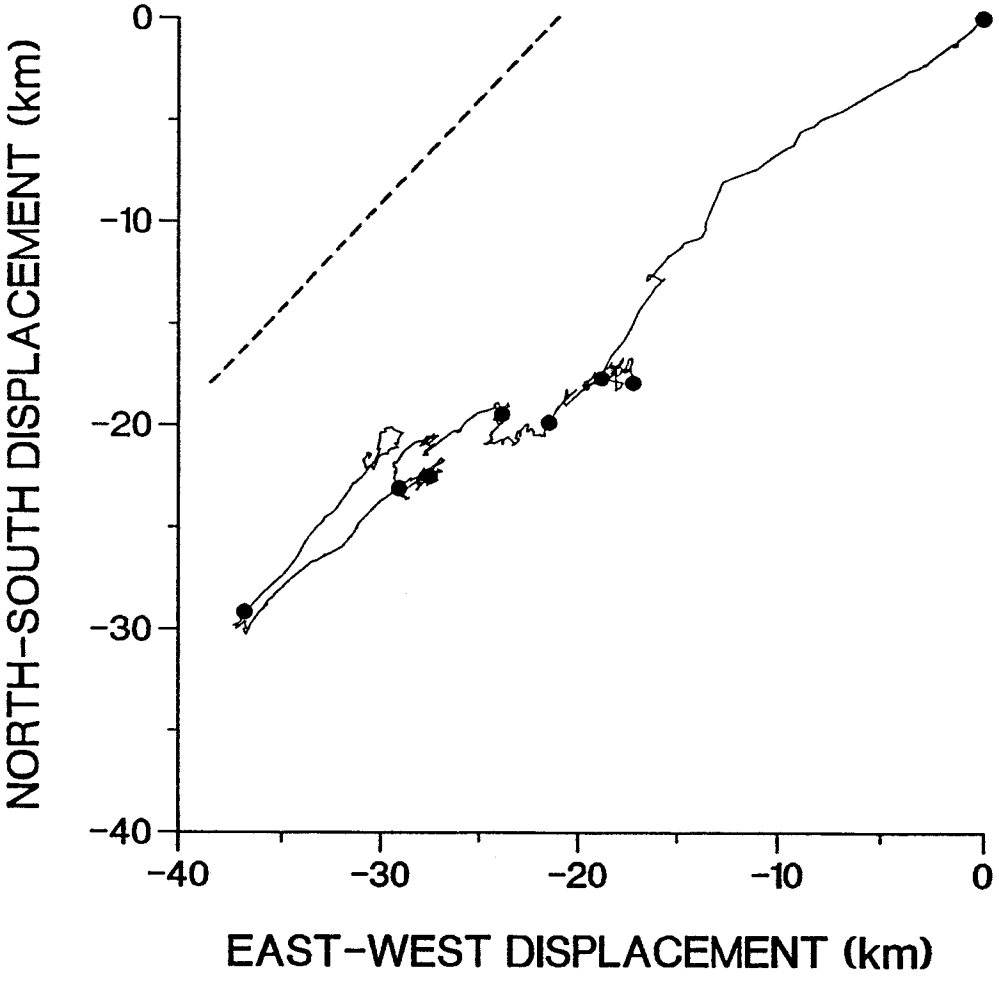


**Figure 26** Progressive vector diagram of currents recorded 2 m above the bottom in 7 m of water in Hawk Channel off Key Largo from December 18, 1991 to February 10, 1992 (see **Figure 26** for station location). Dots are spaced at 1-week intervals along the plot. The hatched line represents the orientation of isobaths at the study site (approximately 044-224°).

of 12,000 μmoles $m^{-3}$ yields an advective transport rate of -18 μmole $m^{-2}$ $s^{-1}$. Again, since the mean across-shelf current component is within the accuracy of the instrument we cannot quantify the advective transport for this time series with confidence. If such a small across-shelf flow results in an advective transport that is an order of magnitude greater than the diffusive transport calculated for representative concentration gradients, however, then these calculations suggest that advective transport should usually exceed diffusive transport.

A progressive vector diagram of currents recorded in Hawk Channel off Long Key from August 8, 1990 to February 6, 1991 is shown in **Figure 27**. Except for a brief reversal during the second week of the record, and again near the tenth week, the net flow is relatively consistent to the southwest. The resultant flow is 4.8 cm $s^{-1}$ at 220°. Thus, on average, there is a slight offshore deflection of an otherwise along-shelf flow. Most of the seaward deflection occurs during the first four weeks of the time series, and again during a brief period about 19 weeks into the record.

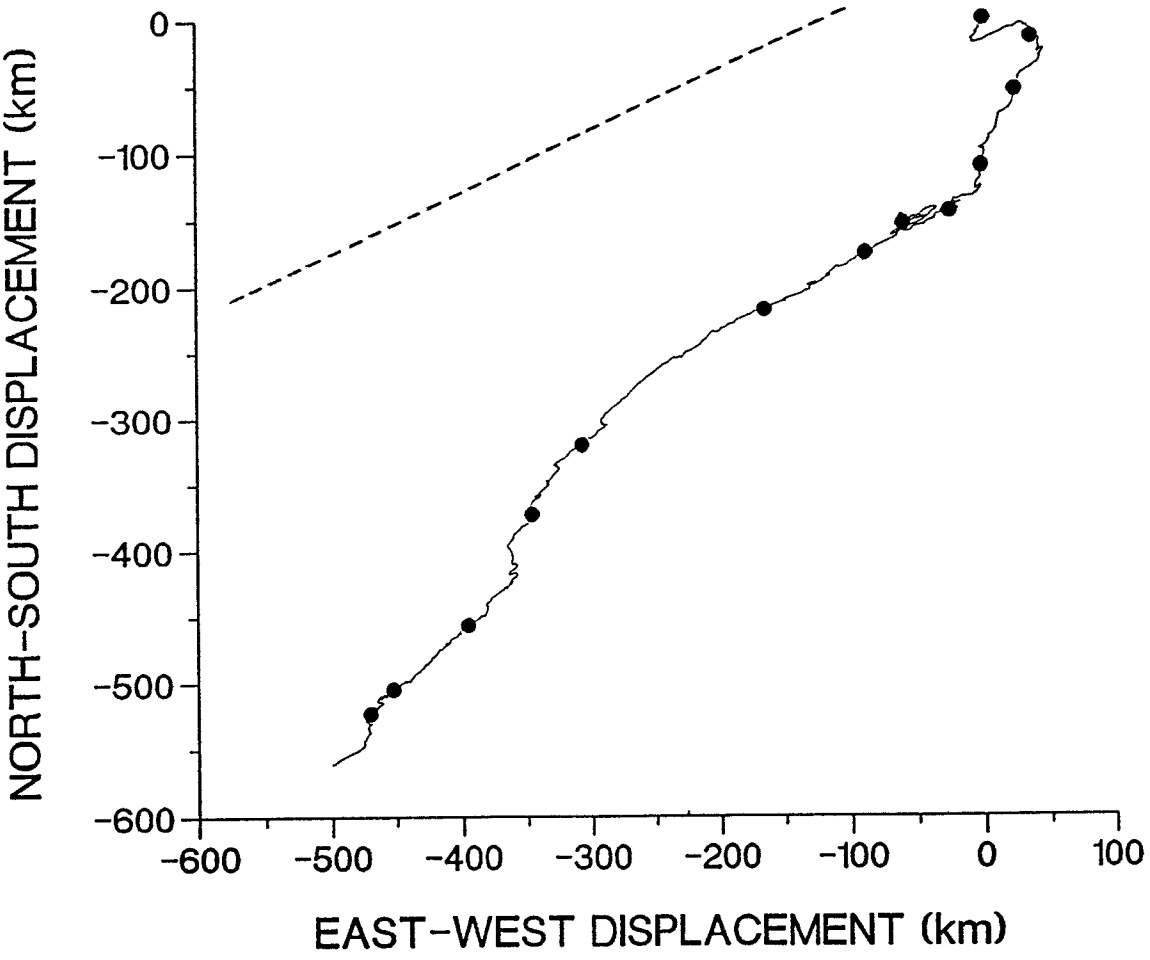


**Figure 27.** Progressive vector diagram of currents recorded 2 m above the bottom in 7 m of water in Hawk Channel off Long Key from August 9, 1990 to February 6, 1991 (see **Figure 24** for station location). Dots are spaced every 2 weeks along the plot. The hatched line represents the orientation of the local isobaths (approximately 055-235°).

Tidal currents at this site have larger amplitudes than those recorded at the Key Largo site, but tidal ellipses are not discernible on the plot. The amplitudes of the along-shelf and across-shelf components of the $M_2$ tidal constituent are 2.9 cm $s^{-1}$ and 3.8 cm $s^{-1}$, respectively. Note that the across-shelf tidal currents are much greater than those recorded off Key Largo which is probably due to this site's close proximity to Channel Five, a major tidal channel connecting Florida Bay with Hawk Channel.

The effective diffusion coefficient of 45.7 $m^2$ $s^{-1}$ is well over an order of magnitude greater than that calculated for the Key Largo site and may reflect the much greater across-shelf tidal currents recorded off Long Key. Combining a nitrogen concentration gradient of 13 µmole $liter^{-1}$ across the 10 km width of Hawk Channel (1.3 µmole $m^3$ per meter) with the effective diffusion coefficient, yields a diffusive transport rate is 59.4 µmoles $m^{-2}$ $s^{-1}$. The mean across-shelf current speed during this study period was 1.90 cm $s^{-1}$ toward the reef tract. Combining this value with the 13 µmoles $liter^{-1}$ of total nitrogen concentration in mid Hawk Channel, the

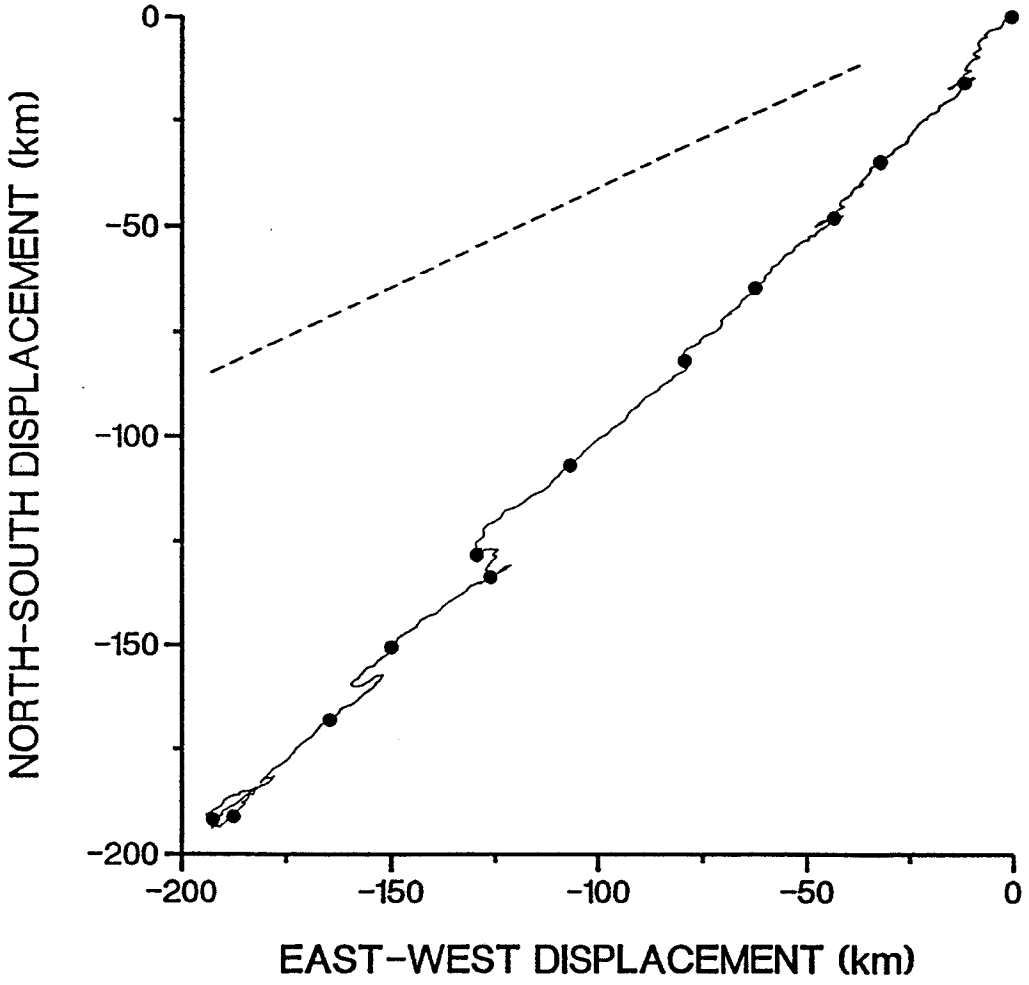


**Figure 28.** Progressive vector diagram of currents recorded 2 m above the bottom in 7 m of water in Hawk Channel off Long Key from November 20, 1992 to February 18, 1993 (see **Figure 24** for station location). Dots are spaced at 1-week intervals along the plot. The hatched line represents the orientation of the isobaths at the study site (approximately 055-235°).

advective transport rate becomes 246 μmoles $m^{-2}$ $s^{-1}$. Note that because the mean across-shelf current speed is outside the accuracy of the instrument the advective transport calculation becomes valid. Thus, the advective transport is in the same direction as and over 4 times greater than the turbulent transport at the study site off Long Key for this time period.

**Figure 28** shows the progressive vector diagram for currents recorded at the same study site off Long Key from November 20, 1992 to February 18, 1993. The pattern shows a predominately along-shelf flow with a significant seaward across-shelf deflection. The resultant heading is approximately 225°, and the resultant speed is 3.5 cm $s^{-1}$.

The average across-shelf current component is seaward at 1.2 cm $s^{-1}$. Applying this value to a cross-sectional area of 1 $m^2$ and using a mid Hawk Channel total nitrogen concentration of 13 μmoles $liter^{-1}$ yields an advective transport rate of 156 μmoles $m^{-2}$ $s^{-1}$. The effective diffusion coefficient, at 9.52 $m^2$ $s^{-1}$, is about a fifth that calculated from the earlier time series from this

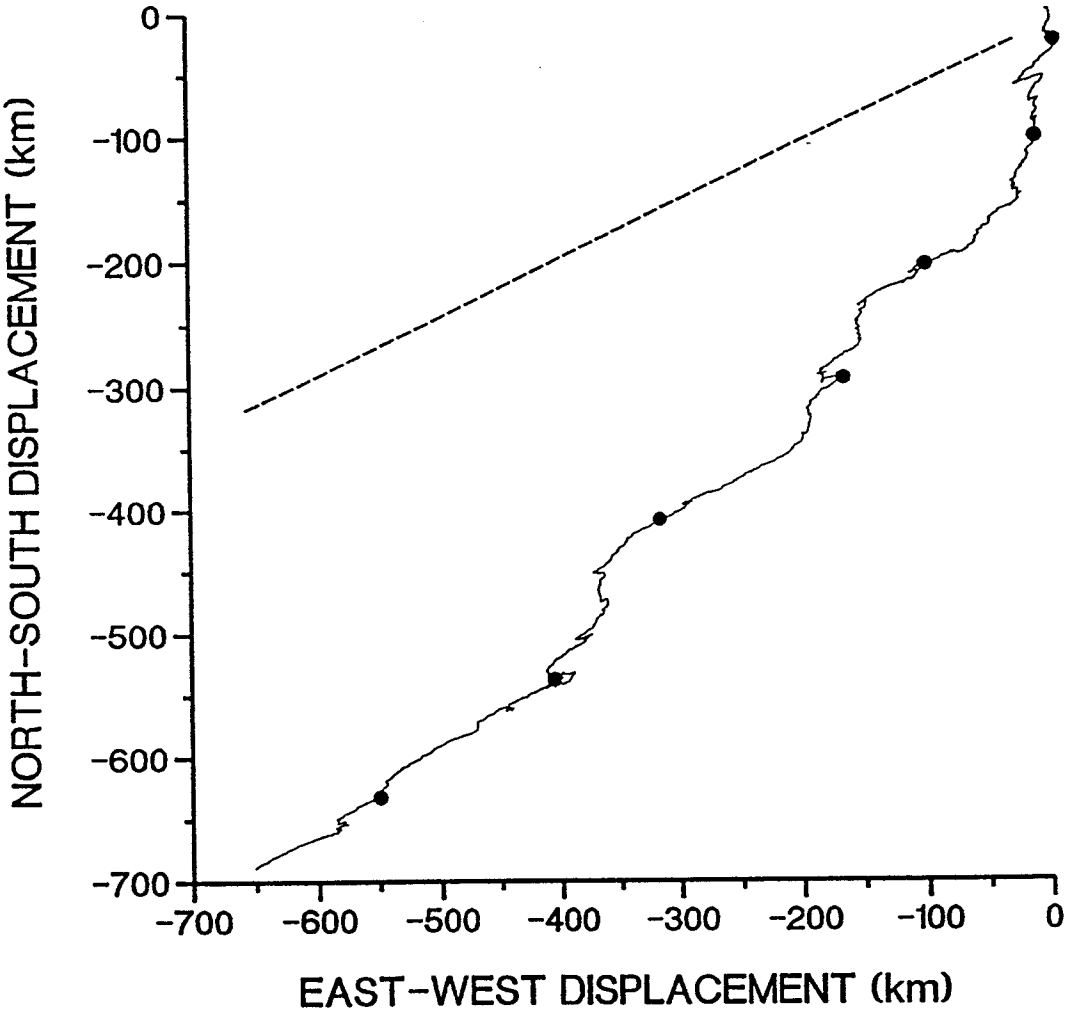


**Figure 29.** Progressive vector diagram of currents recorded 2 m above the bottom in 7 m of water in Hawk Channel off Long Key from July 22, 1993 to February 18, 1994 (see **Figure 24** for station location). Dots appear at the beginning day of each month along the plot. The hatched line represents the orientation of the local isobaths (approximately 055-235°).

location. Combined with a nitrogen concentration gradient of 1.3 μmole $m^{-3}$ per meter yields a diffusive transport rate of 12 μmole $m^{-2}$ $s^{-1}$ across Hawk Channel. Thus, for this time series, advective transport is in the same direction as diffusive transport and over an order of magnitude greater.

**Figure 29** shows a third progressive vector diagram of currents recorded at the Hawk Channel study site off Long Key. These data were recorded from July 22, 1993 to February 18, 1994. The pattern is again characterized by a quasi-steady along-channel flow to the southwest with a distinct offshore deflection. The resultant flow is 5.2 cm $s^{-1}$ at 225° for this 211-day study period. The average across-shelf current component is seaward at 1.9 cm $s^{-1}$. Using the total nitrogen concentration value of 13 μmole $liter^{-1}$ the advective transport rate was determined to be 247 μmoles $m^{-2}$ $s^{-1}$. An effective diffusion coefficient of 47.69 $m^2$ $s^{-1}$ was combined with the nitrogen concentration gradient of 1.3 μmoles $m^{-3}$ per meter for this location to yield a diffusive transport rate of 62 μmoles $m^{-2}$ $s^{-1}$ across Hawk Channel. Again, advective transport is four times

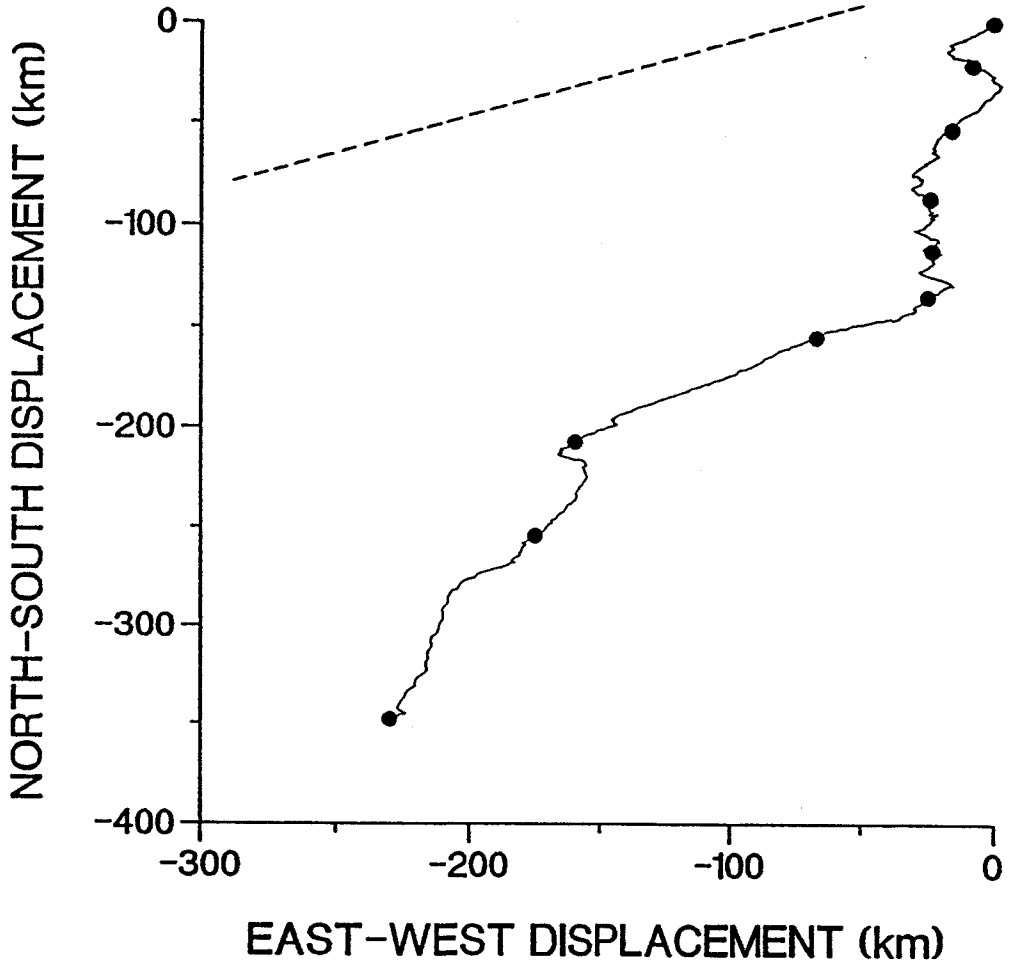


**Figure 30.** Progressive vector diagram of currents recorded 4 m above the bottom in 14 m of water in Hawk Channel off Bahia Honda Key from August 1 to December 5, 1991 (see **Figure 24** for station location). Dots are spaced at 2 week intervals along the plot. The hatched line represents the orientation of the isobaths at the study site (approximately 075-255°).

the turbulent diffusion rate. It is noteworthy that both the advective and diffuse transport rates are nearly identical to those calculated for the August 1990 to February 1991 time period for this location.

The progressive vector diagram of currents recorded in Hawk Channel off Bahia Honda Key from August 1 to December 5, 1991 is shown in **Figure 30**. The pattern shows a prominant seaward flow with quasi-periodic reversals in the along-shelf component during the first half of the study period. The second half of the record is characterized by a relatively consistent along-channel flow with an offshore deflection. The resultant flow over this 127-day study period was 3.8 cm $s^{-1}$ at 220°. Tidal currents at the study site are similar in magnitude to those recorded off Long Key. Amplitudes of the along-shelf and across-shelf components of the $M_2$ tidal constituent are 2.5 and 2.6 cm $s^{-1}$, respectively.

An effective diffusion coefficient of 55.25 $m^2$ $s^{-1}$ was calculated from the across-shelf current components for this study period. Combining this value with a nitrogen concentration gradient of 0.7 µmole $m^3$ per meter yields a diffusive transport rate of 39 µmoles $m^2$ $s^{-1}$ across

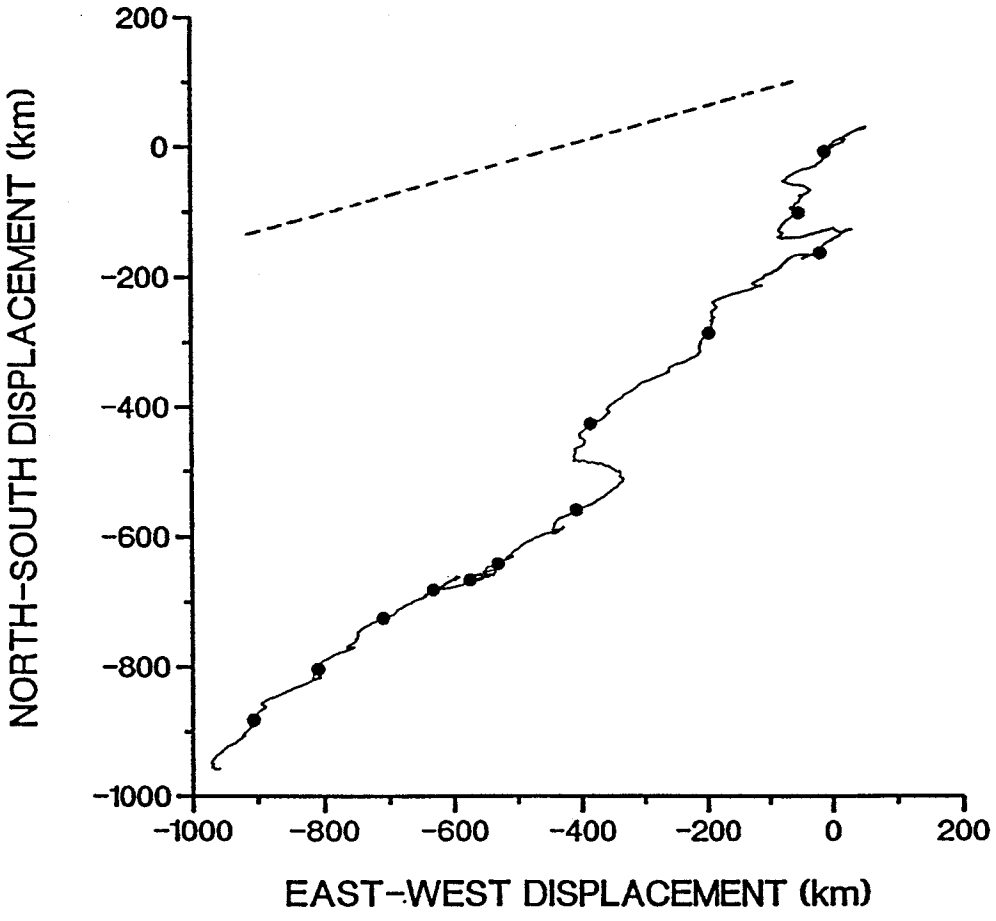


**Figure 31.** Progressive vector diagram of currents recorded 4 m above the bottom in 14 m of water in Hawk Channel off Bahia Honda Key from July 2, 1992 to July 22, 1993 (see **Figure 24** for station location). Dots are spaced at the start of each month along the plot. The hatched line represents the orientation of the local isobaths (approximately 075-255°).

Hawk Channel. The mean across-shelf current speed during this study period was +2.54 cm $s^{-1}$. Using the total nitrogen concentration of 13 µmoles $liter^{-1}$ and the across-shelf current speed one obtains an advective transport rate of 330 µmole $m^{-2}$ $s^{-1}$. Again, both transport processes are toward the reef tract, however, the advective transport rate is nearly an order of magnitude greater than the turbulent transport.

**Figure 31** shows a progressive vector diagram for a 13-month time series from the same study site off Bahia Honda Key. The data were recorded July 2, 1992 to July 22, 1993. The resultant flow during this 385-day study period was toward 223° at 4.1 cm $s^{-1}$, again a generally along-shelf flow toward Key West with an offshore deflection. On several occasions, particularly during mid December, the seaward deflection is very pronounced for periods of up to two weeks.

The mean across-shelf current speed during the study period was seaward at 2.03 cm $s^{-1}$. Using the total nitrogen concentration value of 13 µmoles $liter^{-1}$ and the mean across-shelf current speed, the advective transport rate becomes 264 µmoles $m^{-2}$ $s^{-1}$. An effective diffusion coefficient of 57.89 $m^2$ $s^{-1}$ is the largest value obtained from any time series appearing in this report. Combining the nitrogen concentration gradient of 0.7 µmoles $m^{-3}$ per meter for this location with the effective diffusion coefficient yields a diffusive transport rate of 41 µmoles $m^{-2}$ $s^{-1}$ across Hawk Channel. The advective and turbulent transport rates calculated for this time series are in close agreement for the values obtained from the earlier record from this location.

A progressive vector diagram of currents recorded in Hawk Channel off Key West from July 1 to August 27, 1992 is shown in **Figure 32.** This 8-week time series shows a primarily along-channel flow with low-frequency reversals every 2-3 weeks. The pattern also shows a slight seaward deflection during most of the study period. Superimposed onto the low-frequency east-west flow is a distinct wavelike pattern which reflects tidal ebbs and floods. Amplitudes of the along- and across-shelf current components of the $M_2$ tidal constituent are 3.9 and 6.7 cm $s^{-1}$,

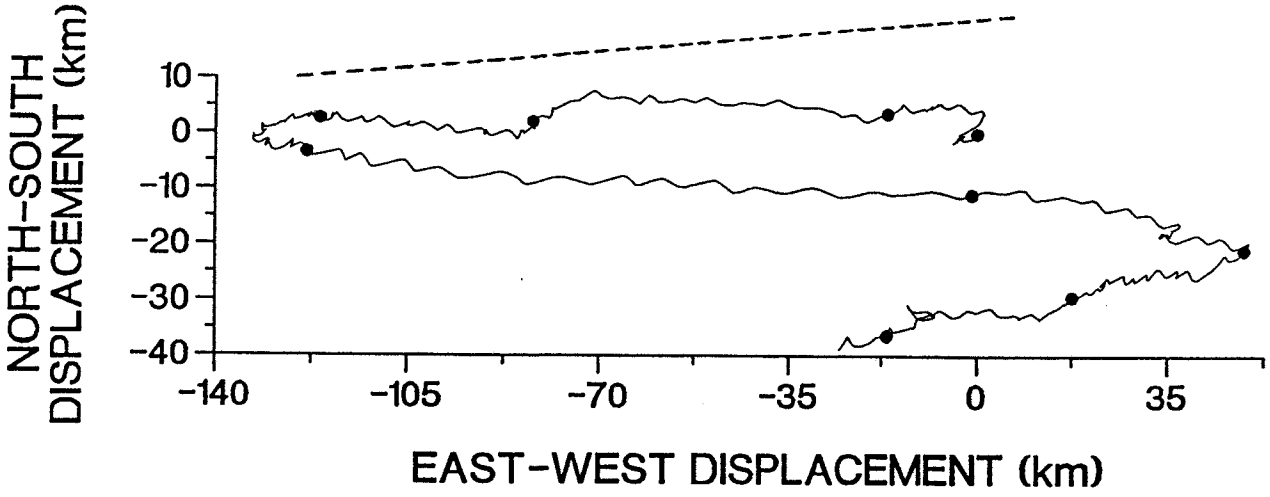


**Figure 32.** Progressive vector diagram of currents recorded 2 m above the bottom in 12 m of water in Hawk Channel off Key West from July 1 to August 27, 1992 (see **Figure 24** for station location). Dots are spaced at weekly intervals along the plot. The hatched line represents the orientation of isobaths at the study site (approximately 085-265°).

respectively. The relatively large across-shelf amplitude probably reflects tidal exchanges occurring between the Gulf of Mexico and the Atlantic Ocean through Northwest Channel, a large tidal channel just west of Key West.

Analysis indicates that the mean along-shelf current speed and the effective diffusion coefficient for this time series are +0.74 cm $s^{-1}$ and 41.93 $m^2$ $s^{-1}$, respectively. Advective and diffusive transport rates cannot be calculated, because values for the total nitrogen concentration and the nitrogen concentration gradient are unavailable for this location. Also, the validity of the advective transport value would have to be questioned, given the fact that the mean across-shelf speed is within the accuracy of the current meter.

**Figure 33** shows another progressive vector diagram constructed from currents recorded off Key West from October 13, 1993 to January 27, 1994. Flow during most of the study period is along-channel; west-to-east for the first 2 weeks followed by east-to-west flow for the remainder of the study period. A significant across-shelf flow occurs during the first half of December. Tidal currents can be observed as wavelike oscillations superimposed onto the long-term flow. The mean across-shelf current speed for this time series is +0.75 cm $s^{-1}$ and the effective diffusion coefficient is 38.83 $m^2$ $s^{-1}$. Both are in close agreement with the earlier record from this location. Again, the mean across-shelf current speed is within the precision of the instrument.

ENDECO current meter data were available from two short (1-day) studies conducted in 1994. Because of a 5 minute sampling period, we were able to use the same analytical techniques to quantify the magnitude of transport by diffusion over shorter time scales. Results therefore extend the results described above by quantifying turbulent mixing over time scales of between five minutes and one hour.

A 24-hour study conducted on January 24-25, 1994 provided current speeds and directions from a study site in Hawk Channel off the mouth of Tavernier Creek (24°58'51" N, 80°30'51" W). Currents were recorded at approximately mid depth in 5 m of water. Results indicate an

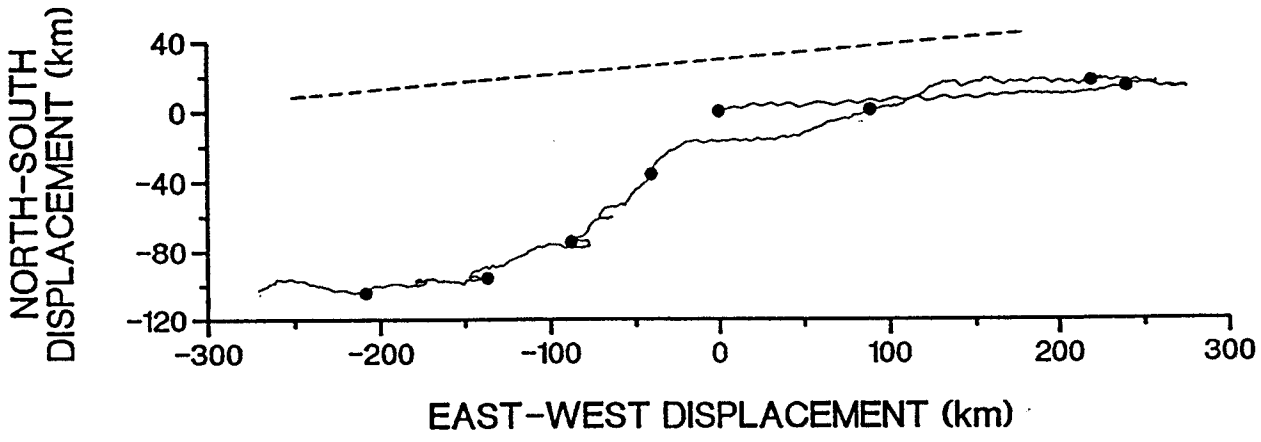


**Figure 33.** Progressive vector diagram of currents recorded 2 m above the bottom in 12 m of water in Hawk Channel off Key West from October 13, 1993 to January 27, 1994 (see **Figure 24** for station location). Dots have been entered every 2 weeks along the plot. The hatched line represents the orientation of isobaths at the study site (approximately 085-265°).

effective diffusion coefficient of 30.6 $m^2 s^{-1}$. This may not be representative of winter conditions in general, but it is noteworthy that $K_e$ is of the same order of magnitude as the values obtained off Long Key and Bahia Honda Key.

A similar study, conducted from June 30 to July 1, 1994 near the entrances to Snake Creek and Whale Harbor Channel (24°55.53' N, 80°34.98' W) provided a time series that lasted 42 hours. Again, analysis focused on turbulent diffusion over time scales between 5 minutes and 1 hour. Results indicated an effective diffusion coefficient of 40.9 $m^2 s^{-1}$. As was the case with the data obtained off the mouth of Tavernier Creek, the tentative conclusion is that turbulent mixing over these shorter time scales is of the same order of magnitude as turbulent mixing over time scales of 1-30 hours.

As a component of the second field study conducted off Bahia Honda Channel (see **Figure 31**), a current meter was maintained on the same tautline mooring 3.5 m below the surface for a 41-day time period between April 14 and May 25, 1993. During this time, the first current meter continued in operation approximately 3.5 m above the bottom in 14 m of water. Analyses of these two time series offer insight regarding differences in across-shelf transport between near-surface and near-bottom levels.

Mean across-shelf transport at both levels was in a seaward direction. The average current speeds at near-surface and near-bottom levels were +1.1 and +1.7 cm $s^{-1}$, respectively, resulting in seaward advective transport of +143 and 221 μmoles $m^{-2} s^{-1}$. The effective diffusion coefficients were 13.6 and 29.0 $m^2 s^{-1}$ at near-surface and near-bottom levels, and the corresponding diffusive transports were +10 and +20 μmoles $m^{-2} s^{-1}$, respectively. It is noteworthy that seaward transport by both mechanisms was strongest in near-bottom levels.

**Table 3.** Harmonic constants (amplitudes, η, in cm $s^{-1}$; local phase angles, κ, in degrees) of the principal tidal constituents for the across-shelf current components at Hawk Channel study sites off Key Largo, Long Key, Bahia Honda Key and Key West. The across-shelf tidal excursion (TE), in kilometers, appears in the last column. Asterisks denote tidal constituent amplitudes that fall within the precision of the instrument and thus become invalid. The tidal excursion calculated for Key Largo is also in question, because the $M_2$ amplitude used to calculate TE is within the precision of the instrument.

| | | Tidal Constituent | | | | | | |
|---|---|---|---|---|---|---|---|---|
| | | $M_2$ | $S_2$ | $N_2$ | $K_1$ | $O_1$ | $P_1$ | TE |
| Key Largo | η | 0.3* | 0.1* | 0.1* | 0.4* | 0.3* | 0.1* | 0.04* |
| | κ | 353 | 060 | 308 | 297 | 287 | 297 | |
| Long Key | η | 2.8 | 1.1 | 0.9* | 3.5 | 2.6 | 1.4 | 0.41 |
| | κ | 092 | 041 | 047 | 318 | 313 | 291 | |
| Bahia Honda Key | η | 2.6 | 0.9* | 0.6* | 0.4* | 0.5* | 0.1* | 0.37 |
| | κ | 027 | 048 | 006 | 025 | 037 | 025 | |
| Key West | η | 6.7 | 2.1 | 1.3 | 1.0 | 0.4* | 0.3* | 0.95 |
| | κ | 186 | 200 | 167 | 164 | 179 | 164 | |

**Table 4.** Statistics calculated from historical current meter data and used in the calculation of advective and diffusive transport. Across-shelf current speed, v, is in cm $s^{-1}$ (positive values represent seaward flow); the effective diffusion coefficient ($K_e$) is in $m^2$ $s^{-1}$. See text for explanations of the total nitrogen concentrations and concentration gradients used in the calculations (not available for Key West). Advective transport ($T_a$) and diffusive transport ($T_d$) are in micromoles $m^{-2}$ $s^{-1}$.

| | v | $K_e$ | $T_a$ | $T_d$ |
|---|---|---|---|---|
| A. Key Largo | | | | |
| 1. Aug 2 91 to Dec 6 91 | +0.03 | 1.2 | +3.6 | +1.0 |
| 2. Dec 18 92 to Feb 10 93 | -0.15 | 1.6 | -18.0 | +1.3 |
| B. Long Key | | | | |
| 1. Aug 9 90 to Feb 6 91 | +1.9 | 45.7 | +246.4 | +59.4 |
| 2. Nov 20 92 to Feb 18 93 | +1.2 | 9.5 | +152.5 | +12.4 |
| 3. Jul 22 93 to Feb 18 94 | +1.9 | 47.7 | +249.0 | +62.0 |
| C. Bahia Honda | | | | |
| 1. Aug 1 91 to Dec 5 91 | +2.54 | 55.3 | +330.7 | +38.7 |
| 2. Jul 2 92 to Jul 22 93 | +2.03 | 57.9 | +264.1 | +40.5 |
| D. Key West | | | | |
| 1. Jul 1 92 to Aug 27 92 | +0.74 | 41.9 | | |
| 2. Oct 12 93 to Jan 27 94 | +0.75 | 38.8 | | |

Unpublished hydrographic data have shown that under some conditions Florida Bay water will move across Hawk Channel as a near-bottom layer by virtue of its density. In winter months, the shallow waters of the bay will cool more rapidly than deeper shelf water following a frontal passage. During the dry season, bay water will have a higher salinity. In both instances, density will increase, and hyperpycnal water will be restricted to the lower layers of Hawk Channel. More generally, it is noteworthy that the effective diffusion coefficient is over twice as large in near-bottom layers. This is surprising, because turbulent mixing might be expected to be greater in near-surface, wind-influenced layers. Nevertheless, results of this sub-study, showing advective transport over an order of magnitude greater than diffusive transport for the same time and location, are consistent with findings obtained with other, longer time series.

**Discussion**

Results presented here suggest that the transport of dissolved or suspended material across Hawk Channel is primarily in response to the across-isobath component of the current. Thus, we tentatively accept our hypothesis that advection is the dominant transport mechanism. The relative importance of advective and diffusive transport must be accompanied by several qualifications, however. For example, estimates of the magnitude of advective transport must be based upon only those current meter records for which the across-isobath flow is greater than the accuracy of the current meter used to make the measurements (1.0 cm $s^{-1}$). This restriction eliminates both time series from the Key Largo study site and both from the Key West study site.

As described in the QAQC Plan, the uncertainty of turbulent transport calculations is approximately ±13 μmoles $m^{-2}$ $s^{-1}$. On that basis as well, results from both Key Largo records and the second Long Key study cannot be used in the comparison. Because we do not have nutrient data from the Key West area, we therefore base our comparison on results from only the two time series off Long Key and two time series from off Bahia Honda Key.

A second qualification stems from the fact that both concentrations and concentration gradients vary substantially from one nutrient to the next. For example, across-shelf transport calculated for total nitrogen would not apply to total phosphorus, because both concentrations and concentration gradients for phosphorus reported by Szmant and Forrester (1996) are significantly less than for nitrogen. In general, transport by turbulent mixing may be limited primarily by the across-shelf gradient of the dissolved or suspended material in question. Even when the effective eddy diffusivity is significant, minimal gradients across Hawk Channel will result in little net transport.

Repeated studies at three of the four study sites tend to confirm that results from a single, sufficiently long time series are adequate to characterize turbulent mixing. Only at our Hawk Channel station off Long Key did we find the effective eddy diffusivity varying significantly from one study to the next. The second time series (November 20, 1992 to February 18, 1993) produced a $K_e$ value that was about 20% of what was calculated with current meter data from the other two studies. It is noteworthy that the second study was less than half as long as either of the other two. This suggests that the intensity of turbulent mixing can vary significantly over seasonal and subseasonal time scales. If so, then transport by diffusion may vary seasonally, just as advective transport may vary with the seasonal shift of the wind.

Results from our four study sites suggest that the intensity of turbulent mixing is relatively weak off Key Largo. As noted earlier, this may be associated with the absence of major tidal channels in the Upper Keys. The intensity of turbulent mixing might be related to the lateral distance to the land boundary, but the width of Hawk Channel varies little between Key Largo and Key West (9-10 km). Water depth may also be a factor. Depth at our Key Largo and Long Key station was on the order of 7-8 m, while depth at the Bahia Honda and Key West stations was on the order of 13-14 m. Regardless of the cause, the potential for turbulent mixing to move dissolved or suspended material across Hawk Channel seems to be greatest off the Middle and Lower Keys.

It is likely that both advective and diffusive transport occur in response to relatively short-term events as much as to mean conditions. Strong across-shelf flow was recorded at all four locations, at least for brief periods of time. Effective eddy diffusion coefficients were not calculated for time periods shorter than the full time period available for each historical record. It is probable that turbulent mixing is no more steady in time than the across-shelf component of the current. This is a subject that should receive further attention.

It is noteworthy that the progressive vector diagrams show that advective transport can be landward across Hawk Channel for time periods of at least several days. Because of the relatively narrow width of Hawk Channel, across-shelf current speeds of only 2-3 cm $s^{-1}$ are required to carry water 10 km in a time period of four days. Diffusive transport, on the other hand, will continue to be seaward as long as the across-shelf concentration gradient is in that direction. Because the Keys or tidal channels probably represent a greater source of nutrients than does upwelling at the reef tract, and because mixing of Hawk Channel and Florida Straits water at the reef tract represents a loss of nutrients, a seaward-directed gradient is probably far more common than a landward-directed gradient. Thus advective transport, while dominant in

magnitude, may reverse in direction. Diffusive transport, on the other hand, while smaller in magnitude, only rarely reverses to carry nutrients landward.

**HYPOTHESIS #5: Seasonally shifting winds alternately increase and decrease the near-bottom export of Florida Bay water from Hawk Channel to the Florida Straits.**

**Introduction**

In this section we examine across-shelf transport at the shelf break in response to tidal currents, wind forcing and density forcing. The analysis is based upon new data collected during the summer of 1996 and winter of 1996-97. Specifically, we test the hypothesis that seasonally shifting winds alternately increase and decrease the near-bottom export of water from Hawk Channel into the Straits of Florida. Results quantify across-shelf flow in response to wind, tidal and density forcing at two shelf break sites during summer and winter seasons.

**Data Base**

The data used to examine flow at the shelf break include current meter data from two levels at each of two stations, and wind data from two nearby offshore stations. Currents were recorded 2 m above the bottom and 6 m below the surface on taut-line moorings near Tennessee Reef (24° 42.40'N, 80° 51.35'W) and near Conch Reef (24° 58.18'N, 80° 26.02'W). See **Figure 34** for study site locations. Data were recorded at both sites from June 20 to October 2, 1996 (summer study) and from December 13, 1996 to April 9, 1997 (winter study). The near-bottom current meter deployed at Conch reef flooded within a few hours of the winter deployment, so no data are available from that location and time period.

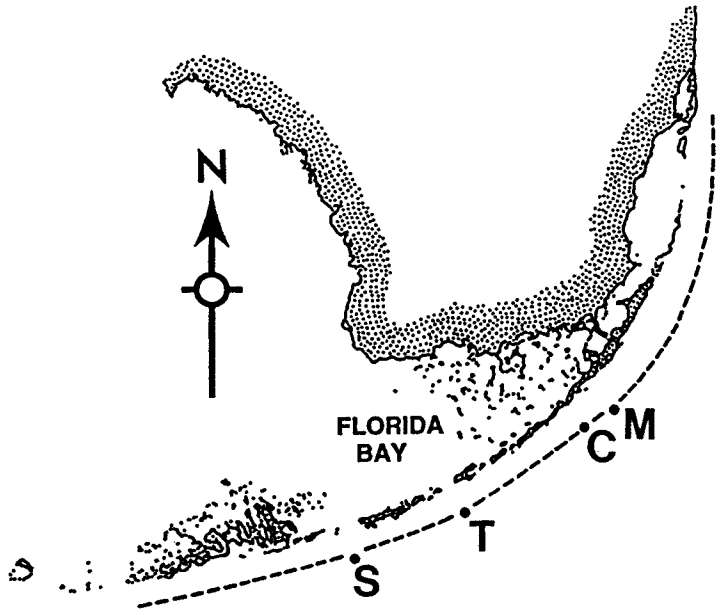


**Figure 34.** Map of the Florida Keys showing the location of study sites near Tenessee Reef (T) and Conch Reef (C); and the anemometers at Sombrero Reef ("S") and Molasses Reef ("M").

Current speeds and directions were recorded hourly. ENDECO Type 174SSM current meters were deployed at the upper level at each study site. ENDECO current meters are designed specifically to be used in wave-influenced layers. General Oceanics Model 6011 Mark II current meters recorded current speed and direction hourly at the bottom of the taut-line moorings.

Wind data were obtained from C-MAN stations on Molasses Reef (25° 00.60'N, 80° 22.80'W) and at Sombrero Reef (24° 37.60'N, 80° 06.60'W) for each of the time periods specified above. Wind speed and direction were recorded with R.M. Young Wind Monitors to the nearest 0.1 m $s^{-1}$ and 1°, respectively. Air pressure and air temperature were recorded to the nearest 0.1 mb and 0.1°C, respectively.

**Methodology**

a. Tidal Forcing

Tidal exchanges between Hawk Channel and the Florida Straits were quantified by harmonic analyses (Dennis and Long, 1971) of the across-isobath component of current vectors recorded at upper and lower levels. Harmonic analyses quantifies the amplitudes and local phase angles (harmonic constants) of 24 tidal constituents. Amplitudes are the highest landward and seaward current speeds attained over the course of each tidal cycle. Inspection of the amplitudes reveals which constituents are physically important. By our definition, tidal constituents with amplitudes greater than 1.0 cm $s^{-1}$ qualify as the "principal tidal constituents." In effect, we use the accuracy of the current meter to decide whether we retain or discard tidal constituents.

The across-isobath excursion for a given tidal constituent, $E_i$, is calculated from the amplitude, $A_i$, and the period, $T_i$, of the $i^{th}$ constituent:

$$E_i = \frac{A_i T_i}{\pi},$$

where the amplitude must be expressed in km $h^{-1}$, and the period must be expressed in hours if the excursion is to be calculated in km.

b. Density Forcing

Steady and time-varying components of across-isobath density-driven transport at the shelf break are quantified using perturbation analysis. Perturbation analysis decomposes density and current speed into their mean and time-varying components, and then calculates the covariance--the mean of the products of the time-varying components of the measured density and across-isobath current speed. Results show whether higher-than-average current speeds (seaward flow) are consistently associated with higher-than-average density, as one would expect if density currents are significant in forcing shelf water seaward.

Time series of water temperature and conductivity are used to calculate salinity in practical salinity units (psu) (Perkin and Lewis 1980), and then water density (Millero and Poisson 1981) in kg $m^{-3}$. Time series of hourly current vectors (speeds and directions) are decomposed into along-isobath and across-isobath components (i.e., flow parallel and perpendicular to the reef tract). The across-isobath flow is retained for comparison with the hourly density values.

In the perturbation analysis used to address this hypothesis, hourly observations of across-isobath current speed (seaward flow defined positive) and density are decomposed into the study mean and the time-varying deviation about the mean. The instantaneous across-isobath current

speed and density for the $i^{th}$ hour of the study ($u_i\rho_i$) are then expanded to four perturbation products, two of which have physical significance. For example, for the $i^{th}$ hour of the study:

$$t_i = \langle u \rangle \langle \rho \rangle + u_i' \rho_i',$$

where <u> and <ρ> are the study mean across-isobath current speed and near-bottom density, u' and ρ' are the deviations ("perturbations") from the mean values at the $i^{th}$ hour. A positive covariance of the perturbation terms (<u'ρ'>) indicates that higher density is commonly associated with seaward flow. This is assumed to be an indication that density currents are leaving Hawk Channel and cascading down the outer shelf.

In most perturbation analyses, the $u_i'\rho_i'$ perturbation products are averaged to make them comparable to the product of the study-mean density and the study-mean across-shelf current speed. The averaging process can obscure considerable variability over tidal and low-frequency time scales, however, and useful information may be lost. In this report, we present not only the study-mean values, but also plots that show the cumulative net mass transport. By accumulating transport values, subtle but persistent differences between flood and ebb contributions stand out clearly. The cumulative net mass transport through the $k^{th}$ hour of the study is given by

$$T_{m,k} = \sum_{i=1}^{k} t_{m,i}.$$

c. Wind Forcing

Wind measurements are available from C-MAN weather stations on Molasses Reef and Sombrero Reef ("M" and "S" in **Figure 34**). Air temperature and air pressure are also recorded. Wind stress is computed from wind speed using the method recommended by Wu (1980):

$$\tau = \rho_a C_D U^2,$$

where $\rho_a$ is the air density, U is the wind speed in m $s^{-1}$, and $C_D$ is a drag coefficient, given by

$$C_D = (0.8 + 0.065\,U)\,x10^{-3}.$$

Our calculations of air density incorporate both air pressure and air temperature. The direction used for the wind stress vector is the same as the wind direction, once the "meteorological convention" has been removed (the direction from which the wind is blowing is 180° from the direction toward which wind stress is directed).

We use progressive vector diagrams (PVDs) to introduce wind conditions during the summer and winter studies. The units along both the x-axis (east-west, with east defined positive) and y-axis (north-south, with north defined positive) are the units of wind stress: dynes $cm^{-2}$. The plot shows how winds, in the form of wind stress, moved past the weather station. We assume that wind conditions at the weather station represent wind conditions at the study sites as well. The end points of the PVDs can be used to calculate the resultant wind stress--the vector average--for any time period. The resultant direction for each seasonal study is the

heading from the start of the PVD plot to the end; the resultant magnitude is the distance (in wind stress units) divided by the number of hourly observations. The PVD is not intended to provide information on hour-by-hour changes in the magnitude or direction of wind forcing. Rather, it is intended to provide a general overview and to characterize temporal variations over time scales of days and longer.

Wind stress components are compared to the across-isobath current component to investigate wind forcing. Correlation coefficients and coherence spectra (Little and Shure 1988) were used to determine the wind stress component to which the across-isobath flow was most sensitive, as well as the time scales over which this coupling occurred.

d. Correlation of the total current

Current meter data collected at two levels can be compared to quantify the correlation of the total current. Kundu (1976) has described a complex correlation coefficient, $\kappa$, that incorporates both along- (v) and across-isobath (u) components of the current, for example. Decomposing current vectors into u- and v-components, and using "T" and "B" subscripts to indicate flow recorded at top and bottom levels, one calculates

$$m = \frac{\langle u_T u_B + v_T v_B \rangle}{\langle u_T^2 + v_T^2 \rangle^{1/2} \langle u_B^2 + v_B^2 \rangle^{1/2}}$$

and

$$n = \frac{\langle u_T v_B - u_B v_T \rangle}{\langle u_T^2 + v_T^2 \rangle^{1/2} \langle u_B^2 + v_B^2 \rangle^{1/2}}.$$

The correlation coefficient is then given by

$$\kappa = (m^2 + n^2)^{1/2}.$$

The average counterclockwise deflection of the flow at the lower level relative to the flow at the upper level, $\alpha$, is given by

$$\alpha = \tan^{-1} \frac{\langle u_T v_B - u_B v_T \rangle}{\langle u_T u_B + v_T v_B \rangle}.$$

The angle given by the deflection equation above gives equal weight to each hourly deflection. An alternate approach, which compares the endpoints of the two progressive vector diagrams, weighs hourly observations at a given level according to the magnitude of the current speed. In the next section, we will include results from both approaches.

**Results**

Results from the summer study are presented first, followed by results from the winter study. Results from each season have been divided into five sub-sections. First, we present PVDs of the currents recorded at each study site to depict the general flow pattern that occurred during the study period. Second, the across-isobath components of the four current meter records are described--upper and lower levels at the Tennessee Reef and Conch Reef study sites. At the study site near Tennessee Reef, isobaths are oriented approximately 065-245°; at the study site

near Conch Reef isobaths are oriented approximately 052-232°. Third, we summarize results related to tidal exchanges across the reef track. Fourth, we present results of our investigation of density currents. Finally, we present results related to comparisons with wind data.

**Summer Study**

a. Overview of currents

We use this section to introduce the reef tract current patterns from which the across-isobath components were extracted. By including PVDs of the current data, flow patterns that occurred during the entire study periods can be depicted.

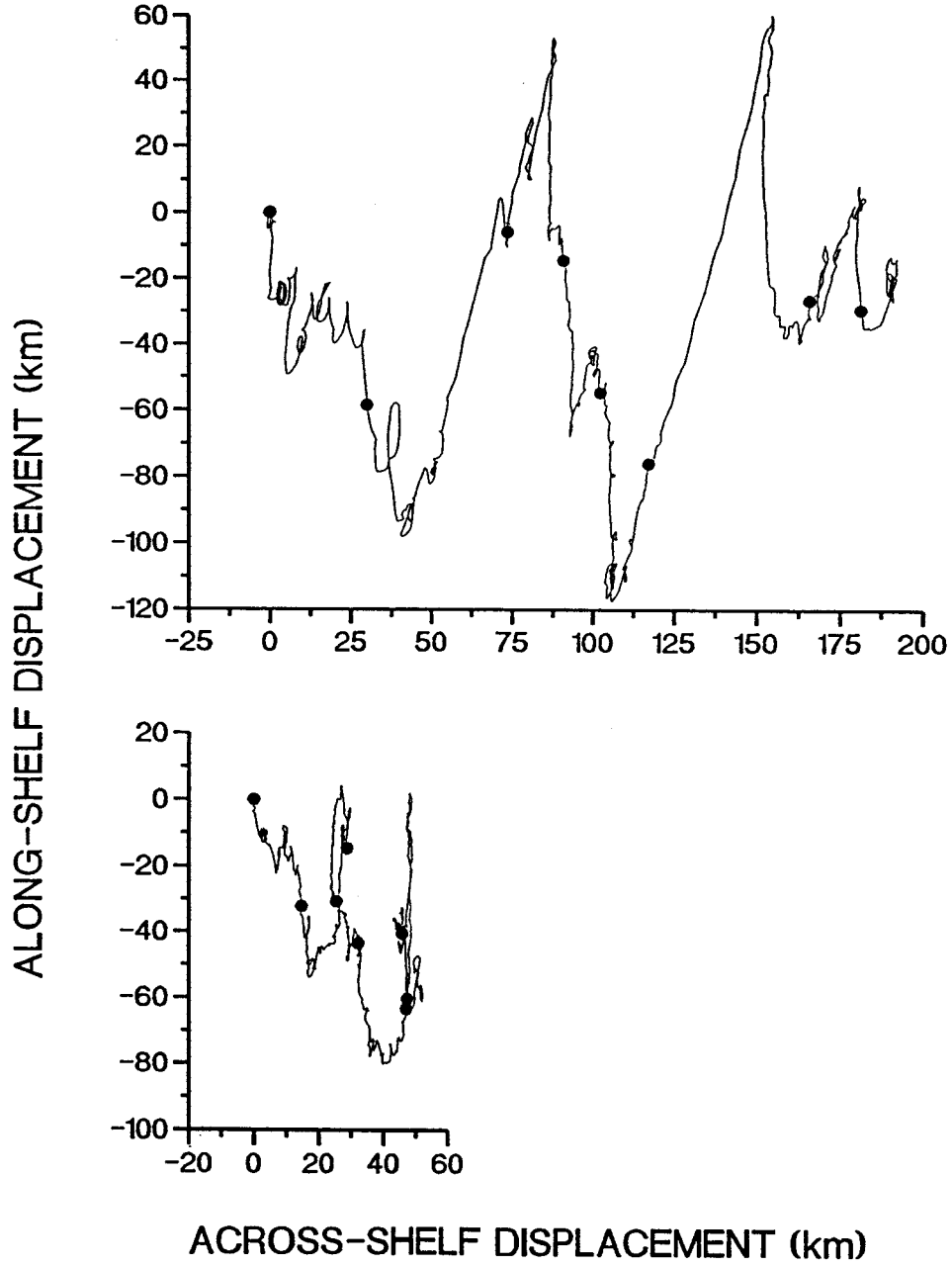


**Figure 35.** Progressive vector diagrams of hourly near-surface (top plot) and near-bottom (bottom plot) currents recorded near Tennessee Reef, June 20 to October 2, 1996.

**Figure 35** shows the PVDs constructed from near-surface (upper plot) and near-bottom currents recorded at the study site near Tennessee Reef, June 20 to October 2, 1996. At both levels, current vectors describe a zig-zag pattern, with a general seaward displacement. The resultant current vector at the upper level (obtained from the endpoints of the PVD) is 2.2 cm $s^{-1}$ with a heading of 162°. The direction is 6° to the right of a directly seaward heading. Near-bottom current vectors have a resultant speed and direction of 0.9 cm $s^{-1}$ and 203°, respectively. Thus, from the PVDs, it appears that near-bottom flow is deflected 41° to the right of the near-surface flow.

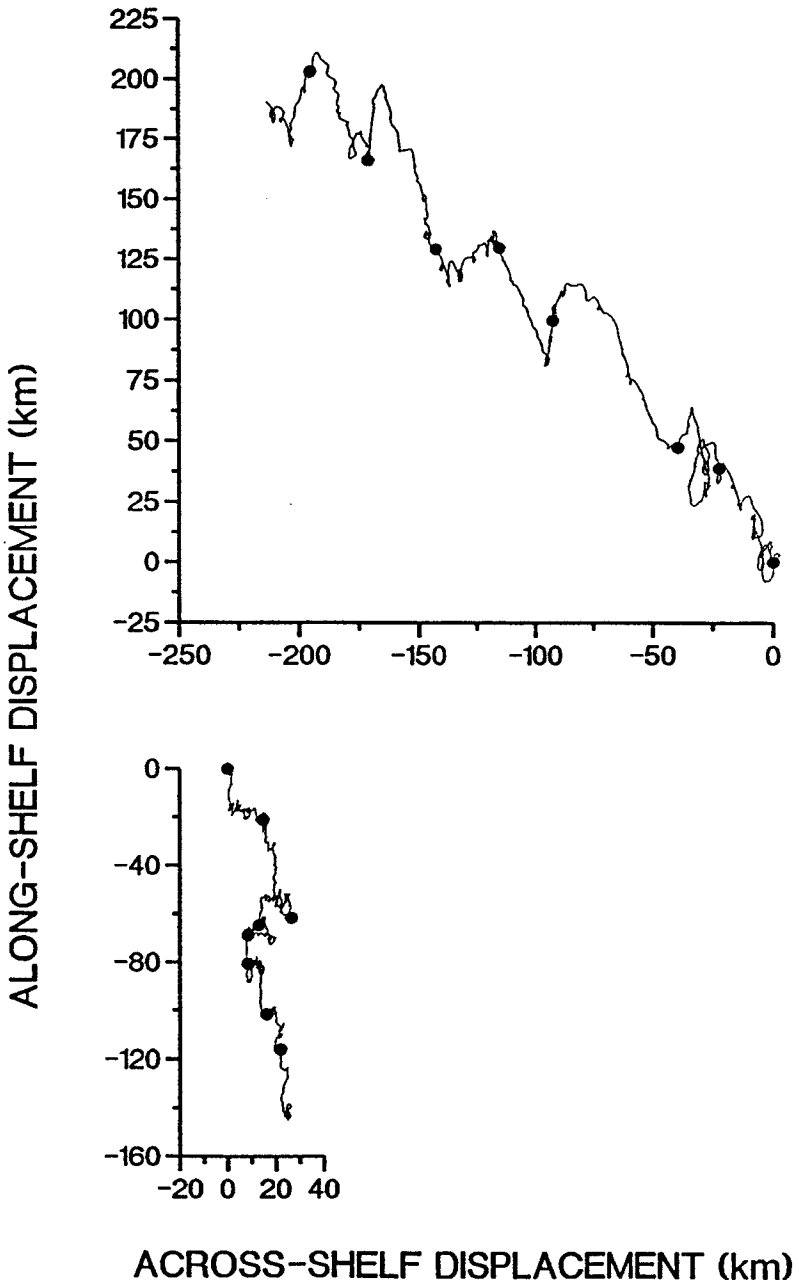


**Figure 36.** Progressive vector diagrams of hourly near-surface (upper plot) and near-bottom (bottom plot) currents recorded near Conch Reef, June 19 to October 3, 1996.

Resultant speeds, mean headings and mean deflections can be misleading, however. Scalar average current speeds (calculated without regard to direction) at the near-surface and near-bottom levels are 18.2 and 9.8 cm $s^{-1}$, respectively--considerably stronger than the resultant speeds. Also, as one can see from **Figure 35**, resultant headings mask completely the zig-zag pattern. The headings of the instantaneous flow at both levels are much more in an along-isobath direction. Values for the mean deflection of the near-bottom flow relative to near-surface flow when equal weight is given to the hourly values are provided below.

**Figure 36** includes the progressive vector diagrams constructed from near-surface and near-bottom currents recorded near Conch Reef, June 19 to October 3, 1996. Near-surface flow has a resultant heading of 004°. Given the 053-233° orientation of the isobaths at this location, the flow is nearly equally distributed between across-isobath in a landward direction and along-isobath northward. The resultant current speed is 3.0 cm $s^{-1}$, compared to a scalar average speed

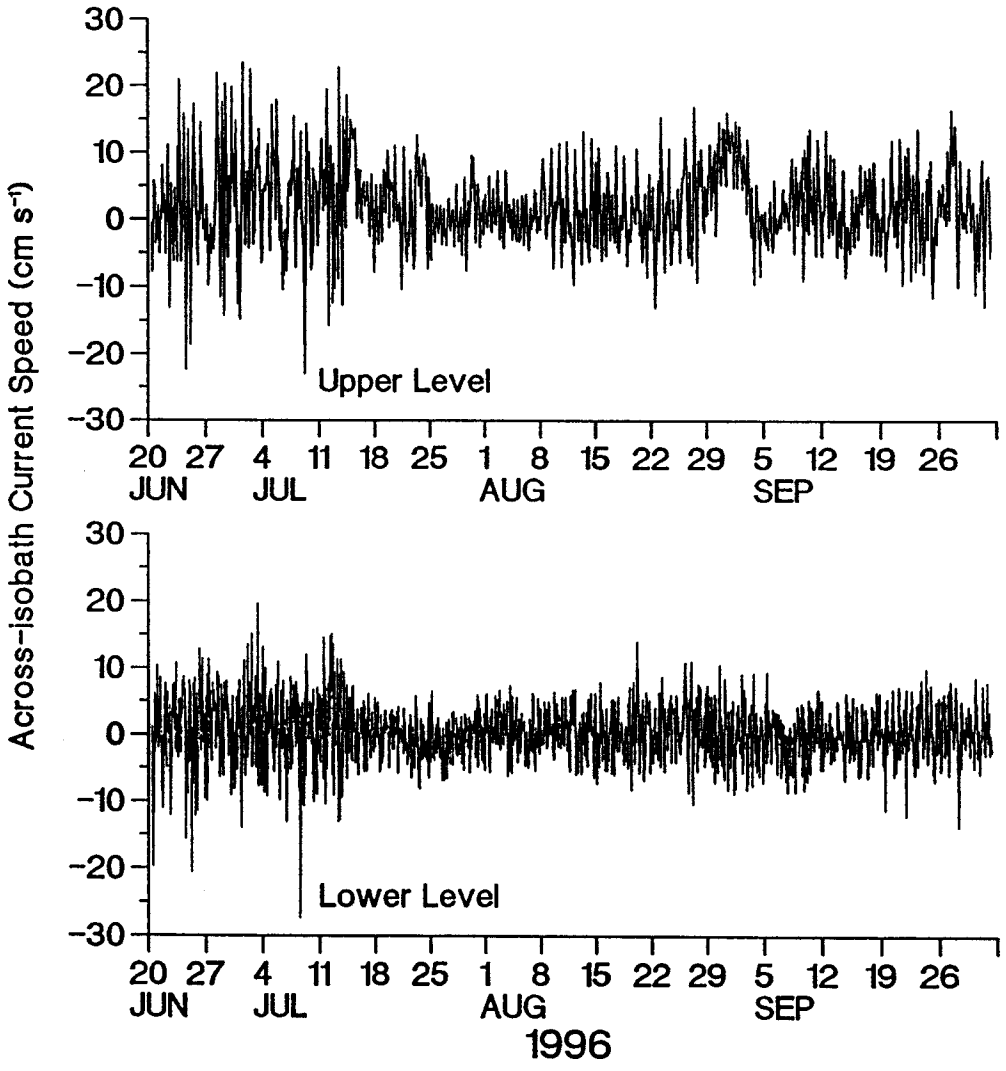


**Figure 37.** Across-isobath current speeds recorded at near-surface and near-bottom levels near Tennessee Reef, June 20 to October 2, 1996. Positive speeds indicate seaward flow.

of 12.2 cm $s^{-1}$. At the near-bottom level, the resultant speed and direction are 1.6 cm $s^{-1}$ and toward 222°. This heading is 11° to the left of a directly along-isobath direction, and it is deflected 142° to the left (counterclockwise) of the near-surface current. Again, the mean deflection and resultant current speed suggested by the PVDs is significantly different from those calculated using the approach suggested by Kundu (1976) (see below).

b. Across-isobath currents

Across-shelf current components from the Tennessee Reef and the Conch Reef study sites are shown in **Figures 37** and **38**. In both figures, currents recorded 6 m below the surface appear in the upper part of the plot, while currents recorded 2 m above the bottom appear in the lower part. At both study sites, across-isobath flow is more active at the upper level, because the flow at the lower level is blocked to some extent by the sloping bottom. At the Tennessee Reef study

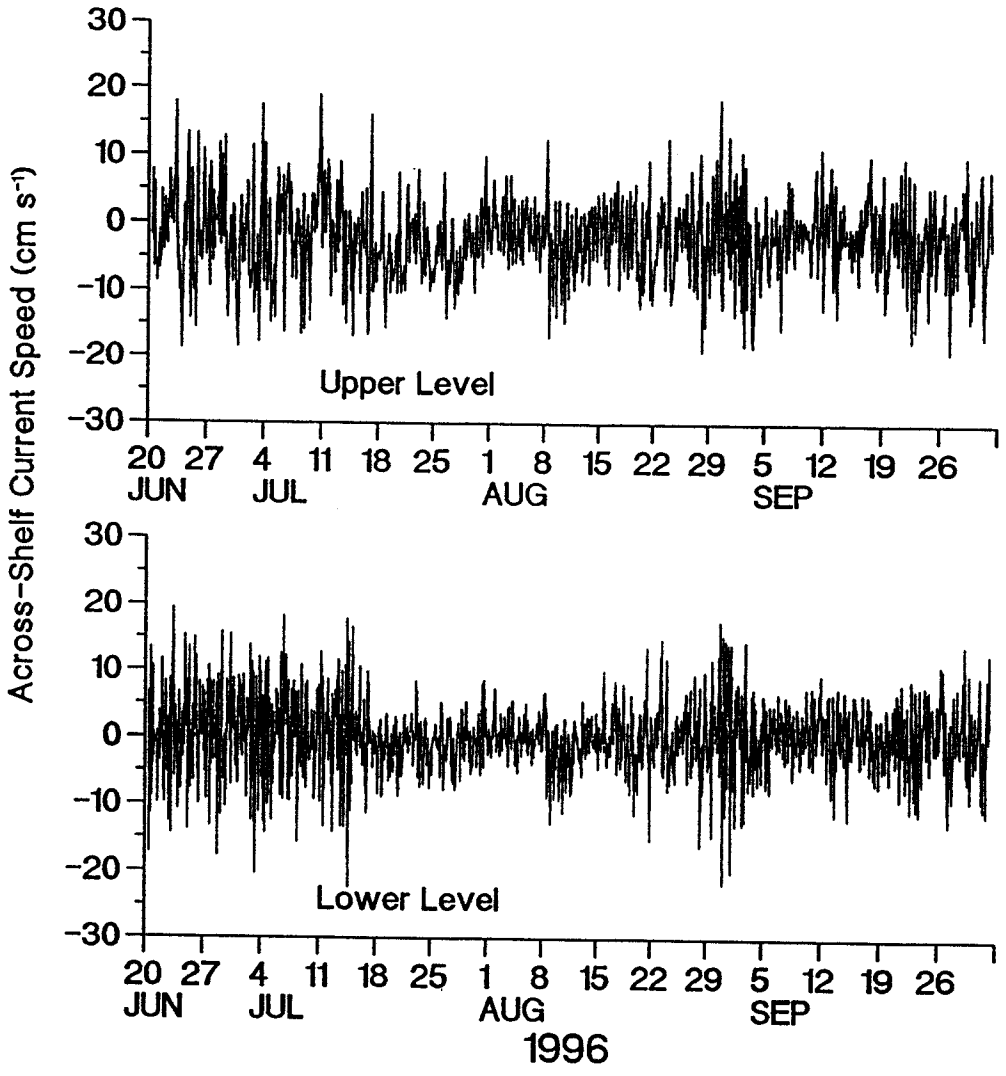


**Figure 38.** Across-isobath current speeds recorded at near-surface and near-bottom levels near Conch Reef, June 20 through October 2, 1996. Positive speeds indicate seaward flow.

site (**Fig. 37**), speeds as high as ±20 cm $s^{-1}$ appear in the early part of the record. Current speeds fluctuate less than about ±10 cm $s^{-1}$ on a day-by-day basis after mid July. Upper level currents are slightly weaker at the Conch Reef study site (**Fig. 38**), and the transition in mid July is less pronounced. A period of sustained seaward flow at the Tennessee Reef study site in late August appears as stronger across-isobath oscillations at the Conch Reef study site.

At the lower level, more active across-isobath flow occurs at both study sites through mid July. The late-August period of greater activity appears only at the Conch Reef study site. At the Tennessee Reef study site, across-isobath flow from mid July to early October is generally between ±5-10 cm $s^{-1}$.

Linear regression correlation coefficients give some indication of the vertical coupling of the flow. Of all the combinations of levels and components that were investigated (e.g., upper level, along-isobath flow vs. lower level, along-isobath flow), across-isobath flow at upper and lower levels was of particular interest. At the Tennessee Reef study site, the correlation coefficient was +0.0749--clearly low, but statistically significant at the 99% confidence level. At the Conch Reef study site, the same combination of current components produced a correlation coefficient of +0.3555. The positive correlation indicates that seaward flow at one level was accompanied by seaward flow at the other.

Although along-isobath flow was not the primary focus of this study, correlation coefficients were computed. As expected, along-isobath flow in the upper and lower layers of the water column is much more highly correlated. At the Tennessee Reef study site, the correlation coefficient of along-isobath flow at the upper and lower levels was +0.8304; at Conch Reef, it was +0.7178.

Similarly, the correlation of the total current at the upper and lower levels was less important in this study than the correlation of the across-isobath components in particular. Nevertheless, for comparison, correlation coefficients were constructed using the approach described by Kundu (1976). At the Tennessee Reef study site, the correlation coefficient for the combined along- and across-isobath components at the upper and lower levels was +0.770, and on average the current direction at the lower level was 7.9° to the left of the current direction at the upper level. At the Conch Reef site, the correlation coefficient was +0.594, and the near-bottom current was 8.4° to the left of the near-surface current, on average.

Comparing the across-isobath current deflections using Kundu's (1976) method with the endpoints of the PVD shows that using resultant speeds, mean headings and mean deflections can be misleading. Scalar average current speeds (calculated without regard to direction) at the near-surface and near-bottom levels near Tennessee Reef are 18.2 and 9.8 cm $s^{-1}$, respectively--considerably stronger than the resultant speeds. Also, as one can see from **Figure 35**, resultant headings mask completely the zigzig pattern. The headings of the instantaneous flow at both levels is much more in an along-isobath direction. Results from the Conch Reef data also shows that the mean deflection suggested by the PVDs is significantly different from the 8° counterclockwise angle calculated from Kundu's (1976) deflection equation, and the resultant speed is substantially less than the scalar average of 7.6 cm $s^{-1}$

c. Tidal exchanges

The investigation of tidal exchanges at the reef tract begins with an analysis of the across-shelf component of the current. At the study site near Tennessee Reef, isobaths are oriented approximately 065-245°; at the study site near Conch Reef isobaths are oriented approximately 052-232°.

Harmonic analysis of the time series shown in **Figures 37** and **38** indicates that the tidal component of the across-isobath current speed is a relatively small part of the total instantaneous across-isobath flow. **Table 5** shows that the across-isobath component of the semidiurnal $M_2$ tidal constituent is only 3 cm $s^{-1}$ at the upper level at the Tennessee Reef station, and less than 3 cm $s^{-1}$ at the upper level at the Conch Reef station. Amplitudes calculated from data recorded at the lower levels are significantly less. In general, amplitudes of diurnal constituents are less than amplitudes of semidiurnal constituents, and amplitudes are less at the lower level for all constituents. The across-isobath displacement calculated from these amplitudes are on the order of 0.5 km or less in all instances. Tidal excursions should be treated with suspicion in regions of spatially varying depth, because currents can accelerate and decelerate as they move into shallower and deeper areas, respectively.

**Table 5.** Amplitudes, A, in cm $s^{-1}$, and tidal excursions, E, in km, of the principal tidal constituents at the study sites near Tennessee Reef and Conch Reef. Near-surface currents were recorded 6 m below the surface; near-bottom currents were recorded 2 m above the bottom. Amplitudes less than the 1 cm $s^{-1}$ accuracy of the current meters are not significant (NS), and tidal excursions are not calculated.

| | | Tidal Constituent | | | | | |
|---|---|---|---|---|---|---|---|
| | | $M_2$ | $S_2$ | $N_2$ | $K_1$ | $O_1$ | $P_1$ |
| 1. Tennessee Reef Site | | | | | | | |
| a. near-surface | A | 3.0 | NS | NS | 1.6 | 1.6 | NS |
| | E | 0.4 | | | 0.4 | 0.5 | |
| b. near-bottom | A | NS | NS | NS | NS | NS | NS |
| | E | | | | | | |
| 2. Conch Reef Site | | | | | | | |
| a. near-surface | A | 2.6 | NS | NS | NS | NS | NS |
| | E | 0.4 | | | | | |
| b. near-bottom | A | 1.0 | NS | NS | NS | NS | NS |
| | E | 0.1 | | | | | |

d. Density-driven exchanges

The investigation of density-driven exchanges at the reef tract begins with a perturbation analysis of near-bottom across-isobath current speeds (**Figures 37** and **38**, bottom) and hourly near-bottom density values calculated from conductivity and temperature measurements (not shown). Results suggest that seaward-directed flow is, on average, associated with higher density (**Table 6**). This is consistent with the hypothesis that high-density water is cascading down the continental shelf past the study site, temporarily deflecting the along-isobath flow in a seaward direction. The association is not a strong one, however. At the Tennessee Reef study site, the average of the $\rho'u'$ perturbation products is +0.00017 g $cm^{-2}$ $s^{-1}$. The positive value indicates that higher than average density is, more often than not, associated with a seaward-deflected current. The magnitude of the covariance, however, indicates that the mass transport is small. In contrast,

the mass transport associated with the mean across-isobath current is three orders of magnitude larger. Taking this one step futher, the correlation coefficient calculated from the 2,495 pairs of $\rho'$ and u' is +0.0642. Again, the positive correlation is consistent with the concept of density currents. A t-test of the correlation coefficient indicates that it is significant at the 95% confidence level, but the low value is a clear indication that density currents are embedded in a significant amount of "noise" that is unrelated to variations in density.

**Table 6.** Perturbation products calculated from near-bottom density (in gm $cm^{-3}$) and across-isobath current speed (in cm $s^{-1}$) recorded at Tennessee Reef and Conch Reef, June 20 through October 2, 1996. Angle brackets, < >, indicate study-mean values; apostrophes indicate instantaneous departures from study mean values.

| | | | |
|---|---|---|---|
| 1. Tennessee Reef | | | |
| | | $\langle\rho\rangle$ | $\rho'$ |
| | $\langle u\rangle$ | 0.587 | 0.0 |
| | u' | 0.0 | 0.00017 |
| 2. Conch Reef | | | |
| | | $\langle\rho\rangle$ | $\rho'$ |
| | $\langle u\rangle$ | 0.280 | 0.0 |
| | u' | 0.0 | 0.00011 |

Similar analysis of the Conch Reef data produces similar results. A perturbation analysis of the near-bottom across-isobath current components and near-bottom density reveals that seaward flow is associated with higher-than-average density. But while the relationship is statistically significant, it is not physically significant. The covariance is +0.00011 g $cm^{-2}$ $s^{-1}$, but the correlation coefficient is only +0.0412. While this is significant at the 99% confidence level, it suggests that much of the variation in near-bottom density, and most of the fluctuations in the across-isobath component of the current are not related. The seaward mass transport associated with the slight mean across-isobath flow is over three orders of magnitude larger than that associated with the hour-by-hour fluctuations in density and current speed.

As noted in the Methodology section, mean values such as those appearing in **Table 6** can mask considerable, and sometimes important temporal variability. **Figure 39** is an analog representation of how the $\rho'u'$ perturbation products increase in time at the two study sites. When the curves are becoming increasingly positive, higher-than-average density is occurring with seaward flow, and lower-than-average density coincides with landward flow. When the curves become more negative, either above average density water is being transported landward or below average density water is moving seaward. Data from Conch Reef (lower plot) show a rapid increase from the start of the study through mid July. Increases and decreases are relatively subtle after that, and little net gain occurs through the rest of the study. At Tennessee Reef, perturbation products increase significantly only during the first three weeks of the study, then again during the second and third weeks of September.

The similarity of the two plots is slight, and across-isobath mass transport at the two study sites appear to respond either to different mechanisms, or to significantly different

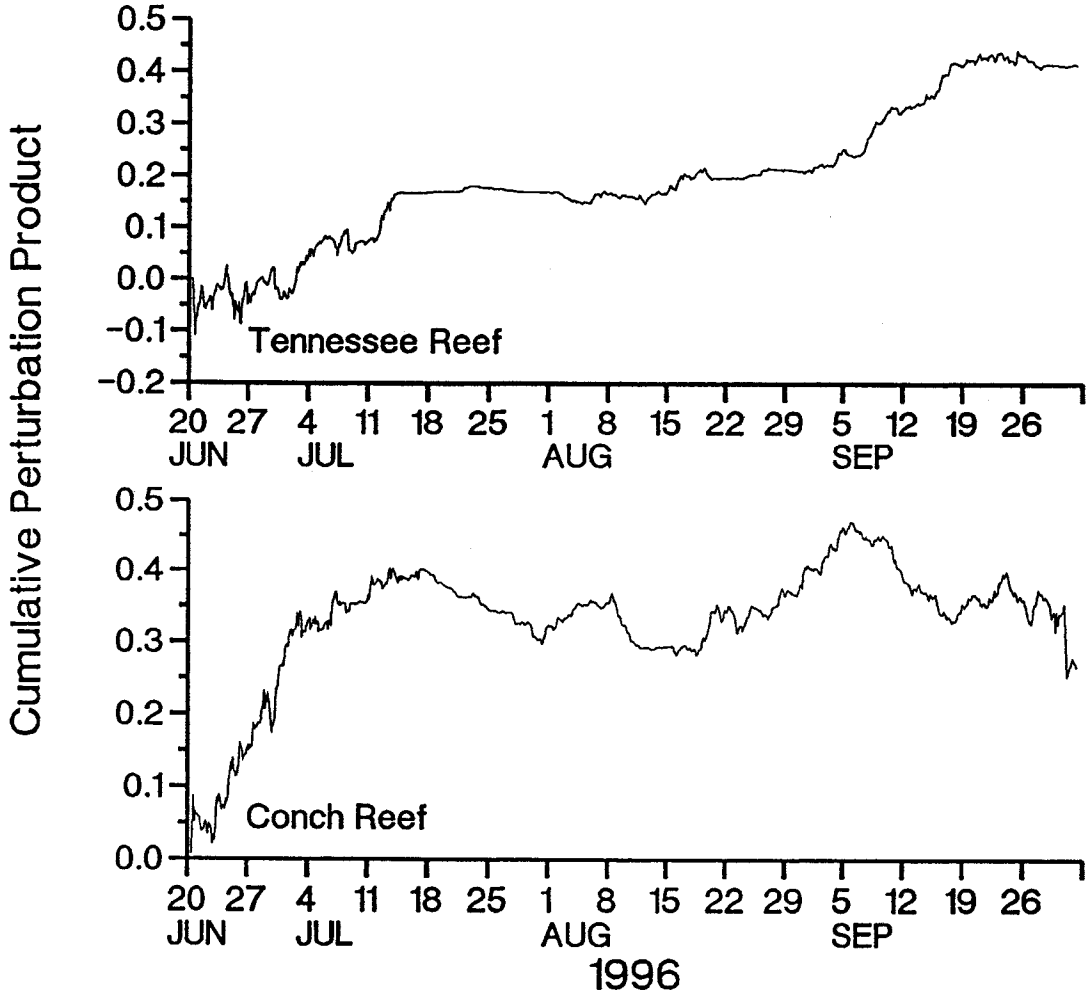


**Figure 39.** Cumulative u'ρ' perturbation products calculated from near-bottom across-isobath current speeds, in cm $s^{-1}$, and near-bottom densities, in g $cm^{-3}$, June 20 through October 2, 1996.

magnitudes of the same mechanisms. This is evidence that different segments of the reef tract experience quite different across-isobath exchanges.

e. Wind-driven exchanges

An overview of wind conditions during the June 20 to October 2 summer study is provided by the progressive vector diagrams shown in **Figure 40**. Dots have been entered at the start of each month to provide some indication of time.

At Molasses Reef, southerly winds produced wind stress directed northward from the start of the study through approximately mid July. From then through the end of the study, wind stress was directed generally toward the west-northwest (290°). Recalling the 052-232° orientation of the reef tract and isobaths at this location, wind stress from the end of July through September was within 30° of a directly landward heading, but with a slight along-isobath component toward Key West.

At Sombrero Reef, the wind stress pattern is generally similar. Recalling the 065-245° orientation of the reef tract at the Tennessee Reef study site, however, wind stress during most of the study had a stronger along-isobath component.

The investigation of wind-driven exchanges at the reef tract began with the determination

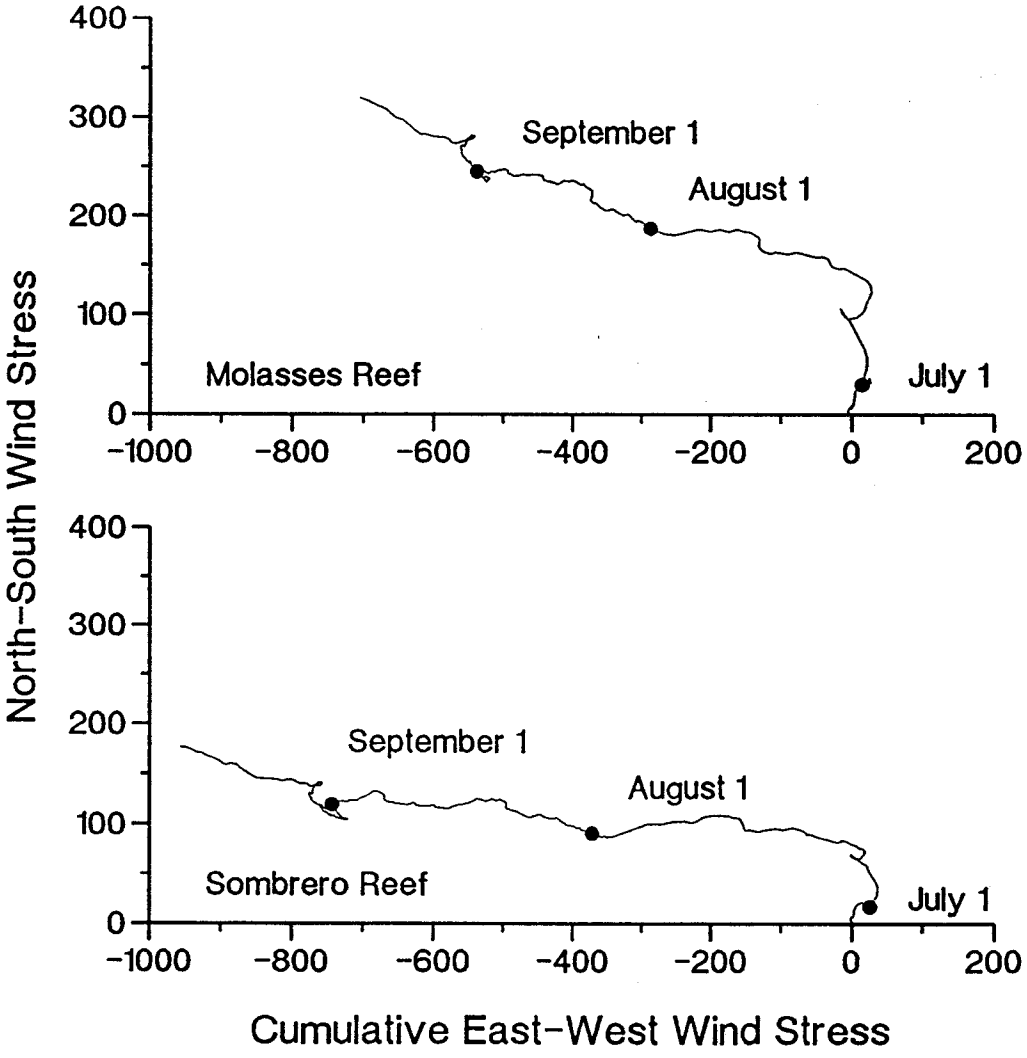


**Figure 40.** Progressive vector diagram of wind stress vectors calculated from hourly winds recorded at Molasses Reef (upper plot) and Sombrero Reef (lower plot), June 20 through October 2, 1996.

of which wind component is most efficient in moving water landward or seaward. Correlation coefficients calculated from low-pass filtered across-isobath currents and low-pass filtered wind components indicated that winds into the northeasterly quadrant were most highly correlated with across-isobath flow. For Sombrero Reef winds and for currents near Tennessee Reef, across-isobath flow at the upper level was most highly correlated with winds toward 013° ($r = +0.3048$), while across-isobath flow at the lower level was most correlated with winds directed toward 024° ($r = +0.1455$).

For Molasses Reef winds and currents recorded near Conch Reef, across-isobath flow at the upper level was most correlated with winds directed toward 048° ($r = +0.2852$), while across-isobath flow at the lower level was most correlated with winds toward 015° ($r = +0.2053$). The positive correlation indicates that northeastward wind stress results in seaward flow. This is consistent with Ekman dynamics, in which currents are to the right of the surface wind (northern hemisphere), although is is likely that the relationship between wind and current reflects a regional flow pattern that is more complicated than a local response to wind forcing. Our results

do not indicate a two-layered flow: Seaward at the upper level but landward at the lower level, for example. As expected, higher correlation coefficients were calculated from currents recorded at the upper level at each study site--where flow should be more responsive to wind forcing.

Spectral analysis of across-isobath flow and the wind stress components listed above provide additional information relating to the time scales over which currents are most responsive to wind forcing and the time lag that occurs between variations in wind stress and the resulting wind-driven current. Spectral analyses paired upper level across-isobath currents recorded near Tennessee Reef with several wind stress components. The along-isobath and across-isobath wind stress components were investigated, as was the 013-193° component that was most highly correlated with across-isobath flow. Similarly, using wind data from Molasses Reef and current meter data from near Conch Reef, across-isobath flow was investigated as a response to several wind stress components. Results (not shown) indicated that the highest coherence occurred over time periods of about 5-6 days. Not surprisingly, highest coherences were found at the upper levels, 6 m below the surface. In several cases, spectral analysis suggested that low-frequency variations in across-isobath flow preceded low-frequency variations in wind forcing--the effect preceded the cause by as much as a day in some cases. As noted above, and as discussed in the following section, we interpret this as an indication that across-isobath flow--the exchange of water between Hawk Channel and the Florida Straits--is not simply a response to local wind forcing.

The low-frequency variations in along-isobath flow recorded at the upper level at the study site near Tennessee Reef provide an opportunity to investigate the wind conditions needed to force flow along the reef tract in either direction. Wind stress components computed from Sombrero Reef winds were compared with along-isobath flow from the upper level near Tennessee Reef, and correlation coefficients were used to guide the analysis. The sign of the correlation coefficient was used to distinguish between winds that would drive currents in the direction of Key Largo (along-isobath flow defined positive) and winds that would drive currents in the direction of Key West (defined negative). Both wind stress and along-isobath flow were low-pass filtered to focus on low-frequency fluctuations.

Zero correlation with along-isobath flow was found for a wind direction of 158° (out of the south-southeast). More southerly winds drove the near-surface flow toward Key Largo; more southeasterly winds drove near-surface flow toward Key West. It is noteworthy that unpublished climatological data from Sombrero Reef (1992-1995) indicate that south-southeasterly winds (157.5 ±11.25°) occur about 5% of the time, although they are somewhat more frequent in summer months (7%) than in winter months (4.5%). Throughout the year, and especially during winter months, winds out of the easterly and northeasterly quadrants are a more common occurrence. This is consistent with the flow toward Key West recorded at this location and in nearby waters of Hawk Channel (Pitts, 1994) in previous studies.

**Winter study**

a. Overview of currents

**Figure 41** shows the PVDs constructed from near-surface (top plot) and near-bottom currents recorded at the study site near Tennessee Reef, December 13, 1996 to April 9, 1997. At both levels, current vectors describe a zig-zag pattern, with a relatively steady and pronounced shoreward displacement at the upper level and a weak seaward displacement near the bottom. Both plots show significant along-shelf flow, but reversals occurring over time scales of a few hours to several days result in little net along-shelf displacement. Flow at the lower level is

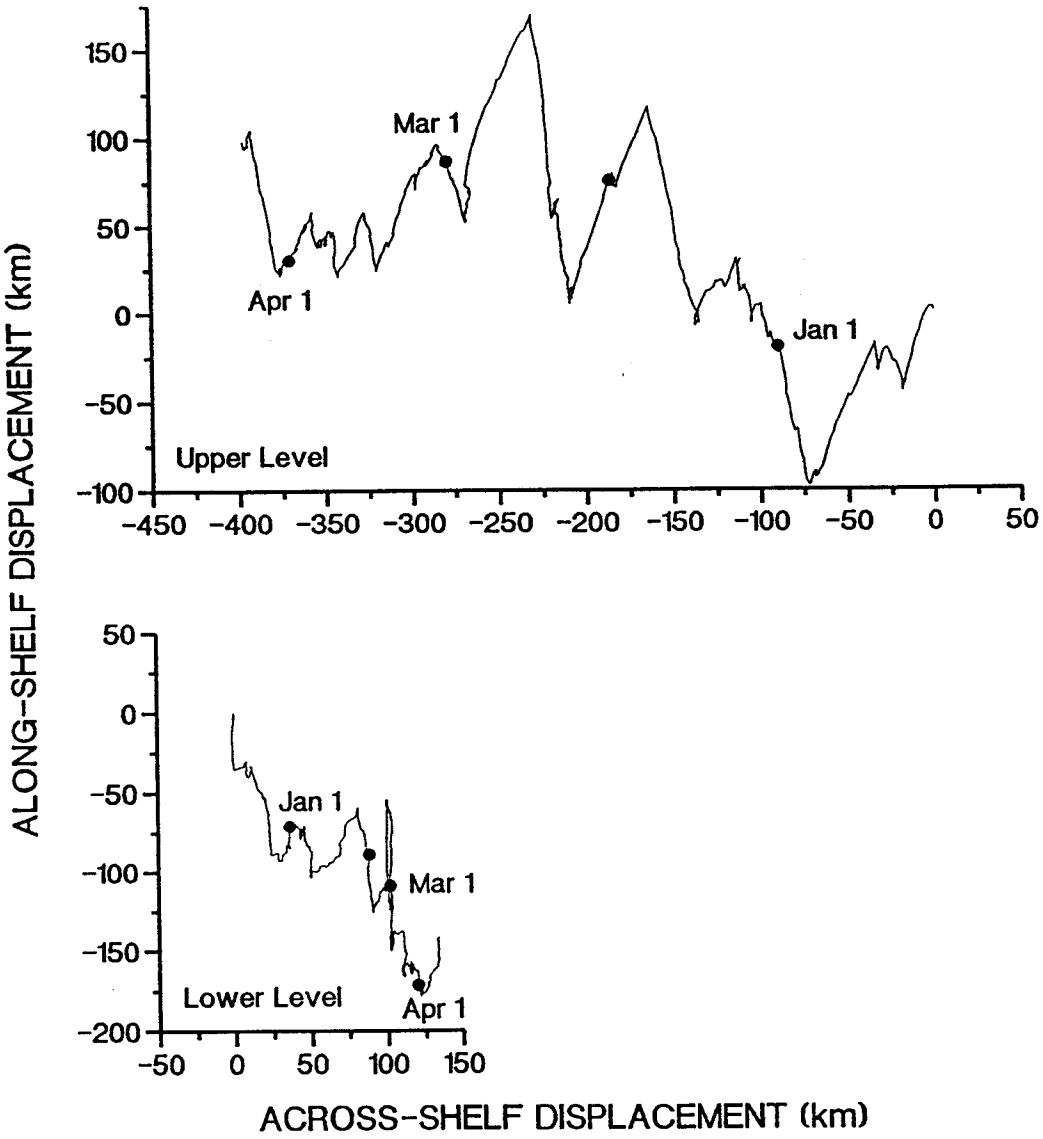


**Figure 41.** Progressive vector diagrams of hourly near-surface (top plot) and near-bottom (bottom plot) currents recorded near Tennessee Reef, December 13, 1996 to April 9, 1997.

almost purely along-shelf for extended periods during the study. The resultant current vector at the upper level (obtained from the endpoints of the PVD) is 4.0 cm $s^{-1}$ with a heading of 348°. Recalling an along-isobath heading at the Tennessee Reef study site of 065-245°, the resultant direction is 13° to the right of a directly shoreward heading. Near-bottom current vectors have a resultant speed and direction of 1.9 cm $s^{-1}$ and 202°, respectively. Thus, from the PVDs, the upper and lower level flow at the Tennessee Reef site is very nearly in opposite directions during the winter study.

Again, resultant speeds, mean headings and mean deflections tell only part of the story. Scalar average current speeds (calculated without regard to direction) at the near-surface and near-bottom levels are 16.3 and 9.5 cm $s^{-1}$, respectively, and considerably stronger than the resultant speeds. Also, as one can see from **Figure 41**, resultant headings mask completely the zig-zag pattern. The headings of the instantaneous flow at both levels is much more in an along-

isobath direction. As seen from calculations using Kundu's (1976) deflection equation, the mean deflection of the near-bottom current vectors is approximately 8° to the left of the near-surface current when equal weight is given to the hourly values.

**Figure 42** shows the progressive vector diagram constructed from near-surface currents recorded near Conch Reef, December 13, 1996 to April 9, 1997. Except for a few minor perturbations the near-surface flow at this site is mostly along-isobath toward Miami with a slight onshore deflection. The resultant speed is 7.5 cm $s^{-1}$ toward 032° during the 117-day study period. The scalar average current speed is 14.0 cm $s^{-1}$.

b. Across-isobath currents

Across-shelf current components recorded 6 m below the surface (top plot) and 2 m above

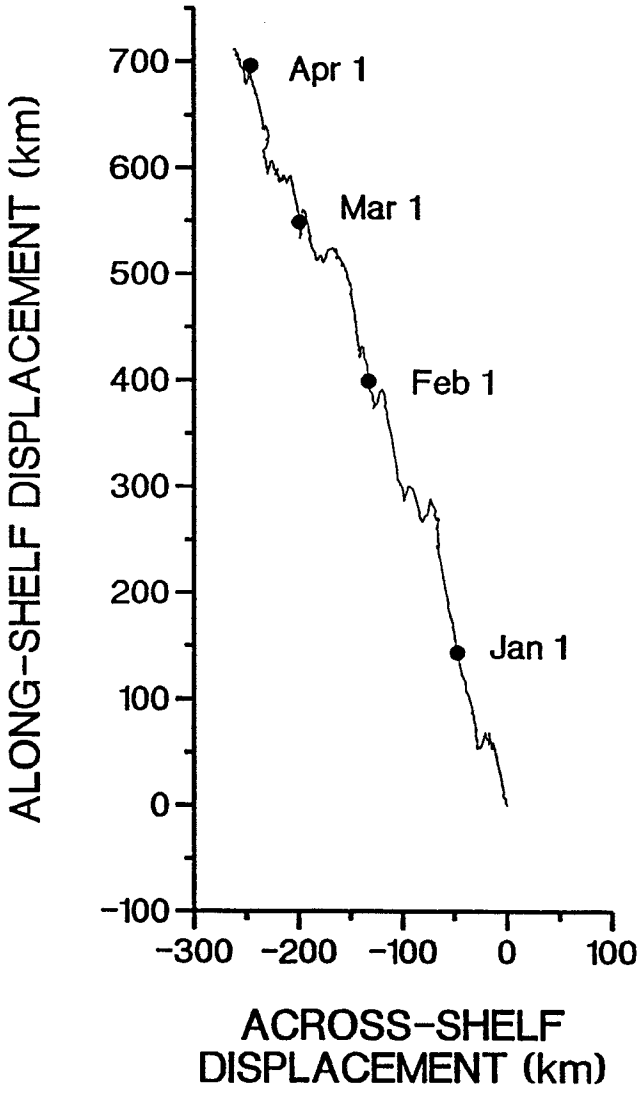


**Figure 42.** Progressive vector diagram of hourly near-surface currents recorded near Conch Reef, December 13, 1996 to April 9, 1997.

the bottom near Tennessee Reef are shown in **Figure 43.** The top plot shows an across-isobath current speed curve that is shifted to the negative side of the plot indicating shoreward flow during this 117-day study period. Current speeds generally range between +10 to -15 cm $s^{-1}$ with a mean of -3.9 cm $s^{-1}$ and a standard deviation of 5.2 cm $s^{-1}$. Fluctuations of ±15 cm $s^{-1}$ occur near the end of the study period. Periods of sustained shoreward flow at this level occur throughout January and from mid to late February. Across-isobath flow near the bottom generally fluctuates ±10 cm $s^{-1}$, has a mean of 1.3 cm $s^{-1}$ and a standard deviations of 4.3 cm $s^{-1}$. The more active across-isobath flow at the upper level may be due to a blocking effect of the sloping bottom on the lower level currents. However, on several occasions lower level currents are stronger than those recorded near the surface. This is most evident in mid January when across-isobath currents near the bottom reach nearly 28 cm $s^{-1}$.

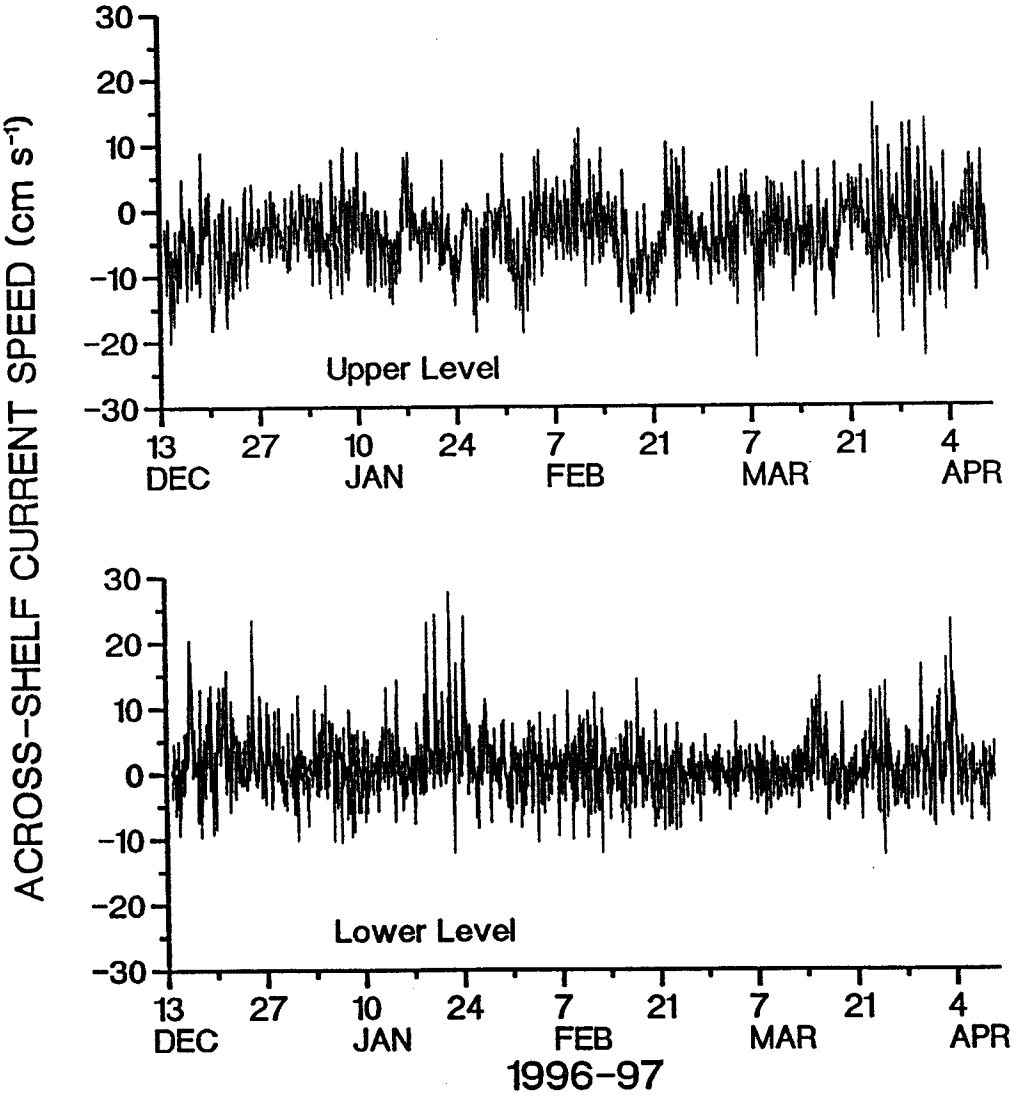


**Figure 43.** Across-isobath current speeds recorded at near-surface and near-bottom levels near Tennessee Reef, December 13, 1996 to April 9, 1997. Positive speeds indicate seaward flow.

Upper level across-shelf currents are slightly weaker at the Conch Reef study site (**Figure 44**) when compared to near surface currents at Tennessee Reef. Like the upper level at Tennessee Reef the near-surface Conch Reef currents are shifted to the negative side of the plot. The standard deviation is 4.7 cm $s^{-1}$ and the time series mean is -2.6 cm $s^{-1}$. The January and February periods of sustained onshore flow recorded at the upper level at Tennessee Reef also occurred at the upper level at Conch Reef.

Linear regression correlation coefficients give some indication of the vertical coupling of the flow at the Tennessee Reef study site. The correlation coefficient of the across-isobath flow at upper and lower levels was -0.106--clearly low, but statistically significant at the 99% confidence level. The negative correlation indicates that seaward flow at one level was accompanied by shoreward flow at the other. Although along-isobath flow was not the primary focus of this study, correlation coefficients were computed. As expected, along-isobath flow in the upper and lower layers of the water column is more highly correlated. The correlation coefficient of along-isobath flow at the upper and lower levels near Tennessee Reef was +0.886.

Similarly, the correlation of the total current at the upper and lower levels was less important in this study than the correlation of the across-isobath components in particular. Nevertheless, for comparison, correlation coefficients were constructed using the approach described by Kundu (1976). At the Tennessee Reef study site, the correlation coefficient for the combined along- and across-isobath components at the upper and lower levels was +0.741, and on average the current direction at the lower level was 8.4° to the left of the current direction at the upper level.

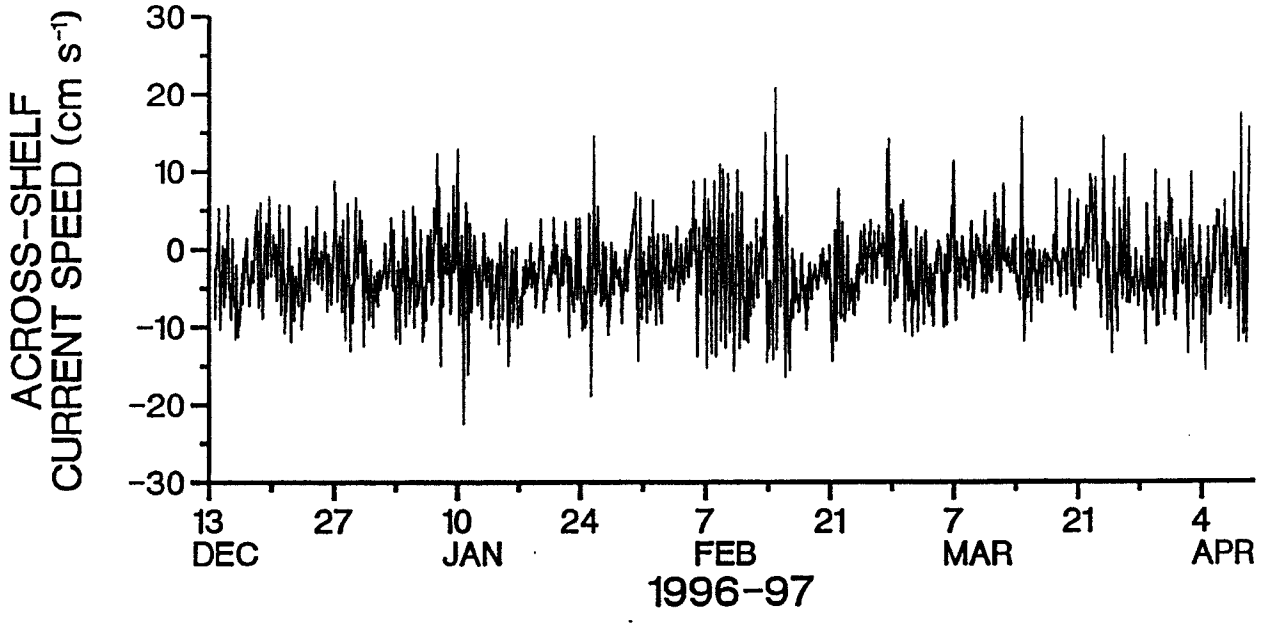


**Figure 44.** Across-isobath currents speeds recorded at the near-surface level near Conch Reef, December 13, 1996 to April 9, 1997. Positive speeds indicate seaward flow.

c. Tidal exchanges

Across-shelf tidal exchanges at the two reef tract study sites during winter months were quantified by harmonic analysis of the time series shown in **Figures 43** and **44** and results appear in **Table 7.** Results indicate that the tidal component of the across-isobath current speed is a relatively small part of the total instantaneous across-isobath flow. In general, amplitudes of diurnal constituents are less than amplitudes of semidiurnal constituents, and amplitudes of all constituents are less at the lower level. The across-isobath component of the semidiurnal $M_2$ tidal constituent is 3.2 cm $s^{-1}$ at the upper level at the Tennessee Reef station, and only 1.4 cm $s^{-1}$ at the upper level at the Conch Reef station. Amplitudes of all diurnal and semidiurnal tidal constituents calculated from data recorded at the lower level near Tennessee Reef are within the precision of the current meter. The across-isobath displacement calculated from the amplitudes of the principal constituents are on the order of 0.5 km or less. As noted above, tidal excursions should be treated with caution in regions of spatially varying depth, because currents can accelerate and decelerate as they move into shallower and deeper areas, respectively.

**Table 7.** Amplitudes, A, in cm $s^{-1}$, and tidal excursions, E, in km, of the principal tidal constituents at the study sites near Tennessee Reef and Conch Reef. Near-surface currents were recorded 6 m below the surface; near-bottom currents were recorded 2 m above the bottom. Amplitudes less than the 1 cm $s^{-1}$ accuracy of the current meters are not significant (NS), and tidal excursions are not calculated.

| | | Tidal Constituent | | | | | |
|---|---|---|---|---|---|---|---|
| | | $M_2$ | $S_2$ | $N_2$ | $K_1$ | $O_1$ | $P_1$ |
| 1. Tennessee Reef Site | | | | | | | |
| a. near-surface | A | 3.2 | NS | NS | 2.0 | 1.3 | NS |
| | E | 0.5 | | | 0.6 | 0.4 | |
| b. near-bottom | A | NS | NS | NS | NS | NS | NS |
| | E | | | | | | |
| 2. Conch Reef Site | | | | | | | |
| a. near-surface | A | 1.4 | NS | NS | NS | NS | NS |
| | E | 0.2 | | | | | |

d. Density-driven exchanges

Density-driven exchanges near Tennessee Reef were investigated by perturbation analysis of near-bottom across-isobath current speeds (**Figure 43,** bottom) and hourly near-bottom density values calculated from conductivity and temperature measurements (not shown). Results are similar to those obtained for the summer study and suggest that seaward-directed flow is, on average, associated with higher density (**Table 8**). This is consistent with the hypothesis that high-density water is cascading down the continental shelf past the study site, temporarily deflecting the along-isobath flow in a seaward direction. The association is not a strong one, however. The average of the $\rho$'u' perturbation products is +0.00034 g $cm^{-2}$ $s^{-1}$, exactly twice the value calculated during the summer study. The positive value indicates that higher than average

density is, more often than not, associated with a seaward-deflected current. The magnitude of the covariance, however, indicates that the mass transport is small. In contrast, the mass transport associated with the mean across-isobath current is four orders of magnitude larger.

Taking this one step futher, the correlation coefficient calculated from the 2,806 pairs of $\rho'$ and u' is +0.1408. Again, the positive correlation is consistent with the concept of density currents and the value is an order of magnitude greater than the correlation coefficient calculated for the summer study. A t-test of the correlation coefficient indicates that it is significant at the 99% confidence level. However, the relatively low value suggests that most of the variation in near-bottom density and the across-isobath component of near-bottom flow are not related.

**Table 8.** Perturbation products calculated from near-bottom density (in gm $cm^{-3}$) and across-isobath current speed (in cm $s^{-1}$) recorded at Tennessee Reef, December 13, 1996 to April 9, 1997. Angle brackets, < >, indicate study-mean values; apostrophes indicate instantaneous departures from study mean values.

1. Tennessee Reef

| | $\langle\rho\rangle$ | $\rho'$ |
|---|---|---|
| $\langle u\rangle$ | 1.352 | 0.0 |
| u' | 0.0 | 0.00034 |

**Figure 45** is an analog representation of how the $\rho'u'$ perturbation products increase in time at the Tennessee Reef study site, which provides some insight regarding temporal variability in the density-driven exchanges. An ascending curve indicates that higher-than-average density is occurring with seaward flow, and lower-than-average density coincides with landward flow. When the curve becomes more negative, the net mass transport is landward. Results show a stairstep pattern through most of the study period indicating rapid increases in perturbation products that are followed by periods of very small decreases. Two events near the end of the study show short-lived but rapid landward mass transport.

e. Wind-driven exchanges

An overview of wind conditions during the December 13, 1996 to April 9, 1997 winter study is provided by the progressive vector diagrams shown in **Figure 46**. Dots have been entered at the start of each month to provide a time reference.

Winds at Molasses Reef are generally out of the eastern quadrant for most of the study period. Clockwise loops occur throughout the record and reflect the passage of cold fronts. Sustained northerly winds associated with these fronts occur near the beginning of the record and again in mid January. The resultant wind stress is nearly due west for the 117-day study period. Recalling the 052-232° orientation of the reef tract and isobaths at this location, the long periods of sustained easterly and south-easterly wind stress have a landward heading with an along-shelf component toward Key West. With the passage of cold fronts, sustained northerly winds have a seaward heading and an along-isobath component toward Key West. At Sombrero Reef, the wind stress pattern is similar. Given the 065-245° orientation of the reef tract at the Tennessee

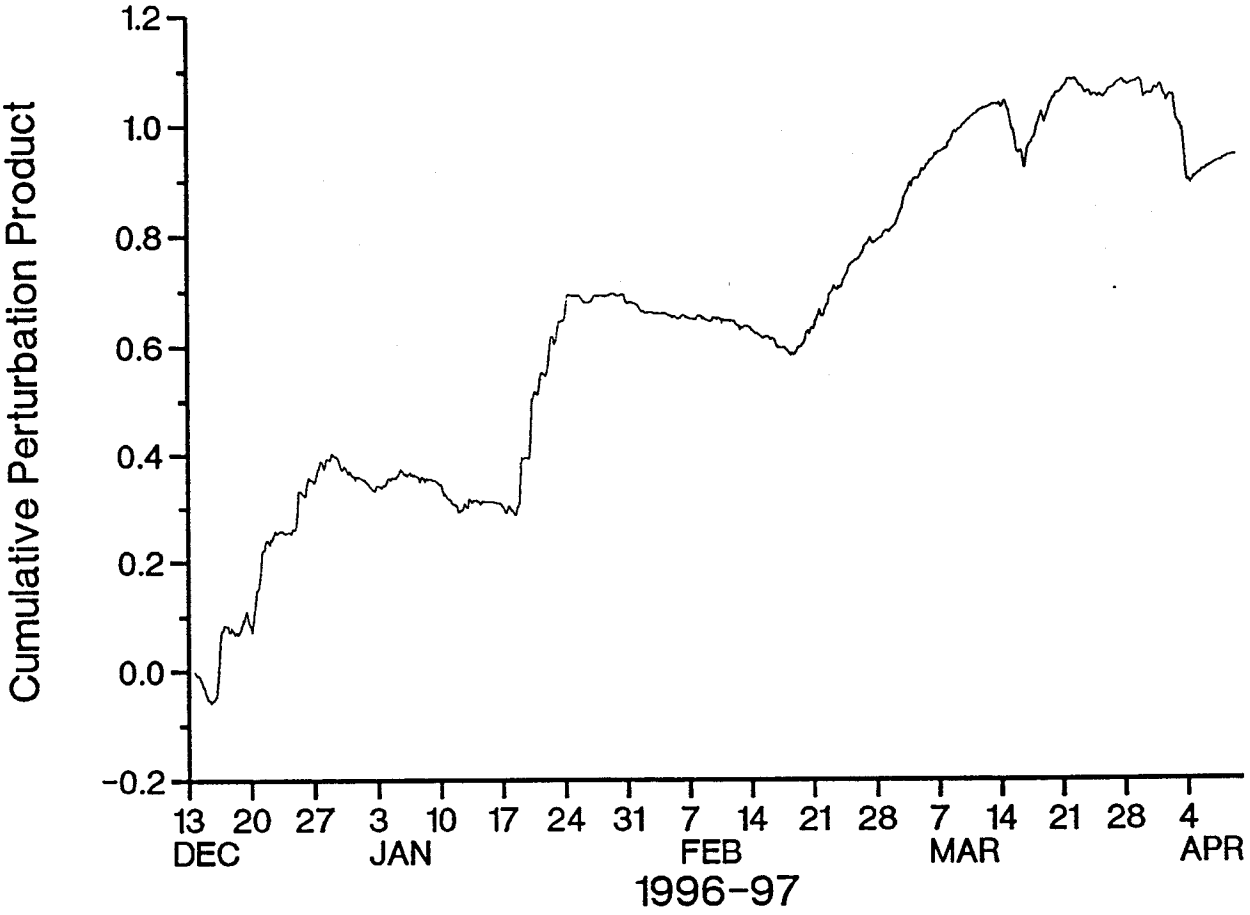


**Figure 45.** Cumulative u'ρ' perturbation products calculated from near-bottom across-isobath current speeds, in cm $s^{-1}$, and near-bottom densities, in g $cm^{-3}$, observed near Tennessee Reef, December 13, 1996 to April 9, 1997.

Reef study site, however, wind stress during most of the study had a stronger along-isobath component. With the passage of cold fronts the seaward component was stronger.

The investigation of wind-driven exchanges at the reef tract during the winter season began with the determination of the wind component most efficient in moving water landward or seaward. Spectral analyses of low-pass filtered across-isobath currents and low-pass filtered wind components (not shown) indicate that the northeast-southwest components of wind stress are most coherent with across-isobath flow near the surface. For Sombrero Reef winds and upper level currents near Tennessee Reef, across-isobath flow is most coherent with the 060°-240° component of the wind stress over time scales of 2-3 days. The phase spectrum indicates that variations in wind stress lead fluctuations of across-isobath flow by 7-8 hours over these time scales. A correlation coefficient of 0.511 (significant well above the 99% confidence limit) was calculated when currents lagged wind stress by five hours. Note that the 060°-240° wind stress component is almost purely along-isobath.

For Molasses Reef winds and currents recorded near Conch Reef, spectral analysis indicates no significant coherence between winds and across-isobath flow. However, a correlation coefficient of 0.318 was calculated for across-isobath currents at Conch Reef and the

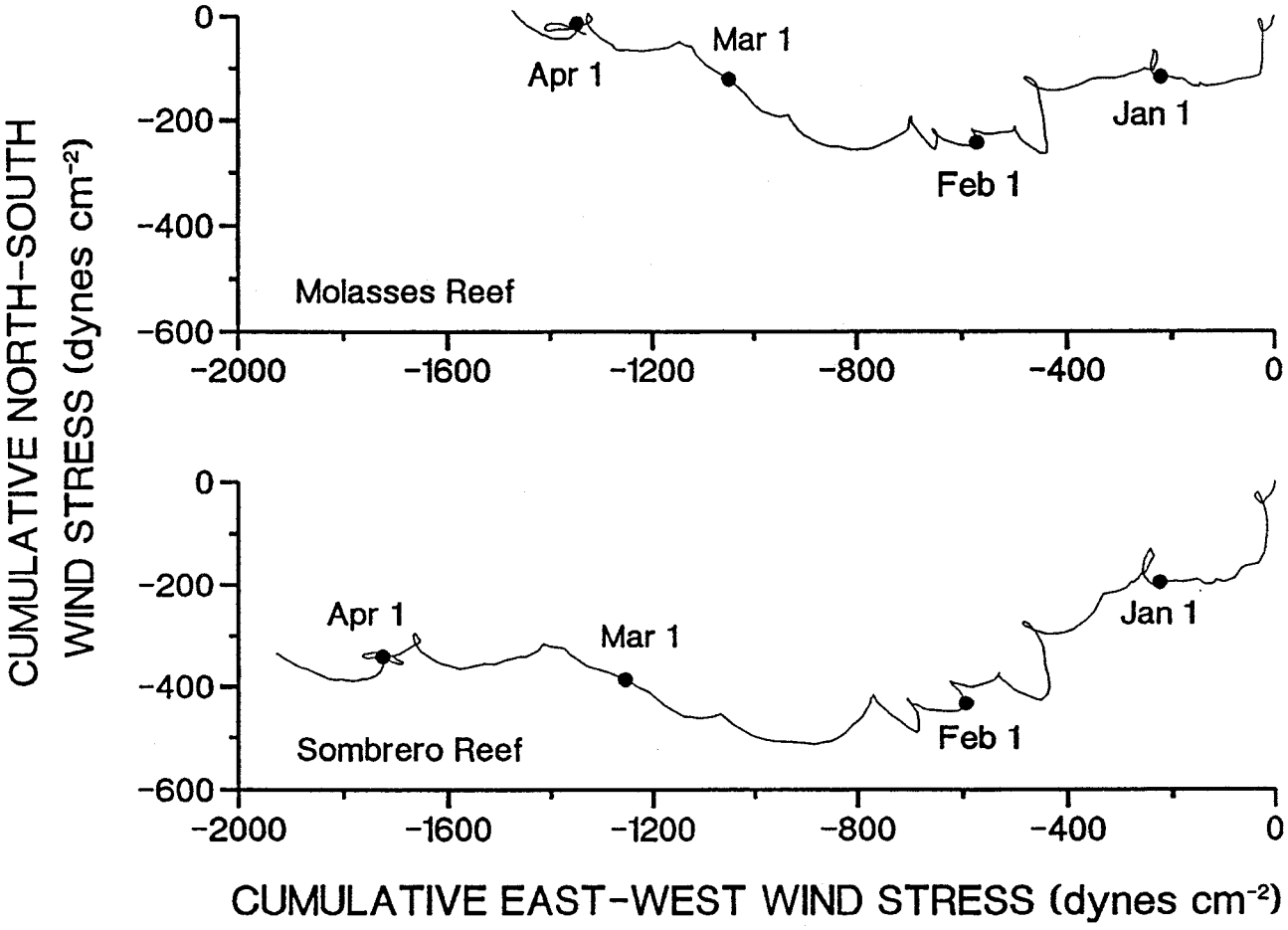


**Figure 46.** Progressive vector diagram of wind stress vectors calculated from hourly winds recorded at Molasses Reef (upper plot) and Sombrero Reef (lower plot), December 13, 1996 to April 9, 1997.

045°-225° component of wind stress with a 5-hour current lag. This is significant above the 99% confidence limit. The positive correlation coefficients and spectral analyses indicate that northeastward wind stress results in seaward flow near the surface at both study sites. This is consistent with Ekman dynamics, in which currents are to the right of the surface wind (northern hemisphere), although is is likely that the relationship between wind and current reflects a regional flow pattern that is more complicated than a local response to wind forcing.

Results from the spectral analyses of Sombrero Reef winds and and near-bottom currents at Tennessee Reef indicate that across-isobath flow was most coherent with the 155-335° wind stress component. Coherence significant at the 95% confidence level occurred over time scales of 2-3 days using this wind stress component. The phase spectrum indicates that winds lead across-isobath flow by 14-16 hours over these time scales. A correlation coefficient of 0.354 was calculated with a 21-hour current lag. The results suggest a two-layered across-isobath flow near Tennessee Reef, with landward flow at the upper level but seaward flow at the lower level.

Strong along-isobath flow was recorded at the upper level at both reef tract sites (**Figures 41** and **42**) during the winter study, and a comparison of wind and current data reveals the wind

directions that are most effective in producing a flow parallel to the reef tract. Analytical techniques were the same as those used to investigate wind-driven across-isobath flow. Results (not shown) indicate that upper level along-isobath flow near Tennessee Reef was most coherent with the 015°-195° component of wind stress from Sombrero Reef at a periodicity of 64 hours. The phase spectrum indicates that currents lag wind stress by about 14 hours at this periodicity. A correlation coefficient of 0.405 was calculated using this wind stress component with a 14-hour current lag.

Results from the study site near Conch Reef indicate a closer coupling between winds and along-isobath flow. Spectral analysis indicates that the 075°-255° component of wind stress is coherent with along-isobath currents at periodicites of 85 and 128 hours (three and five days). The phase spectrum indicates a time lead of currents over winds of 3-7 hours at these periodicities. A correlation coefficient of 0.481 was calculated using the 075°-255° wind stress component and a current lead of 7 hours. As noted earlier, the phase lead of wind stress probably indicates that the response is not a result of purely local forcing.

**Discussion**

A comparison of results from summer and winter studies at a given location, and from the two study sites in a given season reveals several similarities. PVDs of upper level currents at Tennessee Reef exhibit zigzag patterns during both seasons, indicating predominately along-shelf flow with low-frequency reversals ocurring over time scales of a few days to a week or more. The main difference between the two records is that resultant flow during summer months is deflected seaward, while flow during winter months exhibits a landward deflection. Lower level currents recorded near Tennessee Reef show winter and summer patterns that are remarkably similar to one another. Like the upper level currents, flow near the bottom was mostly along-isobath. Across-shelf flow was relatively weak and variable, but mostly offshore during both seasons. Upper level currents recorded near Conch Reef also exhibited similar patterns during the summer and winter studies. Both records show an along-shelf flow toward Miami with an onshore deflection. Reversals in the along-isobath flow are more pronounced in the summer record.

Comparisons of wind patterns reveal distinct differences between summer and winter conditions. At Molasses Reef the resultant wind direction after the 104-day summer study period was 302°, during the winter study the resultant direction was 270°. At Sombrero Reef the resultant wind stress during summer was 285° and during the winter study period resultant winds were at 261°, a counterclockwise rotation very similar to that recorded at Molasses Reef. Winter winds at both stations were much more variable when compared to summer conditions, with the passage of cold fronts accounting for much of the variability. Perhaps just as important as the shift in wind direction is the difference in the wind strength between seasons. At Molasses Reef the average scalar wind speed during summer was 5.2 m $s^{-1}$, compared to 6.8 m $s^{-1}$ during winter months. For Sombrero Reef those values were 5.2 m $s^{-1}$ and 7.5 m $s^{-1}$, respectively. On average, winds were 30-40% stronger during winter months.

Results from the summer and winter field studies suggest that wind probably plays the dominant role in driving across-isobath transport at the shelf break. Across-shelf flow at the upper level of both reef tract study sites is forced primarily by northeast-southwest wind stress components during summer and winter months. However, winds during the summer study were characteristically out of the east and southeast. Thus, winds that drive across-isobath exchanges most effectively along this segment of the reef tract are not common during the summer study

period. Winds out of the northeast quadrant are more common during winter months and account for the resultant shoreward transport of near-surface water at both study sites.

It is noteworthy that the time scales over which upper level currents respond to wind forcing differed appreciably between the two seasons. Spectral analysis indicates that across-isobath currents respond to winds over the 5-6 day periodicities during summer months while during the winter study this coupling occurred at periodicities of 2-3 days.

The analysis of our data base does not support a paradigm that involves a two-layered flow comprised of a downwind-directed near-surface layer and an upwind return flow in near-bottom layers. Results from both seasonal studies indicate that the entire water column moves in roughly the same direction at any given time. While resultant across-isobath flows at the upper and lower levels near Tennessee Reef during winter months exhibit opposite signs, the positive correlation coefficient for the combined along- and across-isobath components (+0.741) together with the 8.4° average deflection of the near-bottom currents is convincing evidence that the water column generally moves as a whole during this time period. Still, the resultant across-isobath flow in opposite directions near Tennessee Reef is significant.

Results indicate a close coupling between the along-shelf component of wind stress from Molasses Reef and along-shelf flow at the reef tract near Conch Reef. However, our analysis shows that along-shelf winds ocurred primarily with the passage of cold fronts which forced short-lived reversals in an otherwise steady flow toward Key Largo. During most of the study period wind stress was landward and with a weak along-shelf component. Thus, the quasi-steady along-shelf flow to the north-northeast at Conch Reef is probably a result of other forcing mechanism. For example, the axis of the Florida Current is closer to the shelf break at Conch Reef than at Tennessee Reef, and it probably contributes to the northeastward resultant flow.

The correlation of near-bottom density with near-bottom across-isobath flow suggests that density currents play a relatively minor role in forcing shelf water seaward. Positive co-variances and correlation coefficients indicate that higher than average density is usually associated with a seaward deflection of the along-isobath current. But data from both seasonal studies seem to relegate density currents to one of the minor roles. While the covariance and correlation coefficient obtained from the perturbation analysis for the Tennessee Reef winter study were double the values calculated from the summer data, all values were very small. It is important to keep in mind, however, that while gravitationally-driven density currents may be small, they provide a one-way transport mechanism. Relatively high density water will not run uphill past the study site. Thus, water moving seaward in a density current is unlikely to return, and this is a relatively efficient exchange mechanism. It is noteworthy that the rapid increases in the plot of cumulative perturbation product calculated at the Tennessee Reef site during the winter field study (**Figure 45**) probably reflect the cascading of cold water down the shelf resulting from the passage of cold fronts. A plot of salinity (not shown) indicates relatively stable salinities at the near-bottom station during the winter study period. Thus, the two-fold increase in the covariance during the winter study may indicate that temperature plays a more important role than salinity in driving across-isobath density currents.

Tidal currents appear to play a minor role in exchanging water between Hawk Channel and the Florida Straits as well. On the one hand, tidal currents are always present; on the other hand, it is likely that the net exchange produced by this oscillatory current is small. The net exchange could not be quantified from the available data base, and it can only be postulated that much of the water passing the study site during the first half of any tidal cycle returns during the second half. Furthermore, the magnitude of the tidal excursion is small. Even combining tidal

excursions associated with individual constituents listed in **Tables 5** and **7**, it appears that under spring or tropic tide conditions the maximum across-isobath excursions are 0.5 km or less.

**HYPOTHESIS 6: Episodic wind events have major perturbing effects in tidal channels and at the reef tract, transporting in a few days volumes of water that are commonly transported in several weeks.**

**Introduction**

Primary attention in this final section is given to an examination of episodic, storm-induced anomalous flow patterns and how they compare to mean conditions. Using historical data collected during Hurricane Andrew, Tropical Storm Gordon and the March 1993 "Storm of the Century," we test the hypothesis that episodic wind events have major perturbing effects in tidal channels and at the reef tract. Results put in perpsective the importance of short-lived transport events that import Florida Bay water into Hawk Channel, advect it across Hawk Channel, or export it to the Florida Straits.

**Data Base**

The data used to address this hypothesis were assembled entirely from archived data collected between 1992 and 1994. Specifically, we include 11 time series of current meter data collected from seven study sites during the passage of three of the most energetic wind events to impact the Florida Keys in the last decade (**Figure 47**). All records extend from well before to well after the passage of a given storm to put its effects in proper perspective.

For Hurricane Andrew (August 24, 1992) we include one record from a tidal channel and two from study sites in Hawk Channel as follows:

1. Long Key Channel (24°47.867'N, 80°52.269'W), July 1, 1992 to September 9, 1993;
2. Hawk Channel off Key West (24°30.22'N, 81°50.44'W), July 1, 1992 to August 27, 1993; and
3. Hawk Channel off Bahia Honda Key (24°36.4'N, 81°16.7'W), August 10 through September 9, 1992.

For the "Storm of the Century" (March 1993), we include one tidal channel time series and one Hawk Channel record as follows:

4. Long Key Channel (24°47.867'N, 80°52.269'W), July 1, 1992 to September 9, 1993; and
5. Hawk Channel of Bahia Honda Key (24°36.4'N, 81°16.7'W), July 2, 1992 to July 22, 1993.

For Tropical Storm Gordon (November 15, 1994), we include current meter data from four tidal channels in the Middle and Upper Keys and from one study site at the reef tract:

6. Snake Creek (24°57.425'N, 80°35.372'W), July 1, 1994 to January 3, 1995;
7. Whale Harbor Channel (24°56.51'N, 80°36.80'W), September 20, 1994 to December 13, 1994;
8. Indian Key Channel (24°53.10'N, 80°40.60'W), September 22, 1994 to March 8, 1995;
9. Long Key Channel (24°47.867'N, 80°52.269'W), August 29, 1994 to July 24, 1995; and
10. Tennessee Reef (24°42.50'N, 80°51.35'W), August 8, 1994 to December 8, 1994 (near-surface and near-bottom).

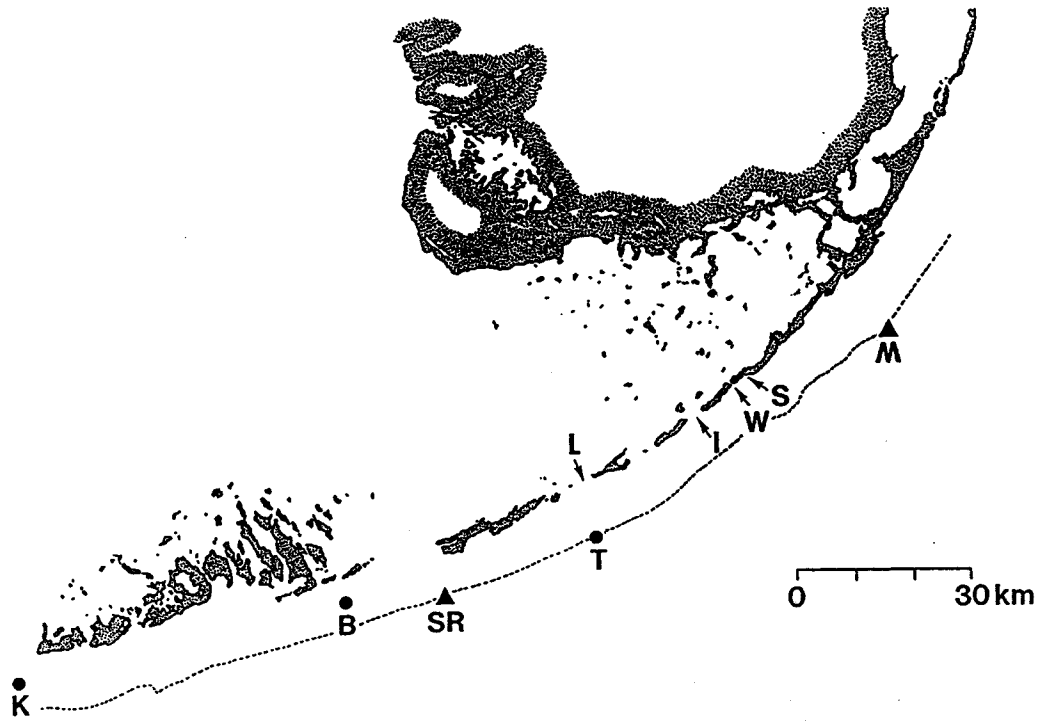


**Figure 47.** Map of the Florida Keys showing the location of study sites in four tidal channels (arrows); including Snake Creek ("S"), Whale Harbor Channel ("W"), Indian Key Channel ("I") and Long Key Channel ("L"). Dots show study sites in Hawk Channel off Key West ("K") and off Bahia Honda Key ("B") and one reef tract site near Tennessee Reef ("T"). Triangles represent the locations of anemometers at Sombrero Reef ("SR") and Molasses Reef ("M").

General Oceanics Model 6011 Mark-II current meters were used in tidal channels, Hawk Channel and the near-bottom station at the reef tract. In tidal channels and Hawk Channel, Mark IIs were suspended anywhere from 1 to 4 m above the bottom on "gallows" type moorings. Total water depths at the tidal channel sites ranged from 3-4 m. Depth at the Hawk Channel sites ranged from 12-14 m. The Mark II used at the near-bottom station near Tennessee Reef was suspended 2 m above the bottom on a taut-line mooring. Near-surface currents at Tennessee Reef were measured hourly using an ENDECO Type 174SSM current meter attached at the top of a taut-line mooring 15 m above the bottom in 21 m of water.

Wind data were obtained nearby from C-MAN stations on Molasses Reef (25° 00.60'N, 80° 22.80'W) and Sombrero Reef (24°37.60'N, 81°06.60'W) to compare with currents recorded during the passage of the storm events ("M" and "SR" in **Figure 47**). Wind speeds and directions were recorded with R.M. Young Wind Monitors.

### Methodology

To describe the relative importance of episodic forcing, we make qualitative comparisons. With recording instrumentation in the water for only three storm events, we do not have a sufficient data base to support the quantitative approach needed to establish empirical relationships. We can, however, compare current speeds recorded during the passage of each storm with values characteristic of the same location before and after the storm. Similarly, we can compare the response to these rare storm events to the response to cold-air outbreaks that

occur several times each winter season.

a. Tidal channels

To investigate the importance of episodic forcing in driving water through tidal channels connecting the Gulf and Atlantic sides of the Keys, current speeds and directions were decomposed into along-channel and across-channel components. Only along-channel components of the hourly current vectors were retained for analysis. To describe the storm-induced flow through a given channel, time series were pruned to cover a period from 1-2 weeks before the storm to 1-2 weeks following its passage. Along-channel components were plotted as hourly current speeds and as cumulative net displacement (Scientific Programming Enterprises, 1985). By our convention negative displacement represents flow from Florida Bay into Hawk Channel.

Harmonic constants of the principal tidal constituents were quantified using the 29-day harmonic analysis program (Dennis and Long, 1971). Transient wind events are put in perspective by comparing tidal current speeds with maximum current speeds recorded during the passage of a storm. Tidal constituents of particular interest included $M_2$, $S_2$, $N_2$, $K_1$, $O_1$ and $P_1$. Nontidal forcing was brought out by subtracting the predicted ebb and flood of the tide (Schureman, 1958) from the total along-channel current. The same six constituents were used in the tidal predictions.

b. Hawk Channel and the reef tract

The response to storm events in Hawk Channel and at the reef tract is examined by plotting the hourly across-isobath and along-isobath current components. Of primary interest in this report are the across-shelf exchanges that represent an exchange of water between Hawk Channel and the Straits of Florida. Isobath orientations for a given study site are provided in the Results section. Again, the entire time series in most cases have been plotted to compare storm effects to average conditions and other forms of meteorological forcing, such as cold air outbreaks.

c. Wind forcing

Wind measurements are available from C-MAN weather stations on the Molasses Reef and Sombrero Reef towers for all three storm events. We compare flow at a given study site with winds recorded at the closest C-MAN station. Wind stress is computed from the square of the wind speed using the method described in the previous section. We use vector plots ("stick plots") of hourly wind stress in dynes $cm^{-2}$ (10 dynes $cm^{-2}$ equals 1 Pascal) to describe wind conditions during the storm events (Scientific Programming Enterprises, 1985). The plots show wind stress from a time interval that completely encompasses the period of anomalous wind forcing. The available data describe only the wind conditions at the weather station. Differences in wind forcing between the weather station and the study sites cannot be estimated from data at hand, but they are assumed to be small.

**Results**

a. Hurricane Andrew

Hurricane Andrew--a very powerful, compact and fast-moving storm--approached South Florida from the east. It crossed the coast south of Miami in the early morning hours of August 24, then passed over Homestead, about 50 km southwest of Miami. After the storm crossed the southern tip of the Florida peninsula it began turning clockwise. Andrew moved across the northeastern Gulf of Mexico. It made landfall a second time two days later along the Louisiana coastline west of New Orleans.

**Figure 48** shows the vector plot of wind stress recorded at the C-MAN station on

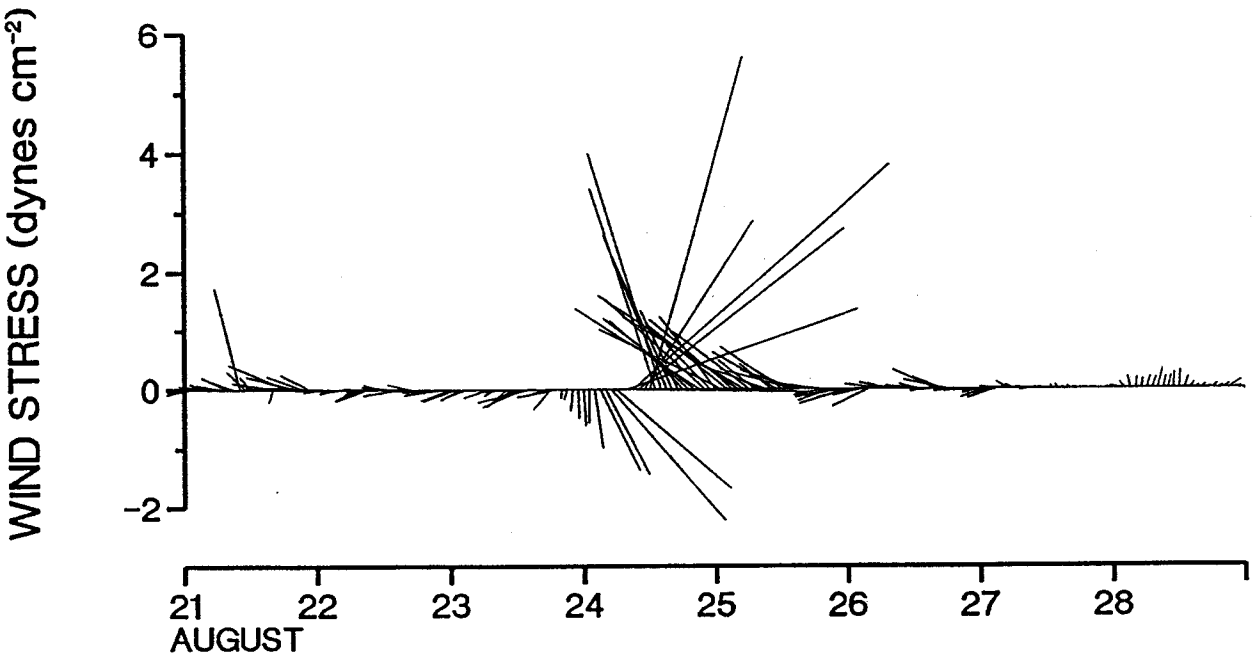


**Figure 48.** Vector plot of wind stress recorded at the C-MAN station on Sombrero Reef from August 21 through August 28, 1992.

Sombrero Reef during the passage of the storm. As the eye of Hurricane Andrew crossed the southern tip of Florida it was about 90 km north of Sombrero Reef. During the 2 days preceding the storm's landfall, wind stress at Sombrero Reef was northwest to southwestward and averaged 0.46 dyne cm$^{-2}$. This corresponds to an average wind speed of 5.5 m s$^{-1}$ (19.8 km hr$^{-1}$). During the late night hours of August 23, wind stress at Sombrero Reef began to rotate counterclockwise. At 0700 EST on August 24 wind stress reached a maximum of 5.81 dynes cm$^{-2}$ (58.7 km hr$^{-1}$) toward 049° at the C-MAN station. Rotation continued during the day and by 1800 EST wind stress was toward 308° at 1.95 dynes cm$^{-2}$. Twenty-four hours after maximum values were recorded at Sombrero Reef, the wind stress vector had completed a full loop and returned to magnitudes and directions characteristic of the summer season (1.25 dynes cm$^{-2}$ toward the west-northwest). Thus, although the eye of this major hurricane passed within 100 km of Sombrero Reef, anomalous wind conditions at that location were short lived.

The response to Hurricane Andrew in Long Key Channel is shown in **Figure 49**. The study site was 50-55 km south of the storm track at its closest point. The top plot shows along-channel current speeds recorded 2 m above the bottom in 3.5 m of water from August 18 through August 31, 1992. By plotting flow through the channel from a week preceding to a week following the storm's passage, the response to the storm itself can be compared to "normal" conditions.

The plot begins with a very regular flood and ebb of the tide. The amplitude of the $M_2$ constituent at the study site is 49 cm s$^{-1}$. Beginning with the second tidal cycle on August 21, every other ebb tide for the next three days is severely damped. This is a result of the diurnal inequality of the tides, however, and not the first effect of the storm. Increasing wind stress as the storm approached would not have such different effects on successive ebb tides, and flood

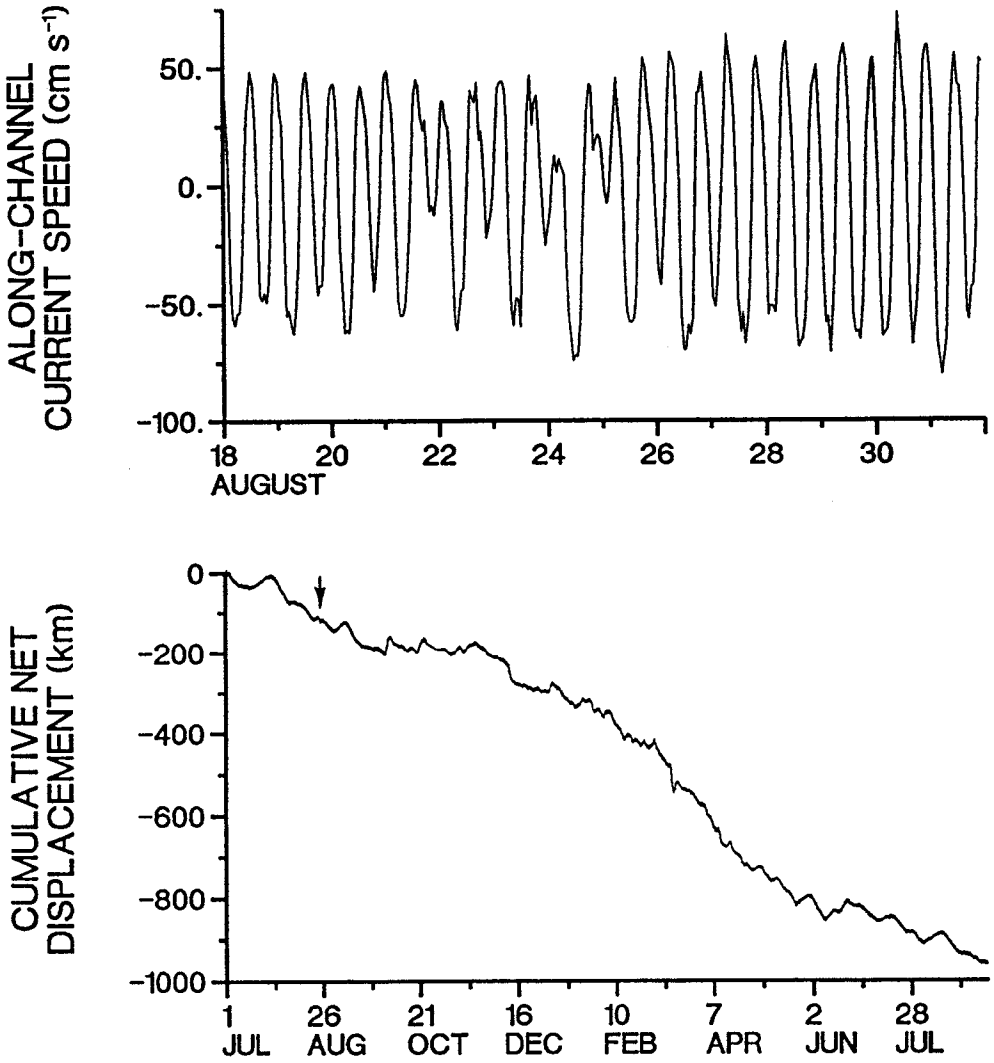


**Figure 49.** Along-channel current speeds recorded 2 m above the bottom at a study site in Long Key Channel, August 18-31, 1992 (top) and cumulative net displacement past the study site from July 1, 1992 to September 9, 1993 (bottom). Negative values indicate flow out of Florida Bay.

tide speeds would increase as ebb speeds diminish. Hurricane Andrew effects appear to be restricted to the day the storm passed closest to the study site, and when strong wind forcing first forced water out of, then into Florida Bay. The weak flood tide recorded in the early morning hours of August 24, the relatively strong ebb at midday, then the prolonged flood followed by a minimal ebb during the next semidiurnal tidal cycle are the extent of the response in Long Key Channel to the passage of the storm.

The bottom plot in **Figure 49** shows the cumulative net displacement of water past the study site in Long Key Channel from July 1, 1992 to September 9, 1993. By including data recorded from well before to well after the storm, effects of the storm can be put in a better perspective, and comparisons can be made with responses to other forcing events. The plot shows a quasi-steady outflow from Florida Bay that averaged -2.6 cm $s^{-1}$ over this 435-day time period. On August 24 outflow from the channel averaged -9.4 cm $s^{-1}$, about a four-fold increase

over the average. However, the plot indicates that the response to the storm (identified by the arrow) is insignificant compared to numerous other perturbations during this time period. For example, the effects of the March 1993 Storm of the Century, which can be seen approximately midway along the plot, were much more pronounced than effects of Hurricane Andrew. Details of flow through Long Key Channel in response to the Storm of the Century appear in the next section. Other fall, winter and early spring perturbations reflect the passage of cold fronts through the region.

Also in operation during the passage of Hurricane Andrew was a study site in the middle of Hawk Channel off Bahia Honda Key, approximately 20 km west of the C-MAN weather station on Sombrero Reef (see **Fig. 47**). The study site was 80-85 km south of the storm track at its closest point. **Figure 50** shows the across-isobath currents recorded 4 m above the bottom in 13 m of water from August 10 to September 9, 1992. This one-month segment was pruned from a much longer time series. Positive values indicate seaward flow (toward 165°). The plot shows that across-isobath current speeds fluctuate generally between +10 and -3 cm $s^{-1}$. Current speeds are positive for much of this one-month record, indicating a net seaward flow. The

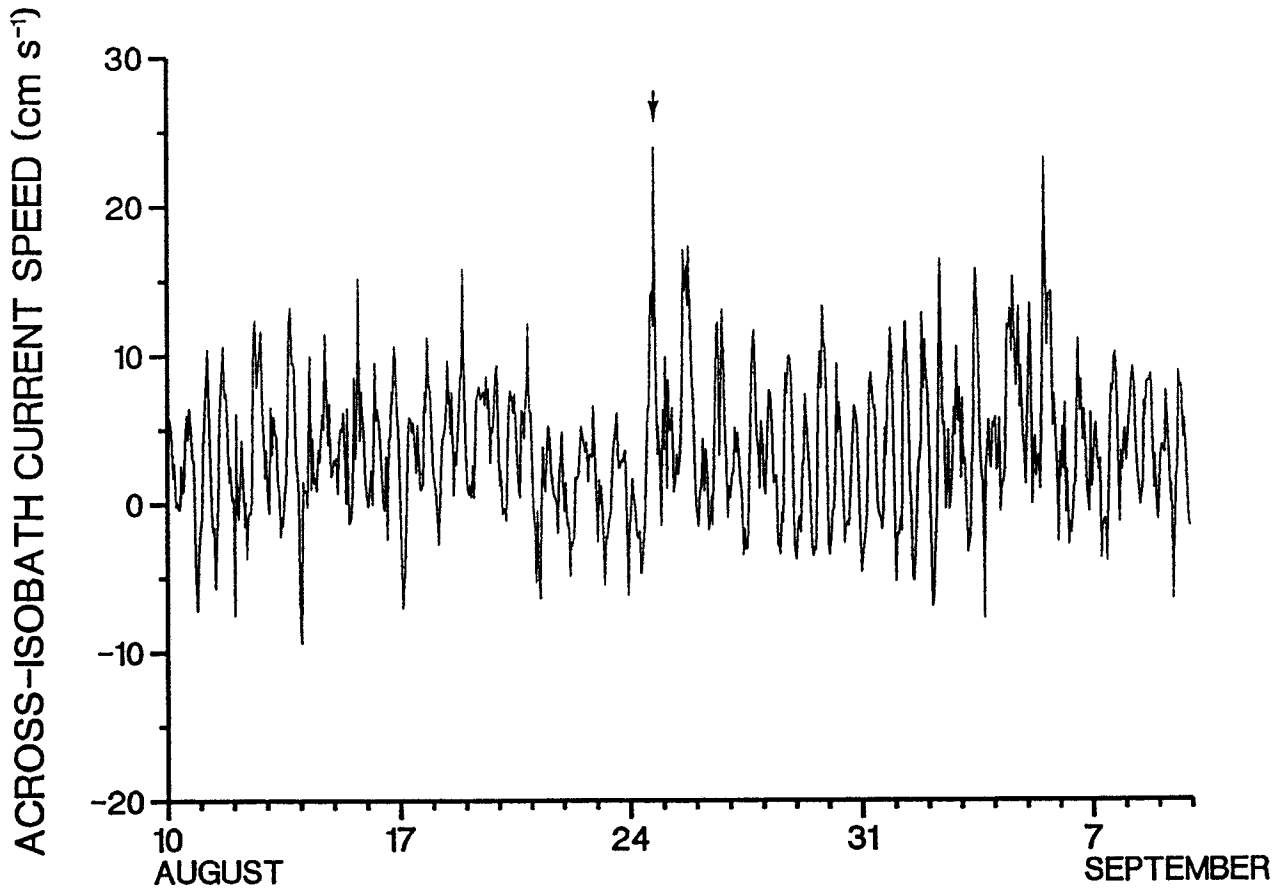


**Figure 50.** Across-isobath current speeds recorded 4 m above the bottom in 13 m of water in Hawk Channel between Bahia Honda Key and the reef tract, August 10 through September 9, 1992. Positive speeds indicate seaward flow (toward 165°) and the arrow marks the response to Hurricane Andrew.

average across-shelf flow during this time period was +3.5 cm $s^{-1}$, and the standard deviation in the across-isobath current component was 4.7 cm $s^{-1}$. For comparison, the amplitude of the $M_2$ tidal constituent for the across-isobath component is 3.7 cm $s^{-1}$. The arrow shows the response of the across-shelf flow to the passage of the hurricane. The storm induced a seaward flow that averaged 9.2 cm $s^{-1}$ over an 11-hour time period on August 24. Across-isobath flow reaches a maximum of +24 cm $s^{-1}$ at 1800 EST.

**Figure 51** shows the along-isobath currents recorded at this Hawk Channel study site. Although the primary focus of the study was on the *across*-isobath flow, the along-isobath component is also of interest. Positive values in the plot indicate flow toward 075°. The pattern indicates a series of low-frequency reversals in along-isobath flow that occur over time scales of about a week. Superimposed onto the reversals are high-frequency fluctuations that range between 15 and 25 cm $s^{-1}$. The standard deviation of the one-month time series is 9.9 cm $s^{-1}$ and the $M_2$ amplitude equals 2.5 cm $s^{-1}$. The response to Hurricane Andrew appears midway through the plot as a temporary interruption of westward flow. For eight hours as the storm passed, northeastward winds (see **Fig. 48**) forced an eastward along-isobath flow that averaged 14.2 cm $s^{-1}$. A maximum speed of 24 cm $s^{-1}$ was recorded at 1300 EST on August 24. For comparison, it is noteworthy that along-isobath flow reached 30 cm $s^{-1}$ in mid September.

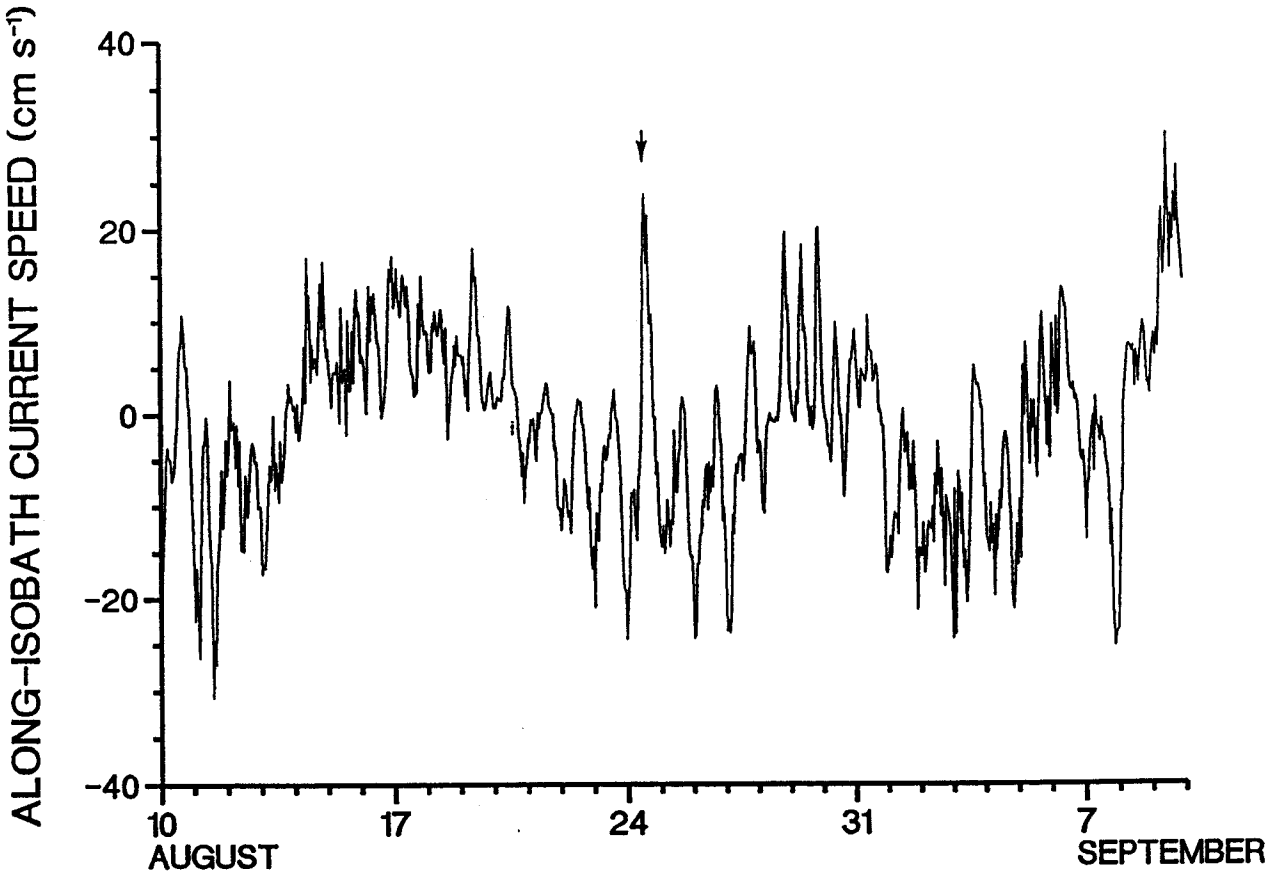


**Figure 51.** Along-isobath current speeds recorded 4 m above the bottom in 13 m of water in Hawk Channel midway between Bahia Honda Key and the reef tract, August 10 through September 9, 1992. Positive speeds indicate flow toward Miami (toward 075°) and the arrow marks the response to Hurricane Andrew.

Current meter data are also available from a third study site off Key West and at the western end of Hawk Channel. Across-shelf flow at this location, 100-105 km south of the storm track at its closest point, is shown in **Figure 52.** The plot shows currents recorded 2 m above the bottom in 11 m of water midway between Key West and Sand Key (see **Figure 47**). Positive values indicate seaward flow (toward 168°). The plot is dominated by tidal ebbs and floods that are superimposed onto low-frequency fluctuations occurring over time scales of several days to about a week. The amplitude of the across-isobath component of the $M_2$ constituent is 6.0 cm $s^{-1}$, and the standard deviation of the 57-day time series is 6.1 cm $s^{-1}$. The effect of the northeastward winds associated with the hurricane (**Fig. 48**) is to force an upwind near-bottom flow at the study site. Seaward flow averaged 11.3 cm $s^{-1}$ during an 8-hour period as the storm passed. A maximum seaward flow of 17.7 cm $s^{-1}$ was recorded at 1200 EST on August 24.

Along-isobath flow in Hawk Channel off Key West is shown in **Figure 53.** Positive values indicate flow toward 078°. The plot shows high-frequency fluctuations that are generally between 10 and 30 cm $s^{-1}$, superimposed onto low-frequency reversals that occur over time scales of several days to about two weeks. The standard deviation of this 57-day record is 11.7 cm $s^{-1}$ and the $M_2$ amplitude is 4.8 cm $s^{-1}$. The response to the storm appears at the end of the record

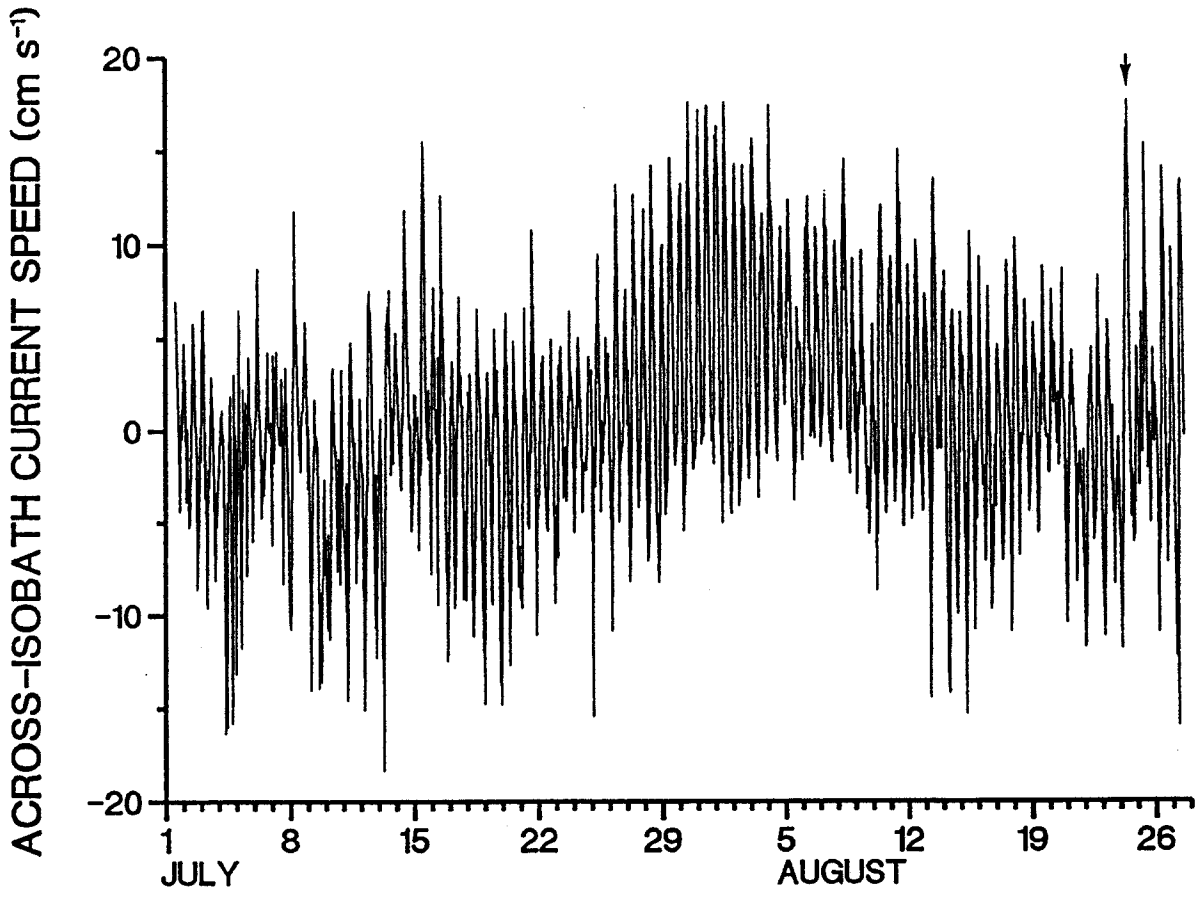


**Figure 52.** Across-isobath current speeds recorded 2 m above the bottom in 11 m of water in Hawk Channel midway between Key West and Sand Key, July 1 to August 27, 1992. Positive speeds indicate seaward flow (toward 168°) and the arrow marks the response to Hurricane Andrew.

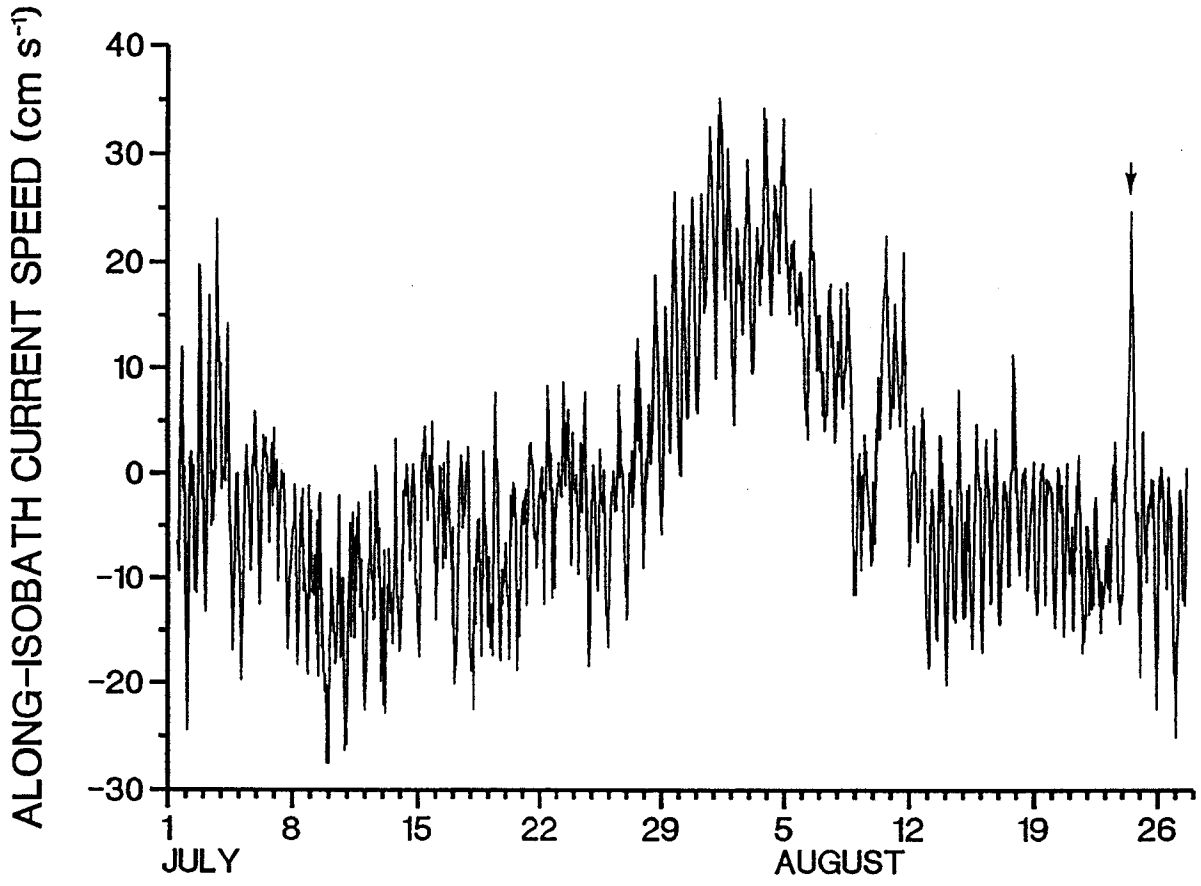


**Figure 53.** Along-isobath current speeds recorded 2 m above the bottom in 11 m of water in Hawk Channel midway between Key West and Sand Key, July 1 to August 27, 1992. Positive values indicate flow toward Miami (toward 078°) and the arrow marks the response to Hurricane Andrew.

(arrow). An 11-day westward flow was temporarily interrupted by the northeastward winds associated with the storm. For 11 hours on August 24 along-isobath flow at the study site averaged 11.3 cm $s^{-1}$. A maximum of 24.7 cm $s^{-1}$ toward 078° was recorded at 1500 EST. Again, however, this is not the strongest along-isobath flow recorded. During a 10-day period in late July and early August, sustained east-northeastward flow is commonly in excess of 20 cm $s^{-1}$.

b. Storm of the Century

The "Storm of the Century" formed in the western Gulf of Mexico early on March 12, 1993 and crossed the coast just east of Tallahassee later that same day. Although the most noteworthy feature of the storm was the large amounts of snow that fell along its path, including 13 inches in Birmingham, wind effects were substantial and equally widespread. Gusts of 37 m $s^{-1}$ (83 miles $h^{-1}$) were recorded in Vero Beach along the Atlantic coast of central Florida.

**Figure 54** shows the vector plot of wind stress recorded at Sombrero Reef, March 10-18. As the storm front approached the study area on March 12, wind stress began to increase and rotate clockwise from a westward heading. At 0300 EST on March 13 wind stress was directed toward 347° at 9.6 dyne $cm^{-2}$, corresponding to a wind speed of 19.8 m $s^{-1}$ (71.3 km $hr^{-1}$). One

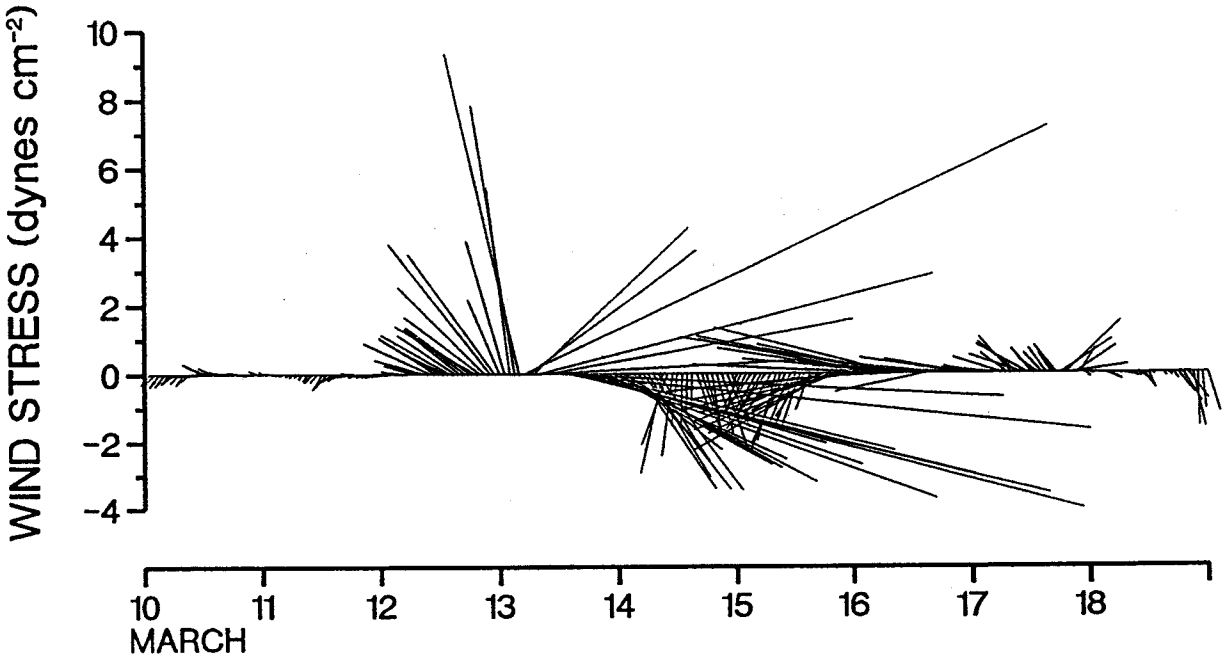


**Figure 54.** Vector plot of wind stress recorded at the C-MAN station on Sombrero Reef from March 10 through March 18, 1993.

hour later it had veered 78° clockwise and was directed toward 065° at 17.1 dyne $cm^{-2}$ (wind speed of 24.5 m $s^{-1}$). From about midday on the 13th to midday on the 14th, wind stress was directed into the southeast quadrant and averaged 8.9 dynes $cm^{-2}$ (17.4 m $s^{-1}$). For the next two days the direction of wind stress alternated mainly between the southwest and southeast quadrants and averaged 2.8 dynes $cm^{-2}$ (10.4 m $s^{-1}$).

The response of flow through Long Key Channel to the Storm of the Century is shown in **Figure 55**. The top plot shows the along-channel current speeds recorded 2 m above the bottom in 3.5 m of water from March 7 through March 20, 1993. Again, positive values indicate flow into Florida Bay. As in **Figure 49**, the plot begins with a very regular flood and ebb of the tide. As the storm moved into the northeastern Gulf of Mexico on March 12, wind forcing produced abbreviated ebbs on two consecutive tidal cycles. The most pronounced effects occurred on March 13, as the center of the storm was moving northward along the coast of Georgia and the Carolinas. Strong wind stress toward the southeast completely overwhelmed two consecutive flood cycles. The maximum recorded current speed during this time was 104 cm $s^{-1}$. Flow through the channel the following day continued to favor the outflow leaving Florida Bay. Then, on March 15 and 16, the flow largely reversed, and the net flow was into Florida Bay. By March 17, storm effects were absent and flood and ebb current speeds were equal in magnitude.

The bottom plot in **Figure 55** shows the cumulative net displacement of water through Long Key Channel from July 1, 1992 to September 9, 1993. The mean outflow from Florida Bay during this 435-day time period was -2.6 cm $s^{-1}$. The storm-induced outflow on March 13 (indicated by the arrow) averaged -51.9 cm $s^{-1}$. This represents a 20-fold increase over the long-term average. Strong outflow continued on the 14th, averaging -25.3 cm $s^{-1}$, then the flow

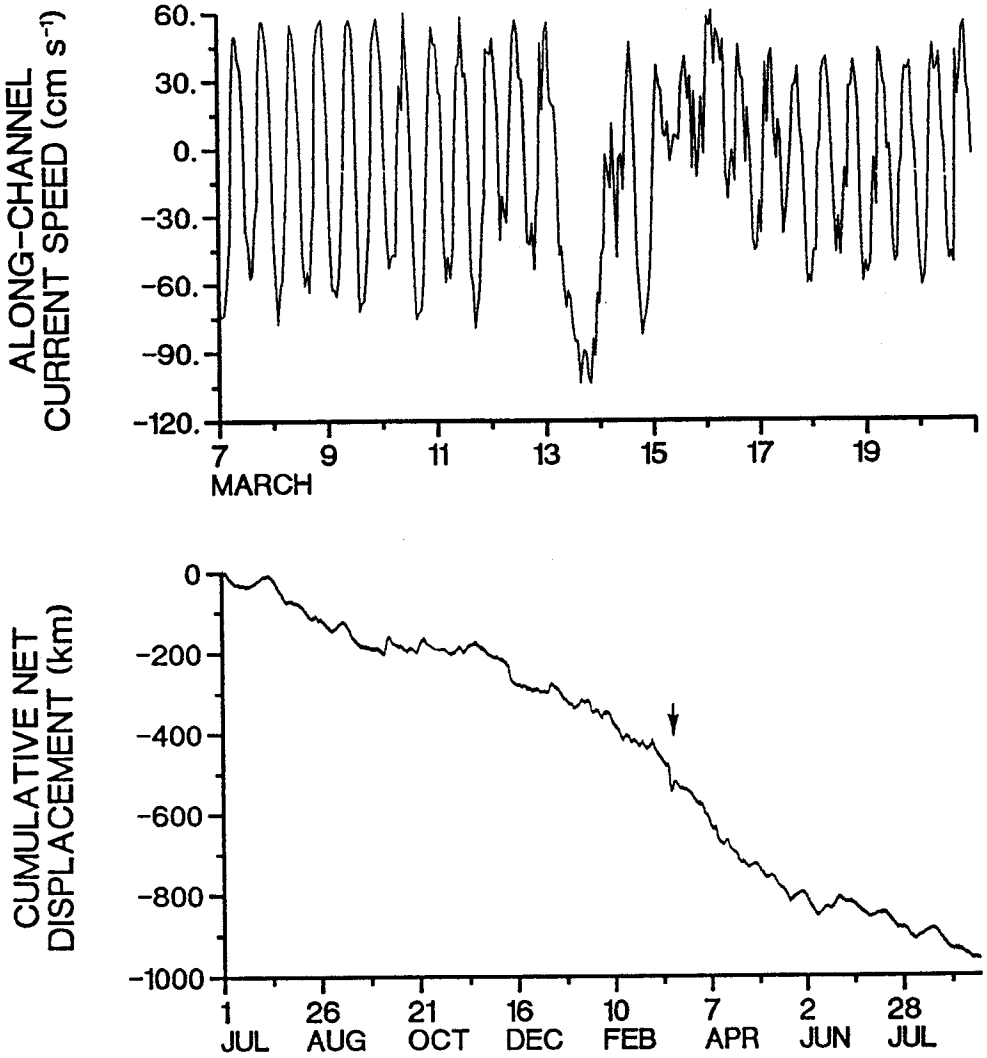


**Figure 55.** Along-channel current speeds recorded 1 m above the bottom at a study site in Long Key Channel, March 7-20, 1993 (top) and cumulative net displacement past the study site from July 1, 1992 to September 9, 1993 (bottom). Negative values indicate flow out of Florida Bay.

reversed. Inflow to the bay recorded March 15-16 averaged 14.3 cm $s^{-1}$. The effects of the storm appear as a significant perturbation on the quasi-steady outflow from the bay through this channel, but the partial recovery significantly lessens the net loss of water from Florida Bay.

The outflow observed on March 13 was the strongest measured for a one-day time period during the 14-month study. However, many other significant perturbations were recorded during the study period. Some represent the passage of cold fronts, while others have unknown causes.

**Figure 56** shows the across-shelf flow in Hawk Channel midway between Bahia Honda Key and the reef tract during March 1-31, 1993. Currents were recorded 4 m above the bottom in 13 m of water. Positive values indicate seaward flow (toward 165°). Across-isobath current speeds vary generally between ±10 cm $s^{-1}$. The average across-shelf flow during this time period was -0.01 cm $s^{-1}$, and the standard deviation was 4.9 cm $s^{-1}$. The amplitude of the across-isobath component of the $M_2$ tidal current is 3.6 cm $s^{-1}$. The response to the Storm of the Century

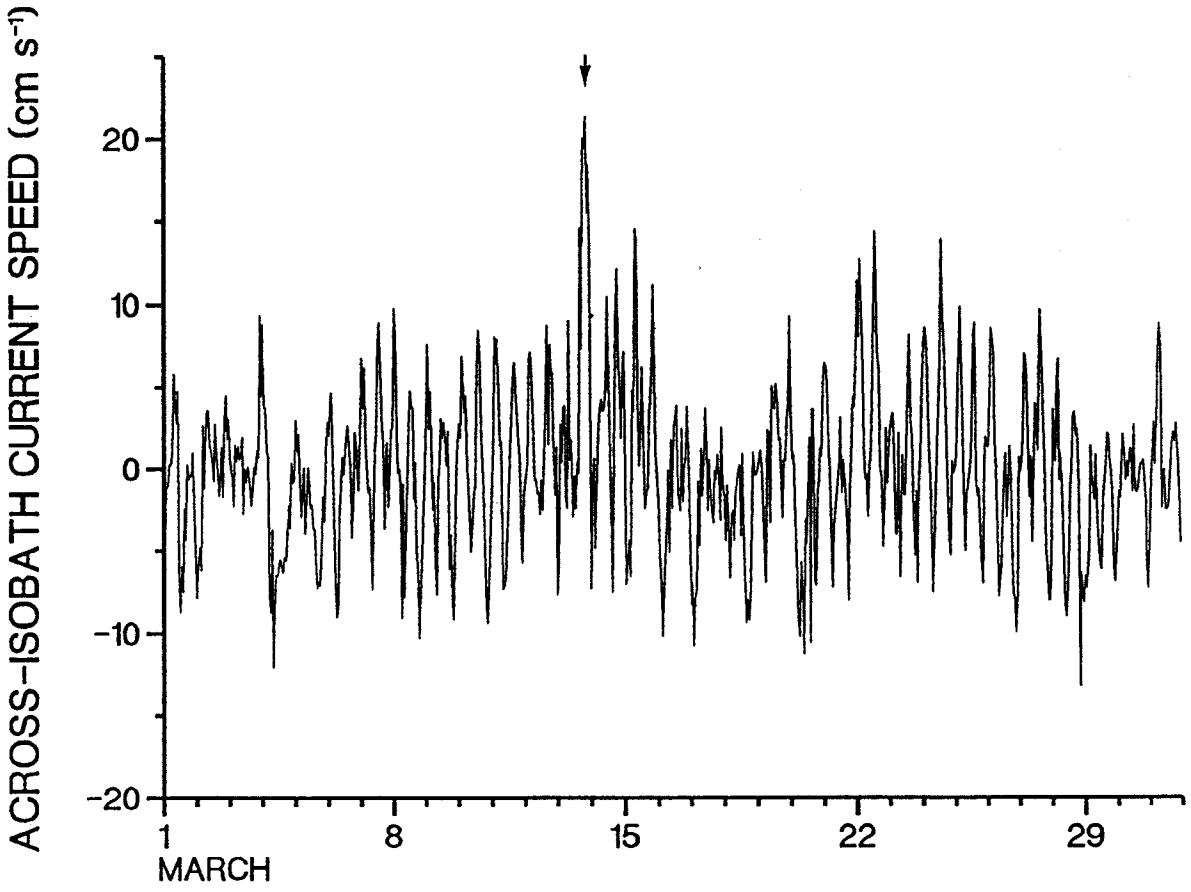


**Figure 56.** Across-isobath current speeds recorded 4 m above the bottom in 13 m of water in Hawk Channel midway between Bahia Honda Key and the reef tract, March 1-31, 1993. Positive speeds indicate seaward flow (toward 165°).

appears at about the midpoint of the plot. The most notable feature is the pronounced seaward flow on March 13 (arrow) that lasted eight hours and averaged 16.3 cm $s^{-1}$. A maximum speed of 21.5 cm $s^{-1}$ was recorded at 2000 EST. Across-isobath currents continue to be predominantly seaward during March 14 and 15. This is followed by a landward flow during March 16-18 that averaged -2.4 cm $s^{-1}$.

**Figure 57** shows along-isobath currents recorded in Hawk Channel off Bahia Honda Key in response to the Storm of the Century. Positive values indicate flow toward 075°. Along-isobath currents speeds are generally between ±10 cm $s^{-1}$. The standard deviation of the one-month time series was 15.0 cm $s^{-1}$, and the amplitude of the $M_2$ tidal current was 3.3 cm $s^{-1}$. The response to the storm is very pronounced in this record. A strong along-shelf flow toward the east-northeast was recorded during March 13. For 31 hours positive along-isobath flow averaged 29 cm $s^{-1}$. A maximum of 55.2 cm $s^{-1}$ was recorded at 1400 EST on March 13. The flow reversed around midday on the 14th and for the next 79 hours currents averaged -32.6 cm $s^{-1}$ toward 255°. A maximum flow of -59.0 cm $s^{-1}$ toward Key West was recorded at 0200 EST on March 16.

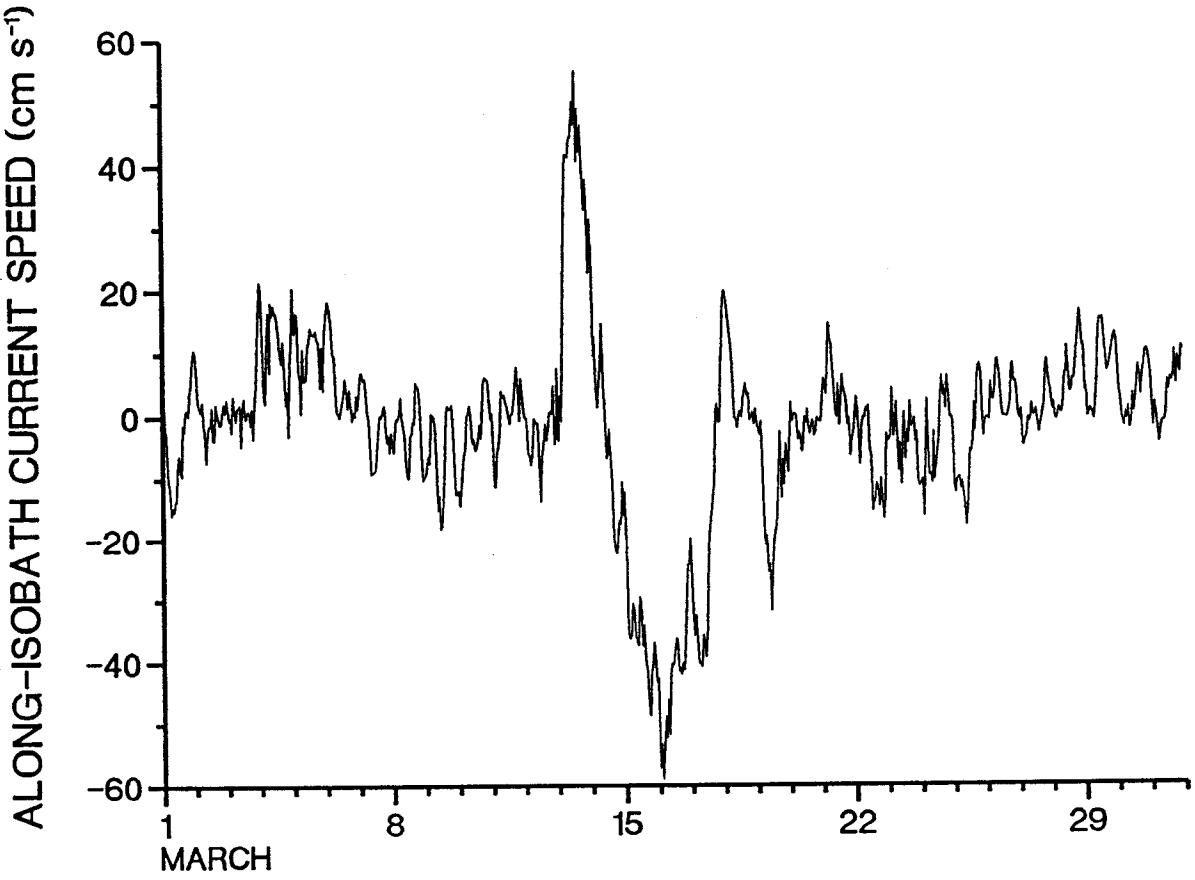


**Figure 57.** Along-isobath current speeds recorded 4 m above the bottom in 13 m of water in Hawk Channel midway between Bahia Honda Key and the reef tract, March 1-31, 1993. Positive values indicate flow toward Miami (toward 075°).

c. Tropical Storm Gordon

Tropical Storm Gordon approached the Florida Keys from the southeast and crossed the island chain at Key West on November 15, 1994. After crossing the Keys, the storm turned clockwise and moved across the Florida peninsula on a northeastward track. **Figure 58** is the vector plot of wind stress recorded at Molasses Reef, November 7-20. At its closest point, the storm center passed 115 km south of Molasses Reef in the early morning hours of November 15th. The plot shows that for approximately two days prior to the passage of the storm, shelf waters near Molasses Reef experienced strong wind stress into the southwest quadrant. A maximum sustained wind stress of 10.2 dynes $cm^{-2}$ directed toward 221° was recorded at 0800 EST November 14. During the early morning hours of November 15 the wind stress vector at Molasses Reef veered clockwise, and for the next 18 hours scalar wind stress averaged 4.7 dynes $cm^{-2}$ toward the northwest. The minimum air pressure recorded at Molasses Reef was 999.6 mb at 0400 EST November 15. By the evening of the 15th, and for the next day wind stress was directed into the northeast quadrant and averaged 5.1 dynes $cm^{-2}$. Wind stress continued veering clockwise and decreased in magnitude as the storm circled the tip of the Florida Peninsula and then continued northeastward across South Florida. By November 18 wind stress was directed toward the south at less than 0.3 dyne $cm^{-2}$.

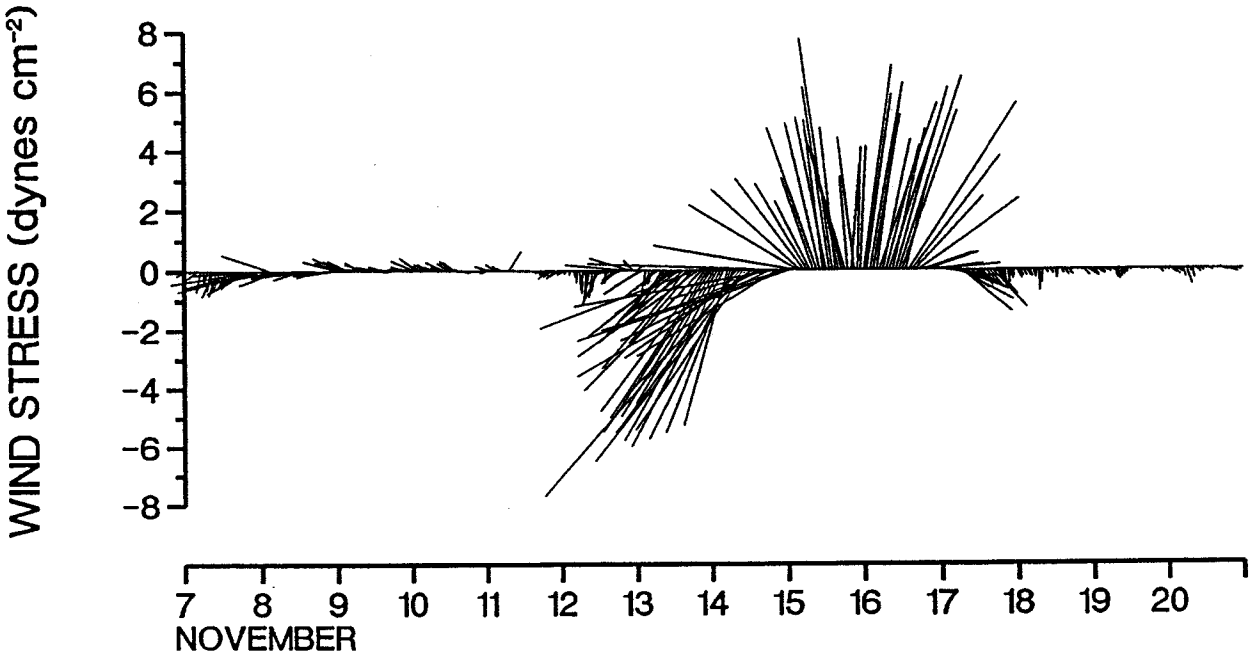


**Figure 58.** Vector plot of wind stress recorded at the C-MAN station on Molasses Reef from November 7 through November 20, 1994.

The response to Tropical Storm Gordon recorded in four tidal channels is shown in **Figures 59-62.** The top plot of each figure shows the along-channel current speed, in cm $s^{-1}$, recorded from November 10-23. The bottom plot shows the cumulative net displacement of water through the channel for the entire time the current meter was in the water. Positive values indicate flow into Florida Bay in all plots.

**Figure 59** shows the response of flow through Snake Creek. The top plot shows that along-channel currents are dominated by tidal ebbs and floods. The amplitude of the $M_2$ constituent at the study site in Snake Creek is 31 cm $s^{-1}$. Measured currents indicate a net flow into Florida Bay during the first four days of the record, but both floods and ebbs were recorded. As the storm approached the study area on November 14 and 15, along-channel flow became almost exclusively positive. This sustained inflow varied in strength, but it reversed only briefly. The average nontidal flow into the bay during this two-day period was 32 cm $s^{-1}$. A maximum inflow of over 73 cm $s^{-1}$ was recorded on November 15. Beginning on November 16, flow through the channel reversed, and water drained out of the bay almost continuously for the next two days. Outflow averaged -16 cm $s^{-1}$ during November 16-18, and it reached a peak of nearly 60 cm $s^{-1}$ early on November 17.

The bottom plot of **Figure 59** shows the cumulative net displacement recorded in Snake Creek from July 1, 1994 to January 3, 1995. The pattern indicates a quasi-steady inflow to the bay that averaged 5.4 cm $s^{-1}$ over this 186-day study period. This is one-sixth of the average inflow during the two days preceding the storm, and one-third of the average outflow during the three days after the storm had passed. Gordon was responsible for one of two significant reversals in inflow to the bay. The other occurred in late December, presumably in response to the passage of a winter cold front.

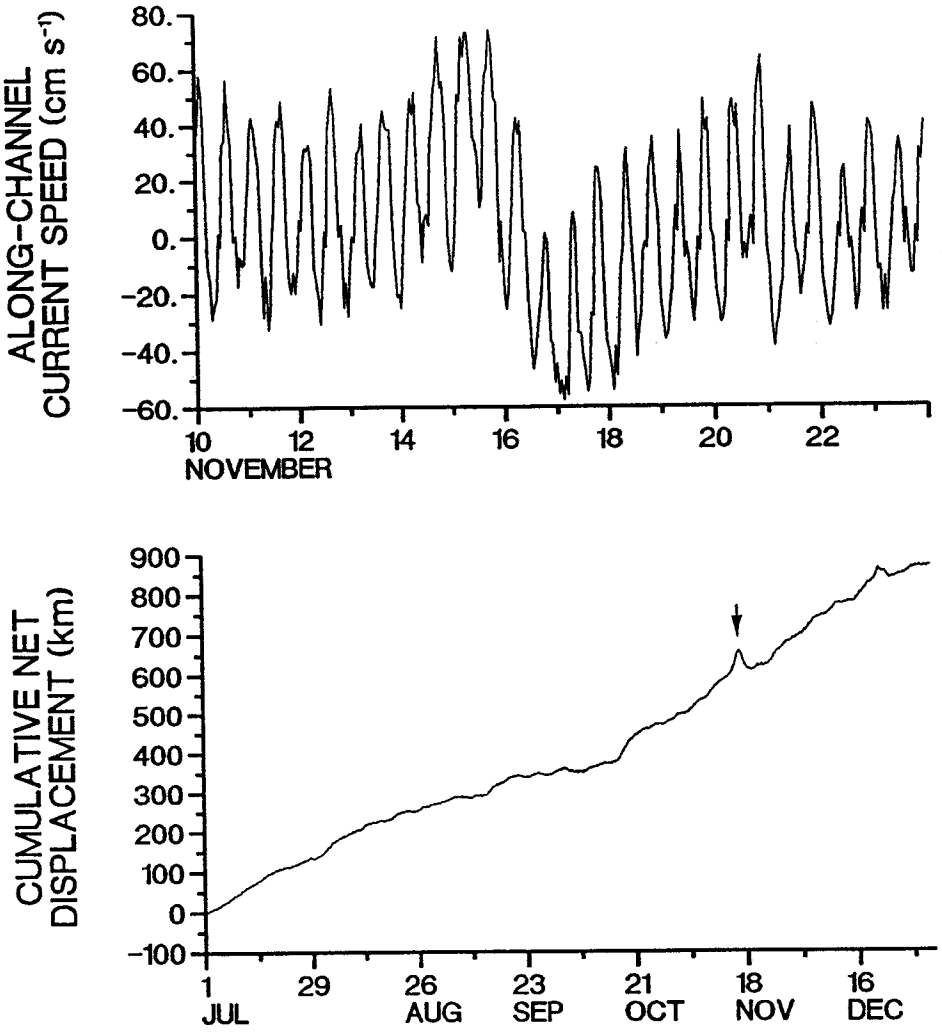


**Figure 59.** Along-channel current speeds recorded 1 m above the bottom at a study site in Snake Creek, November 10-23, 1994 (top) and cumulative net displacement past the study site from July 1, 1994 to January 3, 1995 (bottom). Negative values indicate flow out of Florida Bay.

Effects of the storm on flow through Whale Harbor Channel are shown in **Figure 60**. Whale Harbor Channel is only 3 km southwest of Snake Creek, and the response is similar. Again, tidal ebbs and floods are readily apparent in the record. The $M_2$ amplitude at the study site is 51 cm $s^{-1}$. During the two days preceding the storm's arrival, along-channel flow was mostly into Florida Bay. Nontidal inflow averaged 45.2 cm $s^{-1}$. Inflow reached a peak of over 100 cm $s^{-1}$ late on November 15, and during one tidal cycle on that day, ebb currents were completely overwhelmed by nontidal flow into the bay. Along-channel flow reversed on November 16 and for the next day and a half water flowed out of the bay almost continuously, completely eliminating two flood cycles. Nontidal flow was out of the bay for the next three days at an average speed of -19.3 cm $s^{-1}$.

The bottom plot of **Figure 60** shows the cumulative net displacement through Whale Harbor Channel from September 20 to December 13, 1994. The pattern is similar to the one for Snake Creek, although the Whale Harbor Channel record covers a shorter time period. The flow

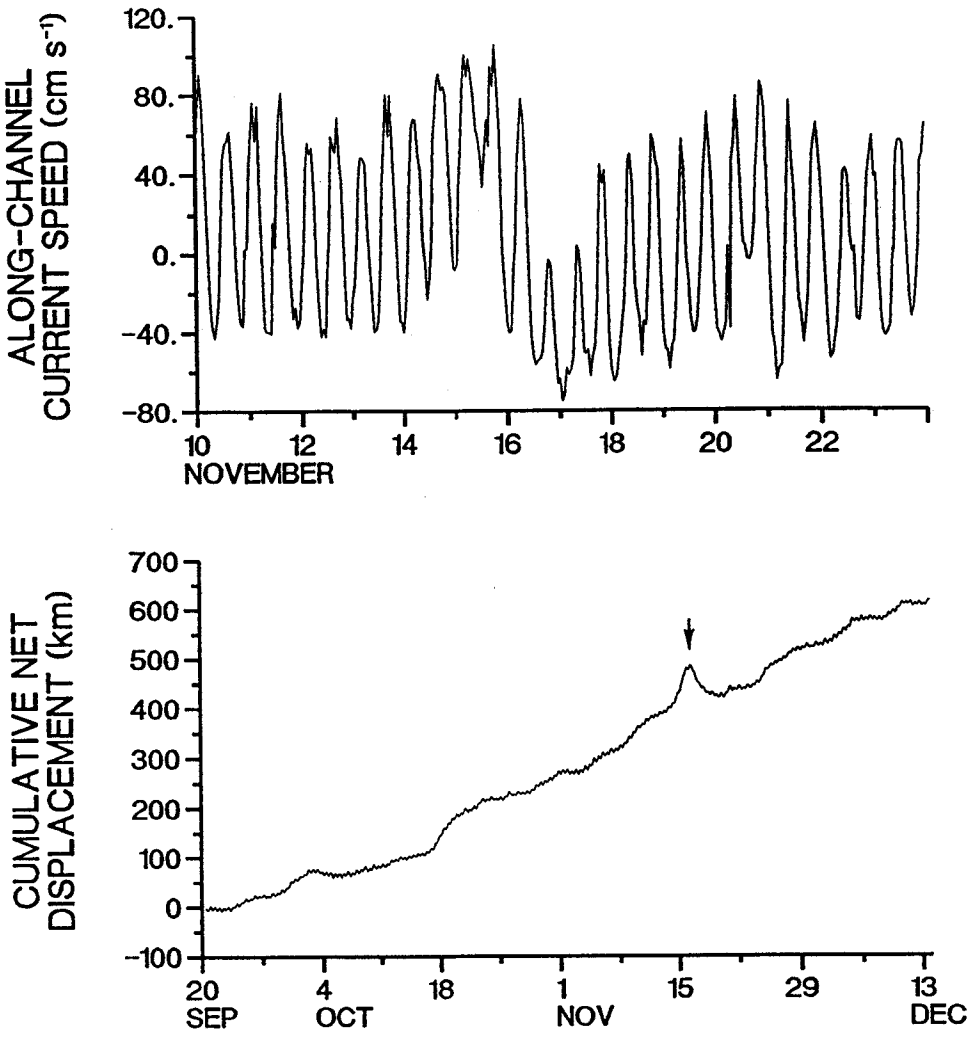


**Figure 60.** Along-channel current speeds recorded 1 m above the bottom at a study site in Whale Harbor Channel, November 10-23, 1994 (top) and cumulative net displacement past the study site from September 20 to December 13, 1994 (bottom). Negative values indicate flow out of Florida Bay.

into the bay during this 84-day study period averaged 8.4 cm $s^{-1}$. By comparison, inflow during the two days preceding the storm averaged 47.0 cm $s^{-1}$, while outflow during the three days following the storm's passage averaged -18.3 cm $s^{-1}$. Tropical Storm Gordon was responsible for the only significant nontidal reversal in inflow through this channel recorded during the 84-day study period.

**Figure 61** shows the flow through Indian Key Channel in response to Gordon. Indian Key Channel is located approximately 9 km southwest of Whale Harbor Channel. The $M_2$ amplitude is 43 cm $s^{-1}$ at the study site. The top plot shows a pattern that repeats many of the features seen in the previous two figures. Along-channel currents are predominantly positive during November 14 and 15, the two days preceding the storm's passage. Nontidal inflow averaged 18.5 through this channel during those two days. The ebb tide is eclipsed by nontidal

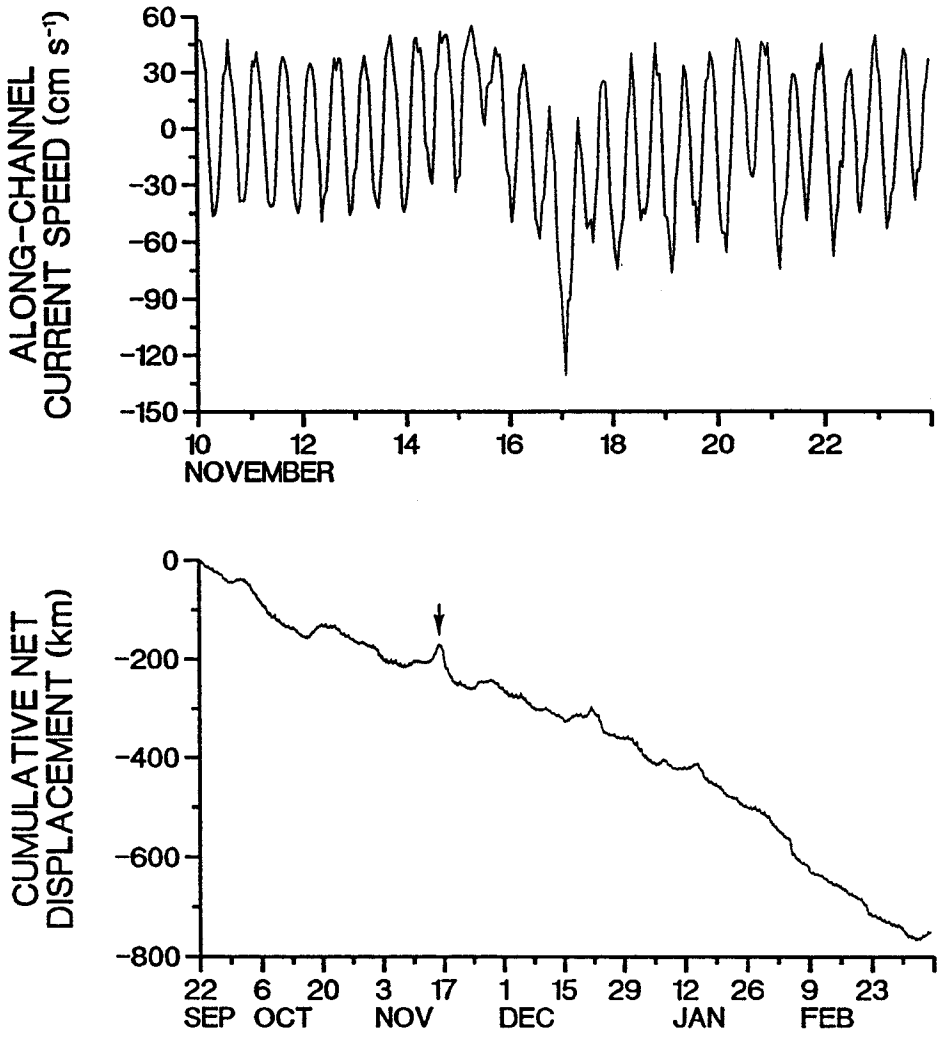


**Figure 61.** Along-channel current speeds recorded 1 m above the bottom at a study site in Indian Key Channel, November 10-23, 1994 (top) and cumulative net displacement past the study site from September 22, 1994 to March 8, 1995 (bottom). Negative values indicate flow out of Florida Bay.

inflow during one of the tidal cycles on November 15. Over the next two days, along-channel currents are mostly negative, indicating an outflow from the bay. Strongest outflow into Hawk Channel was over 130 cm $s^{-1}$ early on November 17. Nontidal outflow from the bay during the three days following the passage of the storm averaged -25.7 cm $s^{-1}$.

Cumulative net displacement through Indian Key Channel from September 22, 1994 to March 8, 1995 is shown at the bottom of **Figure 61**. The plot shows a long-term outflow from Florida Bay that averaged -5.2 cm $s^{-1}$ during the 167-day study period. By comparison, along-channel flow into the bay during the two days preceding the storm averaged +20.1 cm $s^{-1}$, along-channel outflow during the three days following the storm averaged -24.8 cm $s^{-1}$. The storm-induced perturbation is one of several temporary reversals in the quasi-steady outflow from the bay through this channel during the study period. Other significant reversals occur during the

third week of October, the fourth week of December and the middle of January. The December and January perturbations were probably induced by the passage of cold fronts.

**Figure 62** shows data recorded in Long Key Channel. Again, plots are similar to those obtained for Snake Creek and Whale Harbor Channel. As in the other channels, along-channel currents are predominantly positive during November 14 and 15. The mean nontidal flow into the bay during that time averaged 14 cm $s^{-1}$, and a maximum inflow of 68 cm $s^{-1}$ was recorded on November 15. The mean along-channel flow reversed for just over a day following the storm's passage. A maximum outflow of nearly 100 cm $s^{-1}$ was recorded on November 17 and nontidal outflow averaged -11.6 cm $s^{-1}$ during the three days following the storm. For comparison, the amplitude of the $M_2$ tidal constituent at the study site is 46.0 cm $s^{-1}$. It is noteworthy that the response to Tropical Storm Gordon through Long Key Channel was not as pronounced as the response recorded in the other three tidal channels.

Cumulative net displacement through Long Key Channel from August 29, 1994 to July 24, 1995 is shown at the bottom of **Figure 62**. The pattern shows a quasi-steady long-term

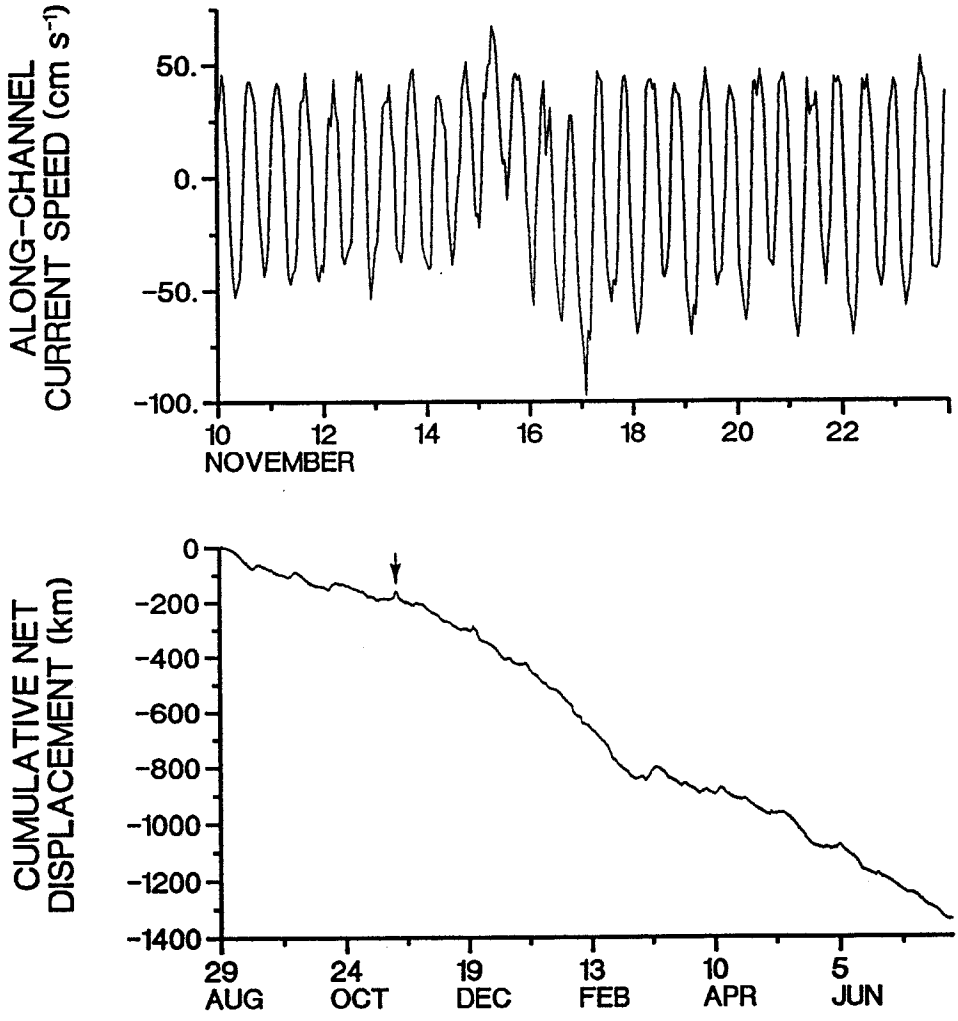


**Figure 62.** Along-channel current speeds recorded 1 m above the bottom at a study site in Long Key Channel, November 10-23, 1994 (top) and cumulative net displacement past the study site from August 29, 1994 to July 24, 1995 (bottom). Negative values indicate flow out of Florida Bay.

outflow from the bay that averaged 4.7 cm $s^{-1}$ during this 329-day study period. By comparison, inflow during the two days preceding the storm averaged 15.7 cm $s^{-1}$, while the outflow during the three days following the storm averaged -11.1 cm $s^{-1}$. The response to the storm appears as a very minor perturbation on the long-term outflow, and the anomalous inflow is largely canceled by the anomalous outflow. Other perturbations appear throughout the time series, the most notable of which occurs in mid March and is presumably a response to a late winter cold front.

Across-shelf flow at the reef tract near Tennessee Reef is shown in **Figure 63**. Positive values indicate seaward flow (toward 158°). The top plot shows the across-isobath currents recorded 6 m below the surface in 21 m of water from August 8 to December 8, 1994. The response to Tropical Storm Gordon (arrow) appears near the end of the plot. The current meter recorded an onshore flow that averaged -2.8 cm $s^{-1}$ during November 14 and 15. A maximum speed of -7.9 cm $s^{-1}$ was recorded on November 14. This onshore flow was immediately followed by two days of seaward flow. A maximum seaward current of 11.1 cm $s^{-1}$ was recorded about a day after the storm had passed. Comparing the mid November time period with the

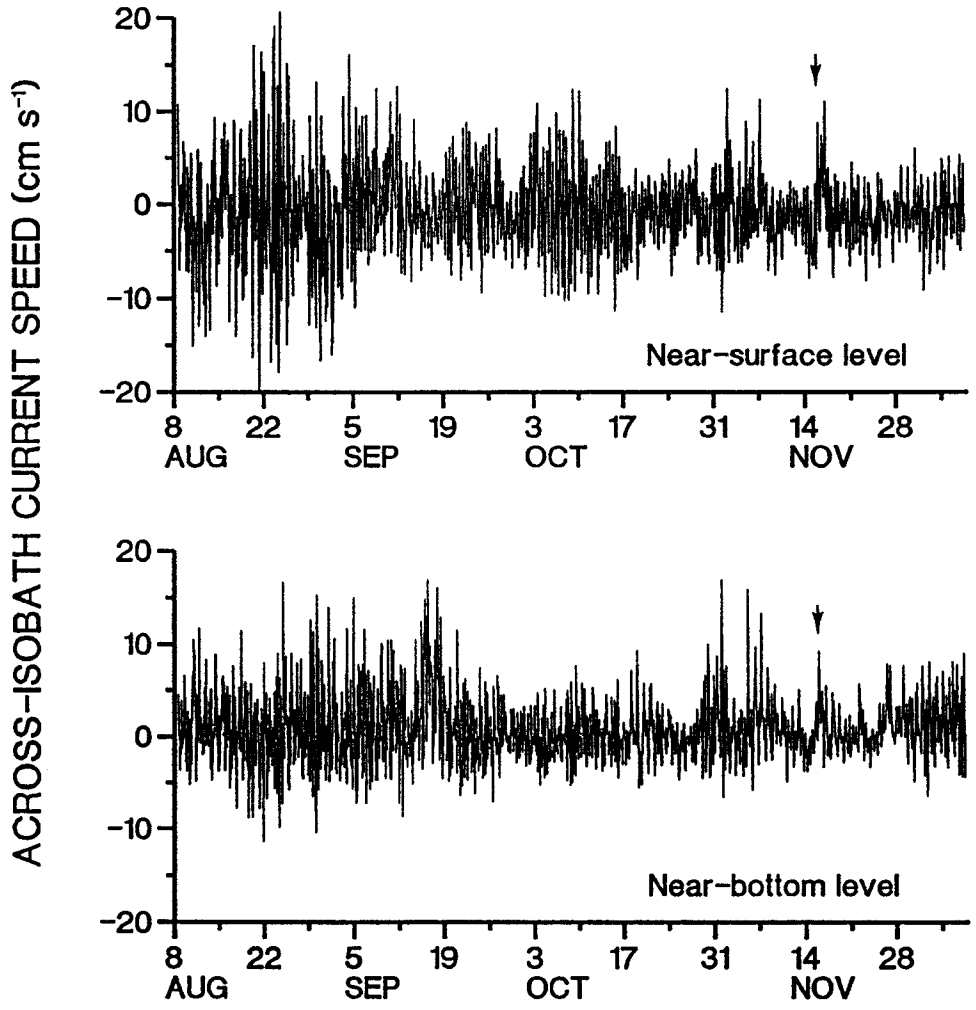


**Figure 63.** Across-isobath current speeds recorded 6 m below the surface (top) and 2 m above the bottom (bottom plot) in 21 m of water near Tennessee Reef, August 8 to December 8, 1994. Positive speeds indicate seaward flow (toward 158°) and arrows mark the response to Tropical Storm Gordon.

remainder of the record indicates that the across-isobath response to Gordon was relatively minor. Relatively large fluctuations in the across-isobath current occurred during late August and early September. Current speeds commonly reached ±10 cm $s^{-1}$ during that time. The standard deviation of this 4-month record is 4.4 cm $s^{-1}$.

The bottom plot in **Figure 63** shows the across-isobath currents recorded 2 m above the bottom at the same study site and during the same time period. Relatively large fluctuations occurred during the first six weeks of the record. Speeds commonly reached +10 cm $s^{-1}$ to -5 cm $s^{-1}$ during that time. The standard deviation of the 122-day time series is 3.3 cm $s^{-1}$. By comparison, near-bottom across-isobath currents attained a maximum onshore speed of only -3.8 cm $s^{-1}$ during the two days preceding the storm. A maximum seaward current of 9.2 cm $s^{-1}$ was recorded the day following the storm's passage.

Along-isobath flow at the reef tract near Tennessee Reef in response to Gordon is shown in **Figure 64**. The top plot in the figure shows along-isobath current speeds recorded near the

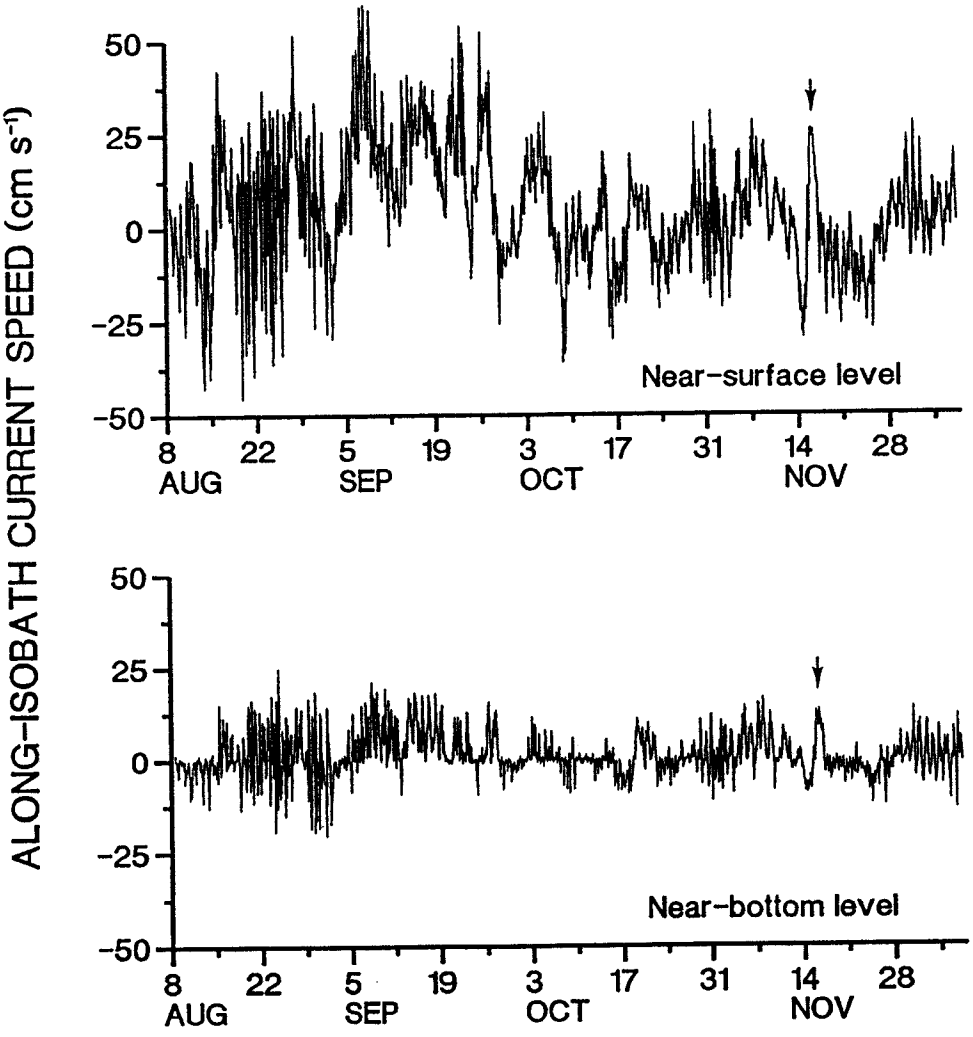


**Figure 64.** Along-isobath current speeds recorded 6 m below the surface (top) and 2 m above the bottom (bottom plot) in 21 m of water near Tennessee Reef, August 8 to December 8, 1994. Positive values indicate flow toward Miami (toward 068°) and arrows mark the response to Tropical Storm Gordon.

surface. Positive values indicate flow toward 068°. Negative flow was recorded during November 14 and 15 as the storm approached the Keys. During that time, flow averaged -13.4 cm $s^{-1}$. A maximum southwestward flow of -29.7 was recorded at 1900 EST on November 24. After the storm had passed the study area along-isobath flow reversed, and for the next 36 hours it averaged 15.4 cm $s^{-1}$ toward 068°. A maximum of 26.4 cm $s^{-1}$ was recorded at 0600 EST on November 16. For comparison, the standard deviation of the 122-day time series is 15.7 cm $s^{-1}$ and maximum along-isobath currents were -45.4 and 60.0 cm $s^{-1}$. Low-frequency fluctuations occurred over time scales of several days to about a week and generally ranged between 25-30 cm $s^{-1}$.

The bottom plot in **Figure 64** shows the along-isobath currents recorded 2 m above the bottom. The response to the storm is similar to that recorded at the surface, although the magnitude is reduced by about half. During November 14 and 15 flow near the bottom averaged -4.6 cm $s^{-1}$ toward Key West in response to the strong southwestward wind stress (**Fig. 58**). A maximum current speed of -9.4 cm $s^{-1}$ was recorded at 1600 EST on November 14. After the storm had passed to the north, along-shelf flow reversed and averaged 7.8 cm $s^{-1}$ for the next 36 hours. Maximum along-isobath currents reached -20.4 and 25.0 cm $s^{-1}$. The current meter recorded a maximum flow of 13.5 cm $s^{-1}$ toward 068° at 1100 EST on November 16. For comparison, the standard deviation of the 122-day record is 5.4 cm $s^{-1}$.

**Discussion**

Although cause-and-effect relationships can only be established qualitatively from the data base discussed above, it is appropriate to recall some of the general principles that relate transient storm events to transport in shallow water.

First, the local response of water level to a storm event will be inversely related to depth. The set-up of water, for example, will be greater in Florida Bay, on the Gulf side of the Keys, than in Hawk Channel, on the Atlantic side. This is because in shallow water there is less room for an upwind near-bottom return flow.

Second, the response to a storm is logically related to the magnitude of the storm. Because wind stress is the driving force, however, the response will be related to the square of the wind speed. The response to a storm event will also be a function of the size of the storm system, and to the storm track relative to the study site. Thus, an intense but relatively small storm such as Hurricane Andrew might have a more local effect than Tropical Storm Gordon, which was larger in size. The storm track, relative to the location of the study site, will determine the distance to the storm center at its closest point, as well as how the wind stress vector veered (turned clockwise) or backed (turned counter-clockwise) as the storm system passed the study site.

Finally, and directly related, is the speed of movement of the storm center. Clearly, a fast-moving storm system will have a more transient effect than a slow-moving storm will have.

Several features brought out in the plots of hourly current speed and cumulative net displacement diagrams in the Results section are worth reviewing in greater detail here. In some cases, the local response to a storm event was equivalent to or less than the response to a cold-air outbreak during the previous or following winter season. For example, **Figure 49** shows that the response to Hurricane Andrew in Long Key Channel was significantly less than the nontidal activity recorded during the following winter season. Similarly, while the flow anomaly in Hawk Channel resulting from Andrew is easily identifiable in **Figure 51**, comparable along-isobath flow in both directions appears earlier and later in the same time series. This is not to say that

hurricanes are less significant than cold fronts, but for the specific channel and time period considered the local response to several forms of meteorological forcing can be significant.

A second feature that is seen most easily in the cumulative net displacement plots involves the long-term net Gulf-to-Atlantic, or Atlantic-to-Gulf movement of water through tidal channels in the Middle and Upper Keys. Our historical data base includes examples of both large and small net volume transports. The response to the Storm of the Century in Long Key Channel (**Fig. 55**) suggests that the outflow of water as the storm moved through the northeastern Gulf of Mexico exceeded the return flow entering Florida Bay as the storm center moved up the Atlantic coast. Alternately, the response to Tropical Storm Gordon in Snake Creek and Whale Harbor Channel (**Figs. 59** and **60**) suggest that the inflow and outflow were much more equal in magnitude. While the net exchange of Hawk Channel water and Florida Bay water cannot be quantified, the cumulative net displacement diagrams suggest little net volume transport occurred in response to this tropical storm.

An important qualifier that applies to the current meter data obtained from tidal channels as well as to the data collected from Hawk Channel is that we cannot accurately quantify volume transport from current meter data alone. Volume transport calculations require information on water level in addition to information on current speed. Thus, when current meter data suggest that inflow was similar to outflow during a storm event, it has been shown only that the flow past the current meter was approximately equal and opposite.

With all the variables related to the size, strength and track of the three storm systems considered here, we can only describe cause-and-effect relationships in terms of the available wind and current meter data. Generalized empirical relationships require a much broader data base. Nevertheless, results presented here, when pooled with results from other studies in the Keys and elsewhere should contribute to model verification exercises.

## LITERATURE CITED

Bowden, K.F. 1983. Physical Oceanography of Coastal Waters. Halstead Press, New York, 302 pp.

Dennis, R. and E. Long. 1971. A user's guide to a computer program for harmonic analysis of data at tidal frequencies. NOAA Tech. Report, U.S. Dept. of Commerce, 41: 31 pp.

Heathershaw, A. and D. Langhorne. 1988. Observations of near-bed velocity profiles and sea-bed roughness in tidal currents flowing over sandy gravels. Estuarine, Coastal and Shelf Science 26:459-82.

Kundu, P.K. 1976. Ekman veering observed near ocean bottom. Journal of Physical Oceanography 6:238-242.

Lewis, E.L. 1980. The practical salinity scale 1978 and its antecedents. IEEE Journal of Oceanic Engineering OE-1:3-8.

Little, J. and L. Shure. 1988. Signal processing toolbox, user's guide. The MathWorks, Inc., Natick MA, 165 pp.

Millero, F. and A. Poisson. 1981. International one-atmosphere equation of state of seawater. Deep-Sea Research 28:625-629.

Panofsky, H.A. and G. Brier. 1963. Some applications of statistics to Meteorology. The Pennsylvania State University, University Park, PA, 224 pp.

Perkin, R. and E. Lewis. 1980. The practical salinity scale 1978: Fitting the data. IEEE Journal of Oceanic Engineering 5:9-16.

Pitts, P.A. 1994. An investigation of near-bottom flow patterns along and across Hawk Channel, Florida Keys. Bulletin of Marine Science 54:610-620.

Pitts, P.A. and N.P. Smith. 1995. Long-term net transport through three tidal channels in the interior of Florida Bay. Final Report, Cooperative Agreement CA5280-4-9022, National Park Service, Everglades National Park, Homestead, Florida, 51 pp.

Pond, S. and G. Pickard. 1983. Introductory Dynamical Oceanography. Second Edition. Pergamon Press, New York, 329 pp.

Schureman, P. 1958. Manual of harmonic analysis and prediction of tides. Spec. Publ. No. 98, U.S. Govt. Printing Off., Washington, D.C., 317 pp.

Scientific Programming Enterprises. 1985. PlotIT Interactive Graphics and Statistics Reference Guide, version 1.0. P.O. Box 669, Haslett Michigan.

Smith, N.P. 1994. Long-term Gulf-to-Atlantic transport in the Florida Keys. Bul. Mar. Sci. 54:602-609.

Szmant, A.M. and A. Forrester. 1996. Water column and sediment nitrogen and phosphorus distribution patterns in the Florida Keys, USA. Coral Reefs 15:21-41.

Wang, J.D., J. van de Kreeke, N. Krishnan and D. Smith. 1994. Wind and tide response in Florida Bay. Bull. Mar. Sci. 54:579-601.

Wu, J. 1980. Wind-stress coefficients over sea surface near neutral conditions--a revisit. Journal of Physical Oceanography 10-727-740.